

UNIVERSIDADE FEDERAL DE PELOTAS
Faculdade de Odontologia
Programa de Pós-Graduação em Odontologia



Tese

**Partículas inorgânicas funcionalizadas em materiais restauradores híbridos em
Odontologia**

Marina da Rosa Kaizer

Pelotas, 2015

Marina da Rosa Kaizer

**Partículas inorgânicas funcionalizadas e materiais restauradores híbridos em
Odontologia**

Tese apresentada ao Programa de Pós-Graduação em Odontologia da Faculdade de Odontologia da Universidade Federal de Pelotas, como requisito parcial para obtenção do título de Doutor em Odontologia, área de concentração Materiais Odontológicos.

Orientador: Prof. Dr. Rafael Ratto de Moraes

Co-orientador: Prof. Dr. Sergio da Silva Cava

Pelotas, 2015

Universidade Federal de Pelotas / Sistema de Bibliotecas
Catalogação na Publicação

K13p Kaizer, Marina da Rosa

Partículas inorgânicas funcionalizadas e materiais restauradores híbridos em odontologia / Marina da Rosa Kaizer ; Rafael Ratto de Moraes, orientador ; Sergio da Silva Cava, coorientador. — Pelotas, 2015.

135 f. : il.

Tese (Doutorado) — Programa de Pós-Graduação em Materiais Odontológicos, Faculdade de Odontologia, Universidade Federal de Pelotas, 2015.

1. Cerâmicas. 2. Estética. 3. Materiais dentários. 4. Partículas. 5. Resinas compostas.. I. Moraes, Rafael Ratto de, orient. II. Cava, Sergio da Silva, coorient. III. Título.

Black : D151

Marina da Rosa Kaizer

Partículas inorgânicas funcionalizadas e materiais restauradores híbridos em
Odontologia

Tese aprovada, como requisito parcial, para obtenção do grau de doutor em Odontologia, Programa de Pós-Graduação em Odontologia, área de concentração Materiais Odontológicos, Faculdade de Odontologia da Universidade Federal de Pelotas.

Data da defesa: 12 de fevereiro de 2015.

Banca examinadora:

Prof. Dr. Rafael Ratto de Moraes (Orientador)
Doutor em Materiais Dentários pela Universidade Estadual de Campinas

Prof^a. Dr^a. Cristiane Wienke Raubach Ratmann
Doutora em Química pela Universidade Federal de São Carlos

Prof. Dr. Fabrício Aulo Ogliari
Doutor em Odontologia (Dentística) pela Universidade Federal de Pelotas

Prof^a. Dr^a. Márcia Borba
Doutora em Odontologia (Materiais Dentários) pela Universidade de São Paulo

Prof. Dr. Paulo Francisco Cesar
Doutor em Odontologia (Materiais Dentários) pela Universidade de São Paulo

Prof. Dr. Mateus Bertolini Fernandes dos Santos (suplente)
Doutor em Clínica Odontológica (Prótese Dentária) pela Universidade Estadual de Campinas

Prof^a. Dr^a. Tatiana Pereira Cenci (suplente)
Doutora em Clínica Odontológica (Prótese Dentária) pela Universidade Estadual de Campinas

Gostaria de dedicar este trabalho à minha mãe, Sonia da Rosa Kaizer, pelo amor e apoio incondicional, atemporal e onipresente. Mãe, tu és maior, melhor e mais forte que teus três filhos juntos! Se não fosse assim, nós três já não caberíamos mais em teu coração. Esta tese e este doutorado são para ti, e só o são por ti. E é por isso que todas as conquistas que virão não serão minhas se não forem tuas também, serão todas nossas! Mãe, te amo e muito obrigada!

Agradecimentos

Primeiramente gostaria de agradecer a Deus, que é por Sua graça que acordo a cada dia com saúde e disposição para novos desafios e conquistas. Que é por Seu amor que recebo tantas bênçãos na forma de experiências, oportunidades, pessoas... é através dessas bênçãos que sabedoria, força e fé me são somadas na construção de um caminho sempre de melhores escolhas e menores tropeços.

Gostaria também de agradecer à minha família, especialmente às pessoas que de forma muito próxima, carinhosa e paciente participaram dessa caminhada: obrigada mãe e tia Vê. Obrigada meus irmãos Gustavo e Maurício, meu sobrinho Pedrinho, e minhas cunhadas Jordana e Dalvane. Obrigada pai, queria muito que o senhor estivesse aqui, seu Pedro, para ver de pertinho o nosso sonho realizado.

Ao Prof. Rafael Ratto de Moraes, meu orientador, muito obrigada! Rafael te admiro imensamente e não poderia ser mais grata por teres acreditado em mim e investido na minha formação. Os aprendizados foram muitos, a parceria de trabalho e amizade estão firmadas e confirmadas.

A caminhada foi longa, são quatro anos com passagem por diversas instituições, presença de muitos mestres e colaboração e amizade de muitas pessoas, aos quais assim agradeço:

À Universidade Federal de Pelotas, à Faculdade de Odontologia, ao Curso de Engenharia de Materiais, ao Programa de Pós-Graduação em Odontologia, ao Programa de Pós-Graduação em Ciência e Engenharia dos Materiais e ao Centro de Desenvolvimento e Controle de Biomateriais. Minha formação de doutorado é desta casa e por ela muito me orgulho. Foram nestes programas de pós-graduação e instalações que aprendi muito, mas mais do que isso, foi aqui que muitas curiosidades e incertezas nasceram, e estas darão frutos durante minha carreira. Um agradecimento especial ao Prof. Sergio da Silva Cava, meu co-orientador, por ensinar uma dentista a ser uma cientista de materiais, aprendiz, mas apaixonada. Obrigada aos professores Fabrício Ogliari, Flávio Demarco, Maximiliano Cenci, Niek Opdam, Noéli Boscato e Tatiana Cenci por todas as oportunidades, conversas, ensinamentos e amizade.

Na UFPel fiz muitos amigos e parceiros de trabalho, mas dois grandes amigos me trouxeram para trabalhar nesta casa e foram especialmente presentes no meu doutoramento, meu muito obrigada à Prof. Patrícia Jardim e ao Prof. Alexandre Masotti. Meu carinho e sincero agradecimento àqueles que fizeram parte dessa jornada, mesmo antes dela iniciada, Anelise Montagner e Jovito Skupien; e também a todas as pessoas especiais que fui encontrando durante o caminho: Adauê Oliveira, Aline Oliveira-Ogliari, Cristina Isolan, Francine Madruga, Gabriela Basso, Lisia Valente, Mário Cruzeiro, Rafael Onofre, Tatiana Ramos, Tiago Delbrücke e tantos mais. Nesta casa também pude aprender a orientar, àqueles que me ensinaram a conduzir o aprendizado de iniciação científica e que hoje são amigos e colegas meu muito obrigada: Aldeci Junior, Ana Paula Gonçalves, Dener Soldati, Gabriela Schmitt, Júlia de Almeida, Luiz Otávio Reis e Roberta da Silva.

A segunda instituição na qual fui acolhida durante meu doutorado, e à qual dedico um agradecimento especial, é a Universidade de São Paulo, especialmente o Programa de Pós-Graduação em Biomateriais e Biologia Oral. Lá tive também um grande mestre, Prof. Paulo Francisco Cesar: muito obrigada pela acolhida, orientação e amizade. Ao Seu Antônio, Eli e Rosinha, pela ajuda e constante disposição e carinho, meu muito obrigada. Agradeço de coração a todos os amigos e parceiros de laboratório, em especial Carina Tanaka, Diego Manarão, Erick Lima, Karen Fukushima, Lucas Hian, Marcela Rodrigues, Ranulfo Miranda, Renata Medeiros e Tamara Tedesco.

Então logo veio o sanduíche, meu estágio e primeira experiência no exterior. I would like to show my gratitude to the New York University – College of Dentistry, the Biomaterials and Biomimetics Department, and the Graduate Program in Biomaterials for receiving me as visiting scholar, allowing me to teach and mentor graduate students, and for the whole experience that is a great part of my PhD training. I am specially thankful to my mentor, Dr. Yu Zhang, for believing and investing in my education and for caring for my personal and professional experiences during my stay in New York. I would also like to thank Dr. Dindo Mijares, Dr. Paulo Coelho, and Dr. Timothy Bromage for the valuable help with my work and all lessons during my internship at NYU. Many thanks to my dear friends and coworkers Anupama Kulkarni, Fatma Shembish, Haifa El Zahawi, Hui Tong, Mary Walczak, Moayed Krawa, Srikanth Ramanathan, and Shweta Saraswast. Living abroad can be tough, but there was always people willing to bear it with me and make

it somewhat easier, and for that I thank Champa Chonzom, Denise Lins, Jean Messner, Marco Aurelio Paschoal and Karine Santos. During my NY experience I met many special people and I can't list them all. But there are three more I have to thank, Nina, Dona Ana, and Chesed, you are special and humbling God blessings for my life and work.

Special thanks to Dr. Jason Griggs, who was always willing to attend my scientific presentations and posters in meetings and critically discuss my work, your help has been of great value in my career and education and in the thesis too.

Aos amigos da vida toda Bianca Santos, Cristano dos Santos, Loise Dresh, Pamela Diesel, Patricia Gindri and Sabrina Vexel, meu obrigada do fundo do coração. Vocês são minha inspiração e porto seguro. Saibam que amo vocês mesmo que não demostre com frequência.

Gostaria muito de agradecer ao Celaniro Junior, secretário do Programa de Pós-Graduação em Odontologia da UFPel, por estar sempre disposto a ajudar e fazê-lo com competência.

Agradecimentos por colaboração científica:

Ao Centro de Microscopia Eletrônica da Universidade Federal do Rio Grande, e às pessoas que lá trabalham, Rudimar, Erica e Caroline, pela importantíssima contribuição à finalização da minha tese.

Ao Instituto de Pesquisas Tecnológicas e ao Instituto de Química da USP, especialmente à Prof^a Catia Fredericci, o Prof. Flávio Vichi e o laboratorista Welber Neves, pela disponibilização das instalações e execução de análises importantes para a realização destes estudos.

To the Chemistry Department at New York University – USA. The Zeiss Merlin FESEM was acquired through the support of the National Science Foundation under Award Number DMR-0923251.

Agradeço ao CNPq – Conselho Nacional de Desenvolvimento Científico e Tecnológico, pelos seguintes auxílios financeiros: Processo 141129/2011-5 (Doutorado - GD); processo 241021/2012-0 (Sanduíche no exterior – SWE); e, processo 475462/2012-2 (Edital Universal).

Enfim, a realização do meu trabalho de doutorado não é minha conquista, é de todos aqui listados e também daqueles esquecidos. Muito obrigada!

*Eu sei que vou. Insisto na caminhada. O que não dá é pra
ficar parado. Se amanhã o que eu sonhei não for bem
aquilo, eu tiro um arco-íris da cartola. E refaço. Colo. Pinto
e bordo. Porque a força de dentro é maior. Maior que todo
mal que existe no mundo. Maior que todos os ventos
contrários. É maior porque é do bem. E nisso, sim, acredito
até o fim. O destino da felicidade, me foi traçado no berço.*

(CAIO FERNANDO ABREU)

Resumo

KAIZER, Marina da Rosa. **Partículas inorgânicas funcionalizadas e materiais restauradores híbridos em Odontologia**. 2015. 135f. Tese (Doutorado em Odontologia) - Programa de Pós-Graduação em Odontologia, Faculdade de Odontologia, Universidade Federal de Pelotas, Pelotas, 2015.

A maioria dos materiais restauradores odontológicos constitui-se de estruturas híbridas, nas quais uma fase de reforço tenaz coexiste com uma matriz mais complacente, de forma a obter-se um balanço entre propriedades estéticas e mecânicas. O reforço entre as duas fases somente é obtido por meio de uma interação interfacial efetiva. Desta forma, este estudo buscou: (1) Obter evidência de como os compósitos resinosos nanoparticulados, submicrométricos e microhíbridos, em uso em odontologia, reagem a procedimentos de polimento e envelhecimento por meio de uma revisão sistemática de estudos *in vitro*; (2) Desenvolver um método de recobrimento por sílica para nanopartículas cerâmicas cristalinas que não contém silício. O recobrimento foi obtido por imersão destas partículas em solução de TEOS, seguida de calcinação; e, (3) Aplicar partículas micrométricas de alumina policristalina nanoestruturada ou monocristalina translúcida, recobertas ou não por sílica, para modelar propriedades ópticas e mecânicas de uma porcelana feldspática no desenvolvimento de novos materiais restauradores híbridos porcelana-cerâmica processados por termoinjeção. Os estudos laboratoriais envolveram uma série de metodologias para caracterização dos tratamentos e materiais, incluindo microscopias eletrônicas de varredura e transmissão, mapeamento elementar por EDS, caracterização das fases cristalinas por DRX, análise por BET, análises de constantes elásticas e propriedades ópticas e análises mecânicas. Os resultados da revisão sistemática indicaram que não há evidência *in vitro* de que compósitos resinosos nanoparticulados e submicrométricos demonstram menor rugosidade e maior brilho que os compósitos microhíbridos tradicionais. Ainda, os compósitos resinosos estudados, em geral, fazem uso de partículas vítreas contendo silício como reforço da fase polimérica. Na segunda fase deste estudo observou-se que o método de recobrimento por sílica proposto resultou na deposição de uma camada de sílica na superfície das nanopartículas; ou ainda, na formação de aglomerados de nanopartículas envoltas em uma matriz de sílica. As partículas funcionalizadas demonstraram alta reatividade superficial, de forma que antecipam-se resultados promissores na sua interação interfacial com silanos ou porcelanas, ou mesmo na formação de estruturas porosas tridimensionais para materiais restauradores indiretos. O uso do método de recobrimento por sílica também mostrou-se efetivo com micropartículas de alumina na terceira fase deste estudo. Para estes experimentos, foram sintetizadas partículas nanoestruturadas de alumina policristalina pelo método dos precursores poliméricos. Estas partículas, bem como pó de alumina monocristalina (adquirido comercialmente), foram recobertos ou não por sílica e empregados na obtenção de materiais híbridos porcelana-cerâmica. As partículas policristalinas parecem funcionar como nanoaglomerados na matriz vítrea

dos materiais obtidos, apresentando deslocamento de nanocristais por fricção. Os materiais com adição de partículas monocristalinas foram consideravelmente mais translúcidos que os demais. O efeito de reforço da adição das partículas de alumina na matriz de porcelana não foi observado devido à porosidade presente nos materiais híbridos testados. A alta reatividade das partículas recobertas por sílica e a efetiva interação superficial entre porcelana e partículas recobertas, observadas neste estudo, são resultados promissores para o desenvolvimento de materiais restauradores híbridos reforçados por partículas cerâmicas cristalinas, com propriedades distintas e melhoradas em relação aos atuais materiais restauradores híbridos em uso em odontologia.

Palavras-chave:cerâmicas; estética; materiais dentários; partículas; porcelanas; propriedades mecânicas; resinas compostas.

Abstract

KAIZER, Marina da Rosa. **Functionalized inorganic particles and hybrid restorative materials in Dentistry**. 2015. 135p. Thesis (PhD in Dentistry) - Programa de Pós-Graduação em Odontologia, Faculdade de Odontologia, Universidade Federal de Pelotas, Pelotas, 2015.

Most dental restorative materials present hybrid structures, where a tough reinforcement phase coexists with a more compliant matrix, in order to exhibit a balance of aesthetic and mechanical properties. The reinforcement can only be achieved with an effective interfacial interaction between the two phases. Therefore, this study aimed to: (1) gather evidence on how nanofill, submicron, and microhybrid resin composites, currently used in dentistry, react to polishing and aging procedures by means of a systematic review of *in vitro* studies; (2) Develop a silica coating method for non-silicate crystalline ceramic nanoparticles. The proposed method was obtained by immersing the particles in TEOS solution, followed by calcination; and, (3) Evaluate the effect of the addition of alumina particles (nanostructured: polycrystalline or translucent: monocrystalline), with or without silica coating, on the optical and mechanical properties of feldspar-based porcelain. The laboratory studies involved a series of methodologies for characterization of the materials and treatments, including scanning and transmission electron microscopy, elemental mapping by EDS, characterization of crystalline phases by XRD, BET analysis, analysis of elastic constants and optical properties, and mechanical tests. The results of the systematic review indicated that there is no current *in vitro* evidence that nanofill or submicron resin composites show improved smoothness or gloss over traditional microhybrids. It was also observed that, in general, the resin composites evaluated in the systematic review have vitreous particles containing silicon as reinforcing phase for the polymer matrix. In the second phase of this study, the silica coating method proposed resulted in the deposition of a silica shell on the surface of the nanoparticles; or, yet in the clustering of nanoparticles embedded in a silica matrix. The functionalized particles showed a high surface reactivity, thus promising results are anticipated for the interfacial interaction of these particles with silanes or porcelain matrices, or in the building of 3D scaffolds for indirect restorative materials. The silica coating method was also proved effective with alumina microparticles in the third phase of this study. For these experiments, polycrystalline nanostructured alumina particles were synthesized by a polymeric precursors method. The polycrystalline particles, as well as a monocrystalline alumina powder acquired, were coated or not with silica and added to a feldspar-porcelain to produce porcelain-ceramic hybrid materials. The polycrystalline particles seemed to work as nanoclusters in the glass matrix of the hybrid material, showing dislodgment of nanocrystals caused by friction. The hybrid materials with addition of monocrystalline particles were considerably more translucent than the other hybrid materials. The effect of addition of alumina particles on the strength of the hybrid

materials was not clear due to the porosity observed. As observed in this study, the high surface reactivity of the silica coated particles, as well as the effective interfacial interaction between porcelain and coated particles are promising results for the development of novel and improved hybrid restorative dental materials reinforced with non-silicate crystalline ceramic particles.

Key-words: aesthetics; ceramics; dental materials; mechanical properties; particles; porcelains; resin composites.

Sumário

1	Introdução	14
2	Capítulo 1	16
3	Capítulo 2	71
4	Capítulo 3	86
5	Considerações finais.....	113
	Referências	115
	Anexo	131

Notas preliminares

A presente tese foi redigida segundo o Manual de Normas para trabalhos acadêmicos da UFPel, adotando o nível de descrição em capítulos não convencionais. Disponível no endereço eletrônico:

http://sisbi.ufpel.edu.br/arquivos/PDF/Manual_Normas_UFPel_trabalhos_acad%C3%AAmicos.pdf

O projeto de pesquisa que originou esta tese foi apresentado em 10 de Maio de 2012 e aprovado pela Banca Examinadora composta pelos Professores Doutores Rafael Ratto de Moraes, César Antonio OropesaAvellaneda e Tatiana Pereira Cenci.

1 Introdução

As duas grandes classes de materiais restauradores na odontologia atualmente são as cerâmicas e os compósitos resinosos. Materiais dessas classes apresentam desempenho mecânico e clínico satisfatórios respeitadas suas indicações (DA ROSA RODOLPHO et al, 2012, LARSSON; WENNERBERG, 2014, OZER et al, 2014). Enquanto restaurações cerâmicas apresentam melhor adaptação marginal, forma anatômica e estabilidade de cor (LANGE; PFEIFFER, 2009), estes são materiais intrinsecamente frágeis, propensos a fraturas e lascamento quando em função (RAIGRODSKI et al, 2007). Por outro lado, compósitos resinosos podem ser indicados para aplicações diretas e indiretas (JOHNSON et al, 2014) e suas restaurações são de fácil reparo; ainda, tendem a não promover desgaste do dente antagonista (GIORDANO, 2006; MIYAZAKI et al, 2009).

A classe dos compósitos resinosos abrange materiais híbridos compostos de distintas fases: uma matriz orgânica polimérica que é reforçada por partículas vítreas/cerâmicas (KAIZER et al, 2014), ou por uma estrutura porosa tridimensional cerâmica (DELLA BONA; CORAZZA; ZHANG, 2014). Assim como na classe dos compósitos resinosos, a grande maioria dos sistemas cerâmicos odontológicos são materiais híbridos, nos quais uma fase cerâmica vítrea coexiste com uma ou mais fases cerâmicas cristalinas (DENRY; KELLY, 2014). O reforço entre as duas fases somente é obtido por meio de uma interação interfacial efetiva. Para que isso ocorra é necessário que as fases sejam quimicamente compatíveis ou que exista outro material entre as superfícies para fazer a interação entre estas. Neste contexto, cerâmicas cristalinas comumente usadas em odontologia, embora apresentem propriedades mecânicas superiores a cerâmicas vítreas (DENRY; KELLY, 2014), usualmente não apresentam silício em sua composição (THOMPSON et al, 2011). Dessa forma, não são silanizáveis para adequada interação com a matriz polimérica de compósitos resinosos, tão pouco são propícias a uma efetiva interação interfacial com a matriz cerâmica vítrea das porcelanas odontológicas.

Para compósitos resinosos em uso em odontologia, o reforço por partículas cerâmicas cristalinas que não contêm silício é um desafio, e a única estratégia efetivamente viável para contornar isso disponível até o momento é o método de agregação de nanopartículas de sílica e zircônia (MITRA; WU; HOLMES, 2003). Apesar de efetivo, este método envolve interferência química com as partículas durante sua síntese, de forma que não é aplicável para a modificação de pós cerâmicos cristalinos já sintetizados. Ainda, esta tecnologia é protegida por patente, e desde sua publicação, seu uso é limitado a nanopartículas de zircônia. Também para materiais híbridos cerâmicos, zircônia é o único tipo de partícula cristalina sem silício empregada no reforço de materiais comercialmente disponíveis: Vita Suprinity (VITA Zahnfabrik, Bad Säckingen, Alemanha) e Celtra DeguDent (DeguDent, Hanau, Alemanha). Apesar do atual interesse em zircônia no campo dos materiais restauradores dentais, a viabilização do uso de toda e qualquer partícula cerâmica cristalina sem silício como fase de reforço de materiais restauradores híbridos ampliaria o campo para investigação, desenvolvimento e aprimoramento destes materiais.

Em vista do vasto campo abrangido pela classificação “materiais restauradores híbridos em Odontologia”, e do exposto anteriormente, os objetivos da presente tese de doutorado são:

- Buscar evidência na literatura, por meio de uma revisão sistemática de estudos *in vitro*, de como compósitos resinosos nanoparticulados e submicrométricos, comparados aos compósitos microhíbridos, reagem a procedimentos de polimento e envelhecimento;
- Desenvolver e caracterizar um método de recobrimento por sílica para nanopartículas cerâmicas cristalinas, de forma que estas tornem-se silanizáveis para uso em compósitos resinosos, bem como apresentem superfície quimicamente compatível para indicação como fase de reforço de porcelanas; e
- Aplicar partículas de alumina policristalina nanoestruturada ou monocristalina micrométricas para modelar propriedades ópticas e mecânicas de uma porcelana feldspática, bem como de recobrimento das partículas por sílica, com o propósito de obter interação interfacial das partículas de alumina com a matriz de porcelana no desenvolvimento de novos materiais híbridos restauradores.

2Capítulo 1

Do nanofill or submicron composites show improved smoothness and gloss? A systematic review of *in vitro* studies¹

Marina R. Kaizer^a, Aline de Oliveira-Ogliari^a, Maximiliano S. Cenci^a, Niek J.M. Opdam^b, Rafael R. Moraes^a

^a Graduate Program in Dentistry, Federal University of Pelotas, Brazil

^b Radboud University Nijmegen Medical Centre, Nijmegen, The Netherlands

Corresponding author:

Prof. Rafael Moraes

School of Dentistry, Federal University of Pelotas

Rua Gonçalves Chaves 457, room 505

96015-560, Pelotas-RS, Brazil

Tel/Fax: 55 53 3225.6741 ext. 135 (moraesrr@gmail.com)

¹ Artigo publicado no periódico *Dental Materials*(FI JCR 2013: 4.16), sendo aqui apresentado com estrutura conforme normas do referido periódico. A licença de uso do texto completo do artigo, cujos direitos autorais pertencem à editora Elsevier, consta no Anexo A.
DOI: <http://dx.doi.org/10.1016/j.dental.2014.01.001>

2.1 Abstract

Objectives: Despite nanofill and submicron composites' aim to provide high initial polishing combined with superior smoothness and gloss retention, the question still remains whether clinicians should consider using these new materials over traditional microhybrids. The aim of this paper was to systematically review the literature on how nanofills and submicrons react to polishing procedures and surface challenges in vitro compared with microhybrids. The paper has also given an overview of the compositional characteristics of all resin composites and polishing systems whose performance was presented herein.

Data: The database search for the effect of filler size on surface smoothness and gloss of commercial composites retrieved 702 eligible studies. After deduplication, 438 records were examined by the titles and abstracts; 400 studies were excluded and 38 articles were assessed for full-text reading. An additional 11 papers were selected by hand-searching. In total, 28 articles met inclusion criteria and were included in the study.

Sources: The databases analyzed were MEDLINE/PubMed, ISI Web of Science, and SciVerse Scopus.

Study selection: Papers were selected if they presented a comparison between nanofill or submicron and microhybrid composites with quantitative analysis of smoothness and/or gloss on baseline and/or after any aging protocol to assess smoothness and gloss retention. Only in vitro studies written in English were included.

Conclusions: There is no in vitro evidence to support the choice for nanofill or submicron composites over traditional microhybrids based on better surface smoothness and/or gloss, or based upon maintenance of those superficial characteristics after surface challenges.

Keywords: aging; finishing/polishing; gloss; nanofill composites; submicron composites; surface challenge; surface roughness; surface smoothness.

2.2 Introduction

Resin-based composites have been used extensively as direct dental restorative materials due to their good esthetic properties and long-lasting clinical performance. Several industry manufacturers offer a wide range of resin composite materials for use in both anterior and posterior areas. Current differences among materials are mainly related to their inorganic filler components, which might affect their handling characteristics [1] and physical properties [2, 3], ultimately influencing the clinical service of restorations [4, 5]. It is known that well-dispersed inorganic particles in a resin matrix effectively improve the polymer strength [6]. Therefore, dental composites have usually been classified according to their filler characteristics, especially particle size.

Numerous adjustments in filler characteristics – most recently, the introduction of nano- and submicron-sized particles – have been proposed in an endeavor to provide a material with high initial polishing combined with superior polish and gloss retention. It is a general belief that smaller filler particles protect the softer resin phase from wear and reduce surface alterations resulting from loss of particles. The size of the fillers is usually ascribed to having a significant impact on composites' surface properties, such as smoothness and gloss [7, 8]. In the same way, appearance and surface luster are often related to clinical performance of restorations, especially in anterior teeth. There is no clinical evidence, however, that nanofill or submicron restoratives show better performance compared to microhybrids regarding restorations' esthetic and surface qualities.

Despite manufacturers' efforts in development and marketing of new materials, the question still remains whether clinicians should consider using nanofill or submicron composites over traditional microhybrids. This question cannot be indisputably answered based on the scarce clinical evidence available; however, in vitro evaluations on the surface characteristics of nanofill and submicron resin-based restoratives are abundant in the literature. Several studies have addressed the effects that challenges such as toothbrushing, thermal cycling, or pH cycling may have on the surface properties of composites. In vitro investigations have the shortcoming of employing different finishing and/or polishing procedures, or distinct methods to evaluate surface properties of the composites, sometimes hindering comparisons among studies or materials.

The aim of this study was to systematically review the literature to gather information on how nanofill and submicron dental composites react to finishing/polishing procedures and surface challenges in vitro, compared with traditional microhybrids regarding surface characteristics. The hypothesis tested was that there is no laboratory evidence to support the choice of nanofill or submicron composites over traditional microhybrid materials based upon better performance regarding surface properties.

2.3 Methods

This systematic review was conducted in accordance with the guidelines of Transparent Reporting of Systematic Reviews and Meta-Analyses [9]. The research question was: Do nanofill or submicron resin composites attain and maintain improved smoothness and gloss in comparison to microhybrid materials?

2.3.1 Search strategy

Three online international scientific databases were used to search for appropriate articles that satisfied the study purposes: National Library of Medicine (MEDLINE/PubMed), ISI Web of Science, and SciVerse Scopus. The databases were searched for studies conducted in the period up to and including August 1, 2012. The structured search strategy was designed to include any published papers that evaluated the effect of filler size on surface smoothness and gloss of commercially available resin composites. The following detailed search terms were used:

- PubMed: (nanofill* OR nanostructure* OR nanocomposite* OR nanoparticle* OR nanoscale* OR submicron*) AND (hybrid* OR microhybrid* OR nanohybrid*) AND (rough* OR smooth* OR luster* OR gloss* OR polish*) AND (resin* OR composite* OR restorative*)
- ISI Web of Science and SciVerse Scopus: (nano* OR submicron*) AND (microhybrid* OR hybrid*) AND (rough* OR smooth* OR luster* OR gloss* OR polish*) AND (resin* OR composite* OR restorative*)

2.3.2 Eligibility criteria

The following eligibility criteria were used:

- Type of studies: in vitro;
- Language: papers written in English;
- Intervention: comparison between nanofill or submicron and microhybrid resin composites;
- Outcomes: quantitative measures of smoothness and/or gloss on baseline and/or after any aging protocol (to assess retention of smoothness and gloss).

Classification of the composites was based on the size range of the particles: nanofills (particle size up to 100 nm), submicrons (particle size between 0.1 and 0.9 μm), and microhybrids (maximum particle size between 1 and 10 μm) [10, 11].

2.3.3 Screening and selection

Two reviewers (A.O.O. and M.R.K.) independently screened titles and abstracts for eligible papers. Whenever information relevant to the eligibility criteria was unavailable in the abstract or if the abstract itself was unavailable, the article was selected for full-text reading. Papers that fulfilled the eligibility criteria were included in the study. The reviewers hand-searched the reference lists of included articles for additional papers. Papers that fulfilled the selection criteria were processed for data extraction. Heterogeneity across the studies was detailed according to the following factors:

- Smoothness: type of polishing system, type of method used to measure the outcome, materials tested, surface challenge protocol (when applicable);
- Gloss: type of polishing system, angle of analysis, materials tested, surface challenge protocol (when applicable).

2.3.4 Data extraction

Data were extracted with regard to smoothness (baseline and post-challenge values, when applicable) and/or gloss (baseline and post-challenge values, when applicable) of nanofill and submicron resin composites compared with microhybrids. Baseline and final evaluation data were used for studies presenting intermediate assessments. Average values and standard deviations were extracted independently by two reviewers (A.O.O. and M.R.K.).

2.3.5 Data analysis

Considerable heterogeneity was present in the selected studies regarding the research design, methods used, outcome variables, and results. Since meta-analysis was considered inappropriate, a descriptive presentation of difference in means was used. Any disagreement between the two reviewers (A.O.O. and M.R.K.) was resolved after additional discussion or after judgment by a third reviewer (R.R.M.).

2.4 Results

2.4.1 Search and selection

The search resulted in 438 unique papers, as shown in Figure 2.1. The screening of titles and abstracts initially resulted in 38 full-text articles. Eleven papers were found by hand-searching. In total, 21 papers were excluded after a full-text reading for the following reasons: 10 studies did not provide statistical comparisons among the materials tested [8, 12-20]; 3 studies did not provide statistical comparisons among the materials tested separately according to the polishing systems applied [21-23]; 3 studies presented initial roughness values only after surface treatments [24-26]; 5 studies did not describe sufficiently their statistical results or tests [27-31].

In total, 28 papers were identified as eligible for inclusion in this review and were processed for assessment of heterogeneity and data extraction. Not all data presented by these 28 papers were included in the present review, mainly because some data did not meet the scope of the study or inclusion criteria. Data regarding materials not classified as microhybrid, submicron, or nanofill composites were not considered (e.g., macrofills or microfills). Data regarding smoothness from da Costa et al. [32] were not considered as there were no statistical comparisons among the materials separately for each polishing system; however, this paper was included because the gloss data met the inclusion criteria. Data regarding smoothness of the control group of Ergücü & Türkün [33] were not considered as there were no statistical comparisons among the composites; this paper was included because data of the other groups met the inclusion criteria. Smoothness data of the test groups of Attar [34] were not included as there were no statistical comparisons among the composites separately for each polishing system; this paper was included because data of the control group met the inclusion criteria. Three papers were not included in

the polish retention analyses as comparisons among the materials regarding final roughness values were lacking [35-37]; these 3 papers presented statistical comparisons required to be included in the baseline smoothness analysis. Finally, the gloss values from Kakaboura et al. [38] were not presented in the paper, but smoothness data met the inclusion criteria. Tables 2.1 and 2.2 present the formulation of the resin composites and finishing/polishing systems tested in the studies selected, as gathered from papers published in the literature or from manufacturers' information.

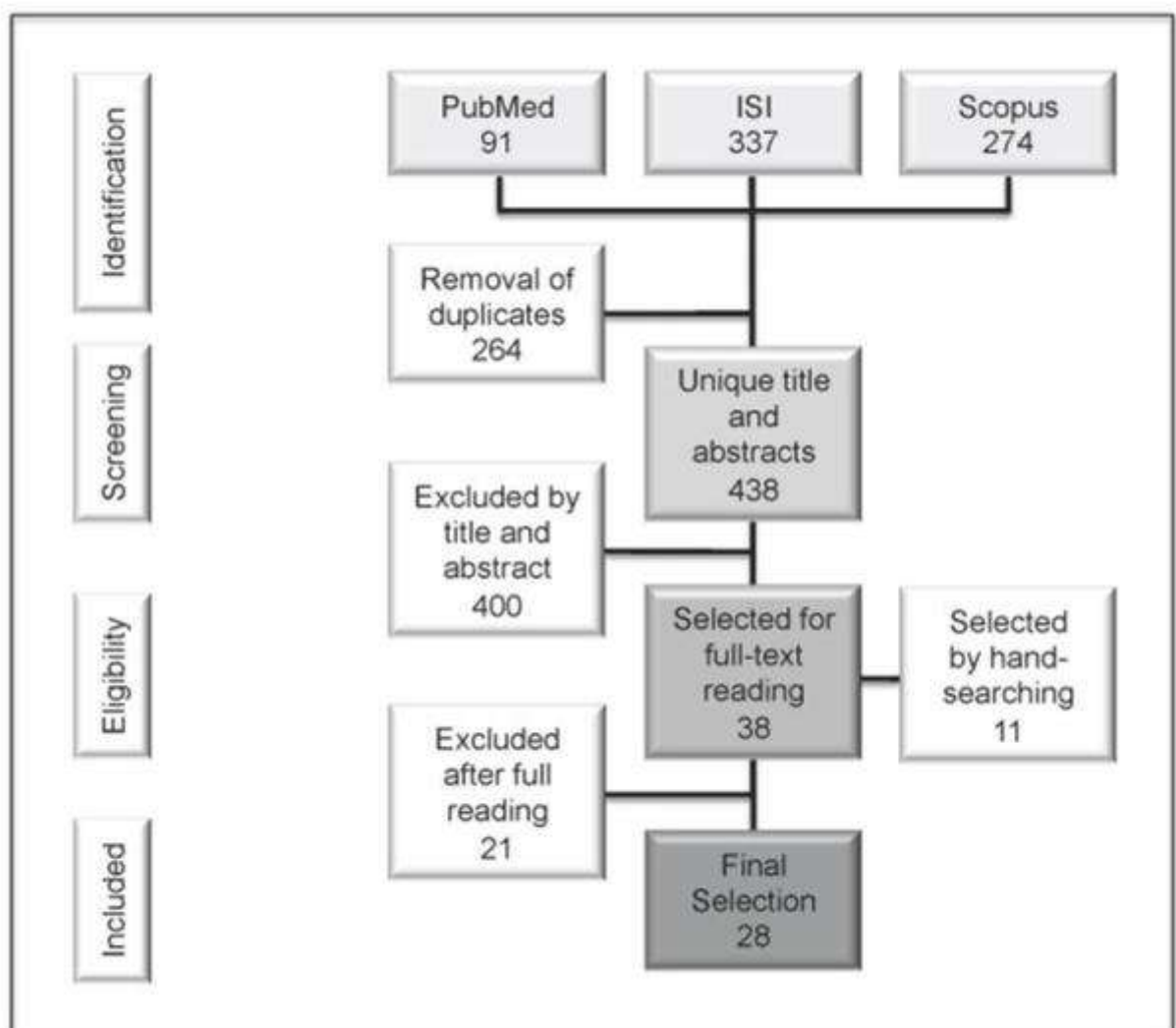


Figure 2.1– Flow diagram of the systematic review.

Table 2.1 - Resin composites evaluated in the included studies

Resin composite	Manufacturer	Classification	Filler load (wt%)	Filler type	Average particle size	Particle size range
Admira	Voco, Anton-Flettner, Cuxhaven, Germany	Microhybrid	78	Barium-Aluminium-Fluoro-Silicate [53]	0.7 µm	0.04 - 1.2 µm [54]
				Silica [53]		
Aelite Aesthetic Enamel	Bisco, Schaumburg, IL, USA	Microhybrid	73	Glass filler	0.7 µm [48]	0.04 - 5.0 µm
				Amorphous silica	0.04 µm [48]	
Artemis	Ivoclar Vivadent AG, Schaan, Liechtenstein	Microhybrid	75 - 77	Barium glass	0.6 µm	0.04 - 3.0 µm
				Ytterbium trifluoride		
				Barium-Aluminium-fluoro-silicate glass		
				Silica		
				Spheroid mixed oxide		
Beautifil II	Shofu, Kyoto, Japan	Microhybrid	83.3	Alumino fluoro-borosilicate glass	0.8 µm	0.01 - 4 µm
				Alumina		
Ceram•X	Dentsply/Caulk, Milford, DE, USA	Microhybrid	76 - 75	Barium-aluminium-borosilicate glass	1.1 - 1.5 µm	n.i.
				Silica	10 nm	n.i.
				Organically modified ceramic	2 - 3 nm	n.i.
Clearfil Majesty	Kuraray Noritake Dental, Kurashiki, Okayama, Japan	Microhybrid	78 [55]	Barium glass	0.7 µm [55]	0.37 - 1.5 µm
				Prepolymer	n.i.	n.i.
Concept Advanced	Vigodent, RJ, Brazil	Microhybrid	77.5 [56]	Barium-Aluminium-silicate glass [56]	n.i.	0.01 - 2 µm [56]
				Silica [56]		
Concept Advanced Magic Kids	Vigodent	Microhybrid	67 (v)* [37]	Barium-Aluminium-silicate glass [37]	0.4 µm [37]	n.i.
Enamel Plus HFO	Micerium - GDF, Rosbach, Germany	Microhybrid	75	Glass filler	0.7 µm	n.i.
				Silica	0.04 µm	n.i.
Estelite Σ	Tokuyama, Taitou-ku, Tokyo, Japan	Submicron	82	Silica-zirconia	0.2 µm	0.1 - 0.3 µm
Estelite Σ Quick	Tokuyama	Submicron	82 [55]	Silica-zirconia	0.2 µm	0.1 - 0.3 µm**
Esthet-X	Dentsply DeTrey,	Microhybrid	73.3 [53]	Barium fluoro alumino silicate glass	1 µm	0.02 - 2.5 µm [57]

	Konstanz, Germany			Silica	0.04 µm	10 - 20 nm [57]
Filtek P60	3M ESPE, St. Paul, MN, USA	Microhybrid	78.8 [53]	Zirconia-silica	0.6 µm	0.01 - 3.5 µm
Filtek Supreme	3M ESPE	Nanofill	78.5	Silica	20 nm	n.i.
				Zirconia-silica clusters	n.i.	0.6 - 1.4 µm
Filtek Supreme Plus	3M ESPE	Nanofill	78.5	Silica	20 nm	n.i.
				Zirconia-silica clusters	n.i.	0.6 - 1.4 µm
Filtek Supreme XT	3M ESPE	Nanofill	78.5	Silica	20 nm	n.i.
				Zirconia-silica clusters	n.i.	0.6 - 1.4 µm
Filtek Z100	3M ESPE	Microhybrid	85	Zirconia-silica	n.i.	0.01 - 3.5 µm
Filtek Z250	3M ESPE	Microhybrid	77.5 [53]	Zirconia-silica	0.6 µm	0.01 - 3.5 µm
Filtek Z350	3M ESPE	Nanofill	78.5	Silica	20 nm	n.i.
				Zirconia-silica clusters	n.i.	0.6 - 1.4 µm
Gradia Direct	GC America, Alsip, IL, USA	Microhybrid	77 [57]	Fluoro alumino silicate glass	0.85 µm [58]	n.i.
				Silica		
				Prepolymer	n.i.	n.i.
Grandio	Voco	Microhybrid	87	Glass-ceramic	1 µm [59]	0,1 - 2,5 µm [60]
				Silica	20 - 60 nm [59]	20 - 60 nm [60]
Herculite XRV	Kerr, Orange, CA, USA	Microhybrid	79 [61]	Aluminium-Boro-Silicate glass [61]	0.6 µm [62]	0.75 - 1.25 µm [63]
				Silica [61]		0.3 - 0.5 µm [63]
Micronew	Bisco	Microhybrid	72	Strontium alumino silicate glass [38]	0.5 µm [38]	0.04 - 7 µm [64]
				Silica [38]		
Miris	Coltène Whaledent, Altstätten, Switzerland	Microhybrid	80	Barium glass	0.6 µm	0.02 - 2.5 µm
				Silica		
Opallis	FGM - Dentscare, Joinville, SC, Brazil	Microhybrid	79.8	Barium-aluminum	0.5 µm	40 nm - 3.0 µm
				Silicate		
				Silica		
Palfique Estelite	Tokuyama	Submicron	82	Silica-zirconia	0.2 µm [47]	0.08 - 0.4 µm***
Point 4	Kerr	Microhybrid	76	Silica [38]	0.4 µm	n.i.
				Barium Aluminium-Silicate [38]		n.i.

Premise	Kerr	Microhybrid	84	Barium glass	0.4 µm	Max. 1.25 µm [63]
				Silica	0.04 µm	
				Prepolymer	30 - 50 µm	
Prisma AP.H	Dentsply/Caulk	Microhybrid	77.5 [65]	Barium boro-alumino silicate glass	n.i.	2.0 - 3.5 µm [63]
				Silica	n.i.	0.5 - 1.0 µm [63]
Simile	Pentron Clinical, Orange, CA, USA	Microhybrid	75 [66]	Barium boro-alumino silicate glass	0.6 - 0.7 µm [52]	n.i.
				Silica	20 - 40 nm [52]	
				Zirconium silicate	5 -20 nm [66]	
Synergy D6	Coltène Whaledent	Microhybrid	80	Barium glass	0.6 µm	0.02 - 2.5 µm
				Silica		
Synergy Duo	Coltène Whaledent	Microhybrid	77	Barium glass	0.6 µm	0.04 - 2.9 µm
				Silica		
Tetric Ceram	Ivoclar North America, Amherst, NY, USA	Microhybrid	74.7 [53]	Silica	0.7 µm [53]	0,04 - 3 µm [48]
				Barium-Aluminium-fluorsilicate glass		
				Barium glass		
Tetric EvoCeram	Ivoclar North America	Microhybrid	82 - 83	Barium glass	5.5 µm	40 - 3000 nm
				Ytterbium trifluoride		
				Mixed oxide		
				Prepolymer	n.i.	0.4 - 3 µm [57]
TPH 3	Dentsply/Caulk	Microhybrid	73 [67]	Barium alumino boro silicate glass	1 µm	Max. 4.0 µm [63]
				Barium fluoro alumino silicate glass		
				Silica	10 - 20 nm	
TPH spectrum	Dentsply/Caulk	Microhybrid	77 [34]	Barium alumino boro silicate glass	1 µm	0.04 - 5 µm [68]
				Silica	0.04 µm	
Venus	Heraeus Kulzer, Hanau, Germany	Microhybrid	73.3 [69]	Barium aluminium fluoride glass	0.7 µm	0.7 - 2 µm [48]
				Silica	0.04 µm	
Vit-I-escence	Ultradent, South Jordan, UT, USA	Microhybrid	75	Barium alumina silicate [70]	0.7 µm	n.i.

* Filler load by weight not found.

** Estelite Σ Quick technical report, provided by Tokuyama, informs that this materials has the same filler composition of Estelite Σ.

*** Information regarding proprietary spherical filler particle used by Tokuyama.

n.i. = not informed: information regarding average abrasive particle size was not found in the scientific literature or manufacturer's informative or technical publications.

Most of the data presented herein were collected from manufacturer's technical or informative publications. When the data required were not found in manufacturer's publications, it was gathered from the scientific literature according to the citations presented within the table.

Table 2.2 - Polishing systems used in the included studies

Polishing system	Manufacturer	Description	Average abrasive particle size
Astrobrush	Ivoclar Vivadent AG	Bristles made of polyamide with silicon carbide incorporated as the abrasive medium	n.i.
Astropol	Ivoclar Vivadent AG	Astropol F - Finishing: silicon rubber and silicon carbide particles	Grey - 45 µm [71]
		Astropol P - Polishing: silicon rubber and silicon carbide particles	Green - 1 µm [71]
		Astropol HP - High gloss polishing: silicon rubber, diamond particles, alumina, titania and iron oxide	Dusky pink - 0.3 µm [71]
Carbide bur	Diatech Dental AC, Heerbrugg, Switzerland	# CF 379-018, tungsten carbide [72]	30-fluted [72]
	KG Sorensen, Barueri, SP, Brazil	# 284, cylindrical with ogive top, 10.4 mm active point [43]	30 blades [43]
	Edenta AG, 9434 Au/SG, Switzerland	Edenta CH, tungsten carbide finishing burs [59]	16-fluted [59]
ComposiPro Diacomp	Brasseler USA, Savannah, GA	Diamond impregnated knife [32]	Green - 20 µm [32]
			Grey - 5 µm [32]
ComposiPro one-step brush	Brasseler USA	Silicon-carbide particles brush [32]	n.i.
Compo System	Komet - Gebr. Brasseler, Lengo, Germany	Transparent discs with honey-comb alumina coating on both sides	Blue - 50 µm
			Red - 30 µm
			White - 5 µm
Diamond bur	Diatech Dental AC	# 859-014, extra-fine diamond [72]	n.i.
	KG Sorensenl	# 4219FF, cylindrical with ogive top, extra-fine granules, 10 mm active point [43]	30 µm [43]
	MDT Dental, Afula, Israel	# 859/014XF, extra-fine diamond finishing bur [59]	n.i.
Diamond Excel	FGM - Dentscare	Paste with micronized diamond, lubricant base, thickener and emulsifier	2 - 4 µm
Diamond Flex	FGM - Dentscare	Polyester disc, adhesive, micro polyester bristles and silicone rubber	n.a.
Diamond Pro	FGM - Dentscare	Polyester disc, adhesive, abrasive (four grit) and silicone rubber	130 - 3 µm [41]
Edenta AG	Edenta AG	Extra-fine diamond finishing bur [59]	n.i.
		Arkansas stone [59]	n.i.
		Yellow rubber [59]	n.i.
Enamelize	Cosmedent, Chicago, IL, USA	Alumina paste [32]	1.5 µm [32]

Enhance	Dentsply/Caulk	Polymerized urethane dimethacrylate resin, alumina, silica	40 µm [73]
Enhance Flex NST	Dentsply/Caulk	Alumina [46]	40 - 100 / 40 - 60 µm [46]
		Diamond-silica [46]	1 µm (diamond), nanoscale silica [46]
EP Esthetic Polishing System	Brasseler USA	Silicon carbide coated discs	Coarse (manual)
			Medium - 40 µm [63]
		Alumina coated discs	Fine - 28 µm [63]
			Super fine - 12 µm [63]
EXL-695	3M ESPE	Proprietary abrasives [45]	n.i.
Hiluster Plus System	KerrHawe, Bioggio, Switzerland	GlossPlus - alumina particle-integrated polishers [58]	10 µm [58]
		HilusterPlus - diamond particle-integrated polishers [58]	5 µm [58]
Jiffy polishers	Ultradent	Silica impregnated disc [32]	Green - 40 µm [32]
			Yellow - 30 µm [32]
			White - 5 µm [32]
One Gloss	Shofu	Synthetic rubber (Polyvinylsiloxane), abrasive grain (Alumina), silica [33]	n.i.
OptraPol	Ivoclar Vivadent AG	Caoutchouc, silicon carbide, alumina, titania and iron oxide	12 µm [74]
PoGo	Dentsply/Caulk	Polymerized urethane dimethacrylate resin, fine diamond powder, silica	20 [74]
Poli-Pro Disks	Premier, Northeast Philadelphia, PA, USA	Alumina coated discs [58]	Medium - 40 µm
			Fine - 30 µm
			Extra-fine - 9 µm
Sof-Lex	3M ESPE	Cured urethane backing, alumina grit and binder, paper	Coarse - 100 µm [71]
			Medium - 40 µm [71]
			Fine - 24 µm [71]
			Extra-fine - 8 µm [71]
Sof-Lex Brushes	3M ESPE	Brushes made from thermoplastic polyester elastomer impregnated with alumina abrasive particles	n.i.
Sof-Lex PoP-On	3M ESPE	Alumina disc [75]	Medium - 40 µm [75]
			Fine - 24 µm [75]
			Extra-fine - 8 µm [75]
Sof-Lex XT	3M ESPE	Polyester film, alumina grit and binder	Dark-orange - Coarse
			Orange - Medium

			Light-orange - Fine
			Yellow - Superfine
Super-snap	Shofu Dental Corp., California, USA	Alumina coated disc system [72]	Green - Fine
			Red - Superfine

n.i. = not informed: information regarding average abrasive particle size was not found in the scientific literature or manufacture's informative or technical publications.

n.a. = not applicable: the polishing system Diamond Flex consists on felt discs with no abrasive particles.

Most of the data presented herein were collected from manufacturer's technical or informative publications. When the data required were not found in manufacturer's publications, it was gathered from the scientific literature according to the citations presented within the table.

2.4.2 Outcomes

Description of the outcomes was based on the results of comparisons; by “comparison” we mean each particular contrast among materials using a different polishing system, method of analysis, or aging process, regardless if those were presented within the same study or in distinct papers. Three possible results were considered when comparing nanofills versus microhybrids: (1) better – all nanofills performed better than all microhybrids tested in the same comparison; (2) poorer – at least one nanofill performed poorer than at least one microhybrid in the same comparison; (3) not different – at least one nanofill tested performed similarly to at least one microhybrid, and no nanofill performed poorer than a microhybrid material in the same comparison. The same situations were considered when comparing submicrons versus microhybrids and nanofills versus submicrons.

2.4.2.1 Initial surface smoothness based on polishing system

In total, 69 initial smoothness comparisons reported in 25 papers were analyzed (Table 2.3). About 60% of those comparisons showed no significant differences among microhybrids and nanofills or submicrons, and around 20% of the comparisons showed better results for the nanofill or submicron materials. Positive results for the nanofills were presented by 6 papers and included 3 different smoothness analyses and 10 finishing methods; they reported 11 microhybrids to be rougher than the nanofills tested. From those 11 composites, 8 had similar or better smoothness to nanofills in other comparisons, and the remaining 3 were tested only once or twice. Poorer results for nanofills compared to microhybrids were found in 11 comparisons from 8 papers, and they included 3 different smoothness analyses and 6 finishing methods. They reported 11 microhybrids as smoother than the nanofills tested. From those 11 composites, 10 had similar or poorer smoothness than did the nanofills in other comparisons.

Four variations of nanofill composites were tested. Filtek Supreme Plus was compared 9 times and was always similar to at least one of the microhybrids tested in the same study. Filtek Supreme XT was compared 35 times and presented varied results in relation to microhybrids. In 63% of the comparisons, Filtek Supreme XT was not different from the microhybrids, whereas it performed better than microhybrids in 11% and poorer in 26% of the comparisons. Filtek Supreme was compared 18 times; it was not different from microhybrids in 56% of the comparisons

and performed better in 44% of the comparisons. Filtek Z350 was tested 5 times and was found similar to microhybrids in 80% of the tests, while it performed better than microhybrids in only 1 comparison. Comparing nanofill and submicron materials, there were 5 comparisons, with 2 of them presenting better results for the submicrons and 3 comparisons showing no significant differences. Ten comparisons between submicron and microhybrid composites were analyzed; submicrons were smoother in 5 comparisons and rougher in 1 comparison. No differences were observed in the other 4 comparisons.

With 69 comparisons among materials, 47 were performed with a rugosimeter, 12 with an atomic force microscope (AFM), 4 with a laser profilometer, 3 with an optical profilometer, and 3 with a laser scanning microscope. Considering the most-used methods for analyzing smoothness – rugosimeter, AFM, and laser profilometer – more than 60% of the comparisons showed no significant differences between nanofills and microhybrids. Better results for the nanofills were observed in ~17% of comparisons made with a rugosimeter or AFM. Laser profilometer was used 4 times, and no differences were found between nanofills and microhybrids in any of those. However, when an optical profilometer was used for analyzing smoothness, nanofills performed better twice and poorer once. The laser scanning microscope was used only in comparisons between submicrons and microhybrids, and it was observed that submicrons were always smoother.

Regarding the surface finishing/polishing protocols before testing, the methods mostly used were Sof-Lex discs (13), polyester matrix (11), carbide bur+polishing system (8), diamond bur+polishing system (5), and SiC abrasive papers (7). When Sof-Lex discs were used, ~61% of comparisons indicated no significant differences between nanofills or submicrons and microhybrids, while ~23% indicated better results for nanofills or submicrons, and ~15% indicated better results for microhybrids. When polyester matrix was used, 55% of the comparisons showed no significant differences among the materials, 36% showed poorer results for nanofills, and 9% showed better results for nanofills. For the use of carbide bur+polishing system, ~63% showed no significant differences, 25% indicated better results for nanofills, and ~12% showed poorer results for nanofills. When the combination of diamond bur+polishing system was employed, 40% of the comparisons showed similar results for nanofills and microhybrids, 40% showed better results for nanofills, and 20% showed poorer results for nanofills. For SiC papers, there were 4

comparisons for nanofills and microhybrids; 3 indicated no significant differences, while 1 indicated better results for nanofills. Three comparisons for submicrons and microhybrids were performed with SiC papers as the finishing method; all showed better results for submicrons.

Table 2.3 - Baseline smoothness measurements according to the different polishing systems used

Polishing system	Author	Method of analysis	N	Material	Roughness (Ra, μm)	Conclusion
Astropol	Antonson et al., 2011 [45]	Laser Profilometer	5	Filtek Supreme Plus	0.13 (0.03)	There were no differences among the materials tested.
				Esthet-X	0.12 (0.02)	
	Senawongse & Pongprueksa, 2007 [71]	Rugosimeter	10	Filtek Supreme XT (dentin shade)	0.038 (0.009)	Nanofills together with the submicron composite and three microhybrids (Premise, Filtek Z250 and Tetric Ceram) presented the lowest roughness values.
				Filtek Supreme XT (transparent shade)	0.038 (0.006)	
				Filtek Z350	0.020 (0.003)	
				Estelite Σ	0.049 (0.041)	
				Ceram•X	0.088 (0.010)	
				Filtek Z250	0.040 (0.012)	
				Premise	0.035 (0.009)	
				Tetric Ceram	0.054 (0.013)	
				Tetric EvoCeram	0.085 (0.017)	
Carbide bur (30 blades)	Botta et al., 2008 [43]	AFM	4	Filtek Supreme XT	0.284 (0.054)	There were no differences among the materials tested.
				Point 4	0.344 (0.127)	
Carbide bur (16 blades)	Gönülol & Yilmaz, 2012 [59]	Rugosimeter	7	Filtek Supreme XT (transparent shade)	0.83 (0.13)	Nanofill together with one microhybrid (Filtek Z250) presented lower roughness values than the other microhybrids.
				Filtek Supreme XT (dentin shade)	0.77 (0.38)	
				Aelite Aesthetic Enamel	1.04 (0.39)	
				Filtek Z250	0.70 (0.19)	
				Grandio	1.51 (0.53)	
Carbide bur (16 blades) + Astropol	Gönülol & Yilmaz, 2012 [59]	Rugosimeter	7	Filtek Supreme XT (transparent shade)	0.41 (0.09)	Only one of the microhybrids (Grandio) was rougher than the nanofill composite.
				Filtek Supreme XT (dentin shade)	0.51 (0.13)	

				Aelite Aesthetic Enamel	0.44 (0.16)	
				Filtek Z250	0.47 (0.08)	
				Grandio	0.97 (0.21)	
Carbide bur (30 blades) + Astropol + Astrobrush	Baseren, 2004 [72]	Rugosimeter	10	Filtek Supreme	0.33 (0.02)	There were no differences among the materials tested.
				Admira	0.29 (0.03)	
				Grandio	0.32 (0.01)	
Carbide bur (16 blades) + Enhance	Gönülol & Yilmaz, 2012 [59]	Rugosimeter	7	Filtek Supreme XT (transparent shade)	0.34 (0.08)	Only one of the microhybrids (Grandio) was rougher than the nanofill composite.
				Filtek Supreme XT (dentin shade)	0.37 (0.07)	
				Aelite Aesthetic Enamel	0.62 (0.13)	
				Filtek Z250	0.48 (0.13)	
				Grandio	0.72 (0.16)	
Carbide bur (12 + 30 blades) + PoGo	Turssi et al., 2005 [76]	Rugosimeter	10	Filtek Supreme	0.1057 (0.0181)	Nanofill composite presented lower roughness values than the microhybrid.
				Filtek Z250	0.1061 (0.0179)	
Carbide bur (16 blades) + PoGo	Gönülol & Yilmaz, 2012 [59]	Rugosimeter	7	Filtek Supreme XT (transparent shade)	0.26 (0.15)	One nanofill composite (Filtek Supreme XT dentin shade) together with one microhybrid (Grandio) presented the highest roughness values.
				Filtek Supreme XT (dentin shade)	0.76 (0.16)	
				Aelite Aesthetic Enamel	0.47 (0.14)	
				Filtek Z250	0.57 (0.14)	
				Grandio	0.91 (0.28)	
Carbide burs (12 + 30 blades) + Sof-Lex Brush	Turssi et al., 2005 [76]	Rugosimeter	10	Filtek Supreme	0.1154 (0.0142)	Nanofill composite presented lower roughness values than the microhybrid.
				Filtek Z250	0.1231 (0.0237)	
Carbide bur (16 blades) + Sof-Lex	Gönülol & Yilmaz, 2012 [59]	Rugosimeter	7	Filtek Supreme XT (transparent shade)	0.24 (0.07)	There were no differences among the materials tested.
				Filtek Supreme XT	0.32 (0.11)	

				(dentin shade)		
				Aelite Aesthetic Enamel	0.44 (0.10)	
				Filtek Z250	0.23 (0.09)	
				Grandio	0.39 (0.10)	
Carbide bur (30 blades) + Super-snap Rainbow	Baseren, 2004 [72]	Rugosimeter	10	Filtek Supreme	0.11 (0.02)	There were no differences among the materials tested.
				Admira	0.13 (0.02)	
				Grandio	0.14 (0.21)	
Compo System	Janus et al., 2010 [42]	Optical Profilometer	6	Filtek Supreme XT	0.123 (0.01)	Nanofill composite presented lower roughness values than the microhybrids.
				Grandio	0.212 (0.017)	
				Synergy D6	0.133 (0.01)	
				Tetric Ceram	0.14 (0.011)	
	Botta et al., 2008 [43]	AFM	4	Filtek Supreme XT	0.510 (0.066)	There were no differences among the materials tested.
				Point 4	0.532 (0.057)	
Diamond bur	Gönülol & Yilmaz, 2012 [59]	Rugosimeter	7	Filtek Supreme XT (transparent shade)	2.28 (0.62)	There were no differences among the materials tested.
				Filtek Supreme XT (dentin shade)	2.11 (0.47)	
				Aelite Aesthetic Enamel	2.08 (0.55)	
				Filtek Z250	2.36 (0.74)	
				Grandio	2.15 (0.25)	
Diamond bur + Arkansas Stone + rubber points	Gönülol & Yilmaz, 2012 [59]	Rugosimeter	7	Filtek Supreme XT (transparent shade)	0.89 (0.24)	One microhybrid (Filtek Z250) presented lower roughness values than one of the nanofills (Filtek Supreme XT transparent shade).
				Filtek Supreme XT (dentin shade)	0.60 (0.09)	
				Aelite Aesthetic Enamel	0.66 (0.13)	
				Filtek Z250	0.49 (0.09)	
				Grandio	1.14 (0.29)	
Diamond bur +	Baseren, 2004	Rugosimeter	10	Filtek Supreme	0.39 (0.04)	There were no differences among the materials

Astropol + Astrobrush	[72]			Admira	0.31 (0.03)	tested.
				Grandio	0.34 (0.02)	
Diamond bur + PoGo	Turssi et al., 2005 [76]	Rugosimeter	10	Filtek Supreme	0.2845 (0.0652)	Nanofill composite presented lower roughness values than the microhybrid.
				Filtek Z250	0.3350 (0.0741)	
Diamond bur + Sof-Lex Brush	Turssi et al., 2005 [76]	Rugosimeter	10	Filtek Supreme	0.1516 (0.0226)	Nanofill composite presented lower roughness values than the microhybrid.
				Filtek Z250	0.1564 (0.0366)	
Diamond bur + Super-snap Rainbow	Baseren, 2004 [72]	Rugosimeter	10	Filtek Supreme	0.13 (0.08)	There were no differences among the materials tested.
				Admira	0.27 (0.05)	
				Grandio	0.15 (0.05)	
Diamond Flex + Diamond Excel	Botta et al., 2009 [41]	AFM	4	Filtek Supreme XT	0.058 (0.006)	Nanofill composite presented lower roughness values than the microhybrids.
				Point 4	0.074 (0.004)	
				Tetric Ceram	0.150 (0.007)	
Diamond Pro	Botta et al., 2009 [41]	AFM	4	Filtek Supreme XT	0.049 (0.001)	Nanofill composite together with one microhybrid (Point 4) presented lower roughness values than the other microhybrid.
				Point 4	0.045 (0.004)	
				Tetric Ceram	0.062 (0.008)	
Diamond Pro + Diamond Flex + Diamond Excel	Botta et al., 2009 [41]	AFM	4	Filtek Supreme XT	0.122 (0.003)	Nanofill composite presented intermediate results compared with the microhybrids: lower than Tetric Ceram and higher than Point 4.
				Point 4	0.079 (0.004)	
				Tetric Ceram	0.156 (0.006)	
Enhance Flex NST	da Costa et al., 2011 [46]	Rugosimeter	5	Filtek Supreme Plus	0.22 (0.04)	There were no differences among the materials tested.
				Esthet-X	0.24 (0.04)	
				Filtek Z250	0.23 (0.02)	
				Premise	0.21 (0.01)	
Enhance / PoGo	Antonson et al., 2011 [45]	Laser Profilometer	5	Filtek Supreme Plus	0.14 (0.02)	There were no differences among the materials tested.
				Esthet-X	0.12 (0.02)	
	da Costa et al., 2010 [35]	Rugosimeter	5	Filtek Supreme Plus	0.04 (0.04)	There were no differences among the materials tested.
				Filtek Z250	0.05 (0.04)	
				Premise	0.05 (0.05)	
	da Silva et al.,	Rugosimeter	12	Filtek Z350	0.32 (n.i.)*	Nanofill composite together with one of the

	2010 [36]			Esthet-X	0.41 (n.i.)*	microhybrids (Opallis) presented lower roughness values than the other microhybrid.
				Opallis	0.30 (n.i)*	
EP Esthetic Polishing System**	Melander et al., 2011 [63]	AFM	10	Filtek Supreme Plus	0.0014 (0.0002)	Nanofill composite together with three microhybrids (Filtek Z250, Herculite XRV and Premise) presented the lowest roughness values.
				Filtek Z250	0.0014 (0.0002)	
				Herculite XRV	0.0017 (0.0003)	
				Premise	0.0014 (0.0004)	
				Prisma AP.H	0.0036 (0.0003)	
				TPH 3	0.0024 (0.0003)	
EXL-695	Antonson et al., 2011 [45]	Laser Profilometer	5	Filtek Supreme Plus	0.11 (0.03)	There were no differences among the materials tested.
				Esthet-X	0.12 (0.01)	
Hiluster	Erdemir et al., 2012 [58]	Rugosimeter	7	Filtek Supreme XT	0.74 (0.41)	There were no differences among the materials tested.
				Gradia Direct	1.02 (0.47)	
One Gloss	Ergücü & Türkün, 2007 [33]	Rugosimeter	10	Filtek Supreme XT	0.528 (0.078)	Two of the microhybrids presented the lowest roughness values (Premise and Ceram•X). Among the other composites including the nanofill, there were no differences.
				Ceram•X	0.346 (0.049)	
				Grandio	0.507 (0.093)	
				Premise	0.338 (0.037)	
				Tetric EvoCeram	0.584 (0.059)	
OptraPol	Ergücü & Türkün, 2007 [33]	Rugosimeter	10	Filtek Supreme XT	0.392 (0.048)	Nanofill composite presented lower roughness values than the microhybrids.
				Ceram•X	0.518 (0.057)	
				Grandio	0.497 (0.114)	
				Premise	0.470 (0.068)	
				Tetric EvoCeram	0.696 (0.096)	
	Korkmaz et al., 2008 [75]	Rugosimeter	5	Filtek Supreme XT	0.12 (0.05)	Nanofill composite together with three microhybrids (Ceram•X, Aelite Aesthetic Enamel and Filtek Z250) presented the lowest roughness values.
				Aelite Aesthetic Enamel	0.14 (0.04)	
				Ceram•X	0.12 (0.05)	
				Filtek Z250	0.16 (0.03)	
				Grandio	0.44 (0.17)	
				Tetric EvoCeram	0.36 (0.11)	

PoGo	Ergücü & Türkün, 2007 [33]	Rugosimeter	10	Filtek Supreme XT	0.198 (0.045)	Nanofill composite together with two microhybrids (Grandio and Ceram•X) presented the lowest roughness values.
				Ceram•X	0.179 (0.046)	
				Grandio	0.171 (0.041)	
				Premise	0.237 (0.044)	
				Tetric EvoCeram	0.223 (0.036)	
	Korkmaz et al., 2008 [75]	Rugosimeter	5	Filtek Supreme XT	0.12 (0.06)	Nanofill composite together with three microhybrids (Ceram•X, Aelite Aesthetic Enamel and Filtek Z250) presented the lowest roughness values.
				Aelite Aesthetic Enamel	0.13 (0.03)	
				Ceram•X	0.12 (0.02)	
				Filtek Z250	0.20 (0.02)	
				Grandio	0.55 (0.21)	
				Tetric EvoCeram	0.38 (0.04)	
Polyester matrix	Attar, 2007 [34]	Rugosimeter	7	Filtek Supreme	0.09 (0.02)	Nanofill composite presented lower roughness values than the microhybrids.
				Artemis	0.33 (0.03)	
				Filtek P60	0.51 (0.07)	
				TPH spectrum	0.29 (0.07)	
	Baseren, 2004 [72]	Rugosimeter	10	Filtek Supreme	0.04 (n.a.)***	Nanofill composite together with one microhybrid (Grandio) presented lower roughness values than the other microhybrid.
				Admira	0.09 (n.a.)***	
				Grandio	0.03 (n.a.)***	
	Botta et al., 2008 [43]	AFM	4	Filtek Supreme XT	0.024 (0.003)	Nanofill composite presented higher roughness values than the microhybrid.
				Point 4	0.013 (0.003)	
	Botta et al., 2009 [41]	AFM	4	Filtek Supreme XT	0.024 (0.003)	There were no differences among the materials tested.
				Point 4	0.013 (0.001)	
				Tetric Ceram	0.015 (0.002)	
	da Silva et al., 2010 [36]	Rugosimeter	12	Filtek Z350	0.18 (0.02)	Nanofill composite together with one microhybrid (Esthet-X) presented higher roughness values than the other microhybrid.
				Esthet-X	0.23 (0.04)	
				Opallis	0.14 (0.02)	
	Erdemir et al., 2012 [58]	Rugosimeter	7	Filtek Supreme XT	0.33 (0.17)	There were no differences among the materials tested.
				Gradia Direct	0.44 (0.11)	
	Gönülol & Yilmaz, 2012 [59]	Rugosimeter	7	Filtek Supreme XT (transparent	0.20 (0.09)	There were no differences among the materials tested.

			shade)		
			Filtek Supreme XT (dentin shade)	0.22 (0.09)	
			Aelite Aesthetic Enamel	0.22 (0.07)	
			Filtek Z250	0.16 (0.08)	
			Grandio	0.18 (0.09)	
Janus et al., 2010 [42]	Optical Profilometer	6	Filtek Supreme XT	0.025 (0.003)	Nanofill composite presented higher roughness values than the microhybrids.
			Grandio	0.017 (0.004)	
			Synergy D6	0.018 (0.003)	
			Tetric Ceram	0.017 (0.002)	
Korkmaz et al., 2008 [75]	Rugosimeter	5	Filtek Supreme XT	0.03 (0.01)	Nanofill composite together with one microhybrid (Filtek Z250) presented lower roughness values than the other microhybrids.
			Aelite Aesthetic Enamel	0.06 (0.01)	
			Ceram•X	0.07 (0.00)	
			Filtek Z250	0.05 (0.00)	
			Grandio	0.07 (0.02)	
			Tetric EvoCeram	0.08 (0.01)	
Senawongse & Pongprueksa, 2007 [71]	Rugosimeter	10	Filtek Supreme XT (dentin shade)	0.016 (0.003)	There were no differences among the materials tested.
			Filtek Supreme XT (transparent shade)	0.020 (0.004)	
			Filtek Z350	0.017 (0.003)	
			Estelite Σ	0.021 (0.002)	
			Ceram•X	0.018 (0.003)	
			Filtek Z250	0.017 (0.002)	
			Premise	0.026 (0.003)	
			Tetric Ceram	0.024 (0.003)	
			Tetric EvoCeram	0.029 (0.009)	
Yap et al., 2004 [77]	Rugosimeter	8	Filtek Supreme XT (body shade)	0.16 (0.04)	Nanofills together with one microhybrid (Admira) presented higher roughness values than the other

				Filtek Supreme XT (transparent shade)	0.15 (0.04)	microhybrids.
				Admira	0.11 (0.04)	
				Filtek Z100	0.04 (0.01)	
Poli-pro disk	Erdemir et al., 2012 [58]	Rugosimeter	7	Filtek Supreme XT	1.20 (0.37)	There were no differences among the materials tested.
				Gradia Direct	0.99 (0.35)	
SiC paper – 180 grit	Hosoya et al., 2010 [55]	Laser scanning microscope	3	Estelite Σ Quick (regular shade)	1.41 (0.23)	Submicron composite presented lower roughness values than the microhybrids, regardless of the shade.
				Estelite Σ Quick (opaque shade)	1.93 (0.44)	
				Estelite Σ Quick (enamel shade)	1.86 (0.18)	
				Beautifil II (regular shade)	5.99 (0.51)	
				Beautifil II (opaque shade)	6.00 (0.48)	
				Beautifil II (enamel shade)	5.59 (0.43)	
				Clearfil Majesty (regular shade)	6.24 (0.51)	
				Clearfil Majesty (opaque shade)	6.10 (0.44)	
				Clearfil Majesty (enamel shade)	6.45 (0.75)	
SiC paper - 1000 grit	Hosoya et al., 2010 [55]	Laser scanning microscope	3	Estelite Σ Quick (regular shade)	0.90 (0.21)	Submicron composite presented lower roughness values than the microhybrids, regardless of the shade.
				Estelite Σ Quick (opaque shade)	1.55 (0.23)	
				Estelite Σ Quick (enamel shade)	0.71 (0.10)	
				Beautifil II (regular shade)	4.68 (0.42)	
				Beautifil II (opaque shade)	4.76 (0.27)	
				Beautifil II (enamel shade)	4.70 (0.25)	

				Clearfil Majesty (regular shade)	4.56 (0.26)	
				Clearfil Majesty (opaque shade)	4.65 (0.12)	
				Clearfil Majesty (enamel shade)	5.10 (0.27)	
SiC paper - 1200 grit	Teixeira et al., 2005 [78]	AFM	10	Filtek Supreme	0.017 (0.006)	There were no differences among the materials tested.
				Filtek Z250	0.051 (0.041)	
	Teixeira et al., 2005 [78]	Rugosimeter	10	Filtek Supreme	0.200 (0.000)	There were no differences among the materials tested.
				Filtek Z250	0.200 (0.000)	
	Turssi et al., 2005 [76]	Rugosimeter	10	Filtek Supreme	0.1266 (0.0180)	Nanofill composite presented lower roughness values than the microhybrid.
				Filtek Z250	0.1394 (0.0277)	
SiC paper - 3000 grit	Hosoya et al., 2010 [55]	Laser scanning microscope	3	Estelite Σ Quick (regular shade)	0.32 (0.04)	Submicron composite presented lower roughness values than the microhybrids, regardless the shade.
				Estelite Σ Quick (opaque shade)	1.52 (0.29)	
				Estelite Σ Quick (enamel shade)	0.30 (0.03)	
				Beautifil II (regular shade)	4.63 (0.32)	
				Beautifil II (opaque shade)	4.77 (0.49)	
				Beautifil II (enamel shade)	4.55 (0.58)	
				Clearfil Majesty (regular shade)	5.01 (0.32)	
				Clearfil Majesty (opaque shade)	4.89 (0.49)	
				Clearfil Majesty (enamel shade)	4.64 (0.67)	
SiC paper - 4000 grit	Barucci-Pfister & Göhring, 2009 [48]	Rugosimeter	10	Filtek Supreme	0.0264 (0.0030)	Nanofill composite together with one microhybrid (Enamel Plus HFO) presented lower roughness values than the other microhybrids.
				Artemis	0.0315 (0.0028)	
				Ceram•X	0.0357 (0.0024)	
				Enamel Plus HFO	0.0297 (0.0028)	
				Miris	0.0315 (0.0040)	

Sof-Lex				Tetric Ceram	0.0337 (0.0041)	
				Venus	0.0335 (0.0024)	
	Antonson et al., 2011 [45]	Laser Profilometer	5	Filtek Supreme Plus	0.08 (0.01)	There were no differences among the materials tested.
				Esthet-X	0.10 (0.02)	
	da Costa et al., 2011 [46]	Rugosimeter	5	Filtek Supreme Plus	0.15 (0.03)	There were no differences among the materials tested.
				Esthet-X	0.12 (0.04)	
				Filtek Z250	0.19 (0.08)	
				Premise	0.15 (0.02)	
	de Moraes et al., 2009 [56]	Rugosimeter	8	Filtek Supreme XT	0.09 (0.02)	Nanofill composite together with two microhybrids (Premise and Concept Advanced) presented lower roughness values than the other microhybrids.
				Concept Advanced	0.09 (0.01)	
				Filtek Z250	0.24 (0.09)	
				Grandio	0.24 (0.04)	
				Premise	0.08 (0.01)	
				TPH 3	0.25 (0.08)	
	Erdemir et al., 2012 [58]	Rugosimeter	7	Filtek Supreme XT	2.05 (0.92)	Nanofill composite presented higher roughness values than the microhybrid.
				Gradia Direct	0.65 (0.24)	
	Janus et al., 2010 [42]	Optical Profilometer	6	Filtek Supreme XT	0.094 (0.007)	Nanofill composite presented lower roughness values than the microhybrids.
				Grandio	0.162 (0.02)	
				Synergy D6	0.109 (0.01)	
				Tetric Ceram	0.12 (0.009)	
	Kakaboura et al., 2007 [38]	AFM (Sa****)	6	Palfique Estelite	0.03 (0.01)	Submicron composite together with one microhybrid (Point 4) presented lower roughness values than the other microhybrids.
				Esthet-X	0.10 (0.02)	
				Point 4	0.05 (0.01)	
				Synergy Duo	0.12 (0.03)	
				TPH spectrum	0.14 (0.05)	
	Kakaboura et al., 2007 [38]	Rugosimeter	6	Palfique Estelite	0.53 (0.06)	Submicron composite together with two microhybrids (Point 4 and Synergy Duo) presented higher roughness values than the other two
				Esthet-X	0.30 (0.03)	
				Point 4	0.52 (0.06)	

			Synergy Duo	0.56 (0.07)	microhybrids.
			TPH spectrum	0.39 (0.05)	
Penteado et al., 2010 [79]	AFM	12	Filtek Supreme	0.055 (0.006)	There were no differences among the materials tested.
			Filtek Z250	0.056 (0.013)	
Senawongse & Pongprueksa, 2007 [71]	Rugosimeter	10	Filtek Supreme XT (dentin shade)	0.038 (0.017)	Nanofill composites together with the submicron and three microhybrids (Tetric Ceram, Tetric EvoCeram and Premise) presented the lowest roughness values.
			Filtek Supreme XT (transparent shade)	0.029 (0.005)	
			Filtek Z350	0.020 (0.003)	
			Estelite Σ	0.054 (0.009)	
			Ceram•X	0.069 (0.012)	
			Filtek Z250	0.105 (0.027)	
			Premise	0.057 (0.014)	
			Tetric Ceram	0.065 (0.015)	
Silikas et al., 2005 [47]	AFM (S_a^{****})	4	Tetric EvoCeram	0.051 (0.013)	
			Filtek Supreme	0.023 (0.002)	
			Palfique Estelite	0.015 (0.001)	
			Filtek Z250	0.032 (0.002)	
Silikas et al., 2005 [47]	Rugosimeter	4	Tetric Ceram	0.034 (0.002)	
			Filtek Supreme	0.125 (0.044)	
			Palfique Estelite	0.101 (0.039)	
			Filtek Z250	0.161 (0.044)	
Valinoti et al., 2008 [37]	Rugosimeter	30	Tetric Ceram	0.169 (0.086)	
			Filtek Supreme	0.103 (n.a.) ^{***}	
			Concept Advanced Magic Kids	0.119 (n.a.) ^{***}	
			Opallis	0.122 (n.a.) ^{***}	
Sof-Lex PoP-On	Rugosimeter	5	TPH 3	0.099 (n.a.) ^{***}	Nanofill composite and one microhybrid (TPH 3) presented the lowest roughness values, although there were no differences between the nanofill and the other microhybrids.
			Filtek Supreme XT	0.09 (0.03)	
			Aelite Aesthetic	0.14 (0.02)	
Korkmaz et al., 2008 [75]	Rugosimeter	5	Filtek Supreme XT	0.09 (0.03)	Nanofill composite together with three microhybrids (Ceram•X, Aelite Aesthetic Enamel and Filtek
			Aelite Aesthetic	0.14 (0.02)	

				Enamel		Z250) presented the lowest roughness values.
				Ceram•X	0.14 (0.01)	
				Filtek Z250	0.17 (0.02)	
				Grandio	0.43 (0.15)	
				Tetric EvoCeram	0.54 (0.12)	
Super-Snap	da Costa et al., 2011 [46]	Rugosimeter	5	Filtek Supreme Plus	0.12 (0.03)	There were no differences among the materials tested.
				Esthet-X	0.13 (0.02)	
				Filtek Z250	0.10 (0.02)	
				Premise	0.18 (0.1)	
	Yap et al., 2004 [77]	Rugosimeter	8	Filtek Supreme XT (body shade)	0.33 (0.06)	Translucent nanofill composite and one of the microhybrids (Admira) presented lower roughness values than the other nanofill and the other microhybrid.
				Filtek Supreme XT (transparent shade)	0.15 (0.02)	
				Admira	0.15 (0.05)	
				Filtek Z100	0.32 (0.13)	

* The paper does not provide standard deviations for baseline roughness values.

**Polishing system is described in the paper as a sequence of polishing discs and identified as PoGo. However, this material is a one-step rubber-based polishing system. In communication with the authors of this work, it was informed that the actual polishing system applied was "EP Esthetic Polishing System".

***The paper presents different baseline roughness means and standard deviations to each material since the groups were already split at that point. We chose to calculate a single mean to each material, yet the same could not be applied to the standard deviations, which are not described here.

****The paper presents roughness measures analyzed with AFM and expressed in Sa values, which is defined as equivalent to Ra.

2.4.2.2 Initial surface gloss based on polishing system

In total, 18 gloss comparisons from 7 papers were analyzed (Table 2.4); ~70% of those showed no significant differences between nanofills or submicrons and microhybrids, ~20% showed better results for nanofills or submicrons, and ~10% showed poorer results for nanofills. Positive results for nanofills were reported in 4 papers and included 3 different gloss analyses and 3 finishing methods; they reported 9 microhybrids as having poorer results than nanofills. Four of those 9 microhybrids performed similar to or better than nanofills in other comparisons; 5 were compared only once. Two studies found poorer gloss results for nanofills compared with microhybrids and included the same gloss analyses (60° angle), 2 finishing methods, and reported 4 microhybrids as having poorer results than nanofills. These 4 microhybrids performed similar to or poorer than nanofills in other comparisons.

Two variations of nanofills were tested. Filtek Supreme Plus was tested 14 times, with ~70% of the comparisons showing no significant difference compared with at least 1 of the microhybrids tested in the same study. In ~15% of the comparisons, nanofills were better than microhybrids, while nanofills had poorer gloss in ~15% of the comparisons. Filtek Supreme was tested 4 times, with 2 comparisons showing similar and the other 2 showing better results than microhybrids. Only 2 comparisons were observed for nanofills, submicrons, and microhybrids all together, with results showing no significant differences among materials in one comparison; in the other, nanofills and submicrons were similar, and both materials performed better than did microhybrids.

Among the 18 comparisons for initial gloss, 15 performed the analysis using a 60° measurement angle, and in ~73% of these cases, there were no significant differences between nanofills and microhybrids. Nanofills performed better than microhybrids in ~13% of the comparisons, and in the other ~13%, nanofills showed poorer performance. Measurement angles of 20° and 45° were applied in one comparison each, and the nanofill composite performed better than microhybrids in both. One study did not inform the measurement angle and found no significant differences between nanofills and microhybrids. Regarding the surface finishing protocol, the method mostly employed was Sof-Lex discs (6); ~67% of these studies indicated no significant differences between nanofills and microhybrids, while 33% showed better results for nanofills.

Table 2.4 - Baseline gloss measurements according to the different polishing systems used in the studies

Polishing system	Author	Measurement angle	N	Material	Gloss (GU)	Conclusion
Astropol	Antonson et al., 2011 [45]	60°	5	Filtek Supreme Plus	57.1 (5.6)	There were no differences among the materials tested.
				Esthet-X	57.9 (5.6)	
ComposiPro Diacomp	da Costa et al., 2007 [32]	60°	5	Filtek Supreme Plus	26.6 (3.77)	There were no differences among the materials tested.
				Esthet-X	20.1 (1.38)	
				Filtek Z100	22.3 (8)	
				Filtek Z250	23.6 (6.97)	
ComposiPro Diacomp + Enamelize	da Costa et al., 2007 [32]	60°	5	Filtek Supreme Plus	23.6 (2.88)	Microhybrid composite Filtek Z100 presented the highest gloss values. Among the other composites, including nanofill, there were no differences.
				Esthet-X	30.5 (6.29)	
				Filtek Z100	51.2 (7.35)	
				Filtek Z250	20.2 (4.79)	
ComposiPro one-step brush	da Costa et al., 2007 [32]	60°	5	Filtek Supreme Plus	36.5 (3.41)	Nanofill composite and one microhybrid (Esthet-X) presented the highest gloss values. However, there were no difference between the nanofill composite and the other microhybrids.
				Esthet-X	42.8 (1.44)	
				Filtek Z100	28.2 (3.15)	
				Filtek Z250	31.0 (9.21)	
Enhance Flex NST	da Costa et al., 2011 [46]	60°	5	Filtek Supreme Plus	44.57 (1.04)	Nanofill composite presented lower gloss values than the microhybrids.
				Esthet-X	58.76 (0.94)	
				Filtek Z250	51.38 (2.17)	
				Premise	57.57 (0.75)	
Enhance / PoGo	Antonson et al., 2011 [45]	60°	5	Filtek Supreme Plus	56.2 (8.7)	There were no differences among the materials tested.
				Esthet-X	56.0 (7.6)	
	da Costa et al., 2010 [35]	60°	15	Filtek Supreme Plus	66.67 (n.a.)*	There were no differences among the materials tested.
				Filtek Z250	63.00 (n.a.)*	
				Premise	67.00 (n.a.)*	
EXL-695	Antonson et al., 2011 [45]	60°	5	Filtek Supreme Plus	67.0 (10.0)	There were no differences among the materials tested.
				Esthet-X	62.2 (6.6)	
Jiffy polishers	da Costa et al., 2007 [32]	60°	5	Filtek Supreme Plus	28.7 (1.73)	There were no differences among the materials tested.
				Esthet-X	24.5 (3.48)	

				Filtek Z100	19.9 (3.80)	
				Filtek Z250	26.6 (3.74)	
PoGo	da Costa et al., 2007 [32]	60°	5	Filtek Supreme Plus	77.4 (4.44)	Nanofill composite presented higher gloss values than the microhybrids.
				Esthet-X	66.2 (11.07)	
				Filtek Z100	59.5 (3.79)	
				Filtek Z250	64.05 (14.17)	
SiC paper	Barucci-Pfister & Göring, 2009 [48]	45°	10	Filtek Supreme	51.0 (1.4)	Nanofill composite presented higher gloss values than the microhybrids.
				Artemis	38.6 (6.1)	
				Ceram•X	25.8 (3.2)	
				Enamel Plus HFO	32.9 (6.4)	
				Miris	27.9 (2.4)	
				Tetric Ceram	38.8 (4.0)	
				Venus	32.4 (2.4)	
Sof-Lex	Antonson et al., 2011 [45]	60°	5	Filtek Supreme Plus	63.9 (6.0)	Nanofill composite presented higher gloss values than the microhybrid.
				Esthet-X	47.1 (2.9)	
	da Costa et al., 2007 [32]	60°	5	Filtek Supreme Plus	55.6 (5.03)	Nanofill composite together with one microhybrid (Esthet-X) presented the highest gloss values.
				Esthet-X	47.3 (5.40)	
				Filtek Z100	35.7 (5.33)	
				Filtek Z250	43.7 (2.51)	
	da Costa et al., 2011 [46]	60°	5	Filtek Supreme Plus	63.6 (1.43)	There were no differences among the materials tested.
				Esthet-X	61.82 (1.20)	
				Filtek Z250	57.6 (0.84)	
				Premise	60.96 (1.24)	
	Gurgan Yalcin Cakir, 2008 [52]	n.i.	30	Filtek Supreme	94.7 (n.a.)*	There were no differences among the materials tested.
				Simile	94.6 (n.a.)*	
	Silikas et al., 2005 [47]	60°	5	Filtek Supreme	77.8 (2.4)	Nanofill together with the submicron and one microhybrid (Filtek Z250) presented the highest gloss values.
				Palfique Estelite	77.7 (2.1)	
				Filtek Z250	74.2 (2.8)	
				Tetric Ceram	69.5 (1.8)	
	Silikas et al., 2005	20°	5	Filtek Supreme	24.0 (2.2)	Nanofill together with the submicron

	[47]			Palfique Estelite	29.2 (3.3)	composite presented the highest gloss values.
				Filtek Z250	19.5 (3.9)	
				Tetric Ceram	12.5 (1.9)	
Super-Snap	da Costa et al., 2011 [46]	60°	5	Filtek Supreme Plus	64.22 (1.80)	There were no differences among the materials tested.
				Esthet-X	62.47 (1.22)	
				Filtek Z250	62.60 (1.61)	
				Premise	65.60 (1.00)	

* The paper presents different baseline roughness means and standard deviations to each material since the groups were already split at that point. We chose to calculate a single mean to each material, yet the same could not be applied to the standard deviations, which are not described here.

2.4.2.3 Smoothness retention

The smoothness retention was tested mainly after simulation of surface wear (5), toothbrushing (4), or “other methods” (4). Wear and “other methods” did not generate any differences between nanofills and microhybrids. The tests that applied toothbrushing indicated better results for nanofills in 1 comparison, poorer performance in 1 comparison, and no significant differences in the other 2 comparisons.

In total, 13 comparisons from 7 papers were analyzed for the retention of smoothness (Table 2.5). About 85% of those found no significant differences between nanofills and microhybrids. Only 1 comparison showed better results for nanofills, and 1 comparison presented poorer results for nanofills. Those came from the same paper, varying just the smoothness analysis (rugosimeter versus AFM). One comparison for submicron, nanofills, and microhybrids all together showed poorer results for the submicron compared to 3 nanofills and 3 microhybrids, although the submicron performed better than 2 other microhybrids.

Three variations of nanofills were tested. Filtek Supreme XT was compared 3 times and always performed similar to at least one of the microhybrids. Filtek Supreme was compared 10 times; in 80% of the comparisons, the material was similar to microhybrids, while it performed better in 1 comparison and poorer in 1. Filtek Z350 was tested only once, showing better results than the microhybrids to which it was compared.

Among 13 comparisons, 9 performed the analysis with a rugosimeter and 3 with an AFM. Between 70% and 90% of the comparisons indicated no significant differences for nanofills and microhybrids, depending on the method used to measure the smoothness, while the remaining comparisons indicated 1 better and 1 poorer result for nanofills. Regarding the surface finishing protocols, the methods mostly used were SiC papers (5) and Sof-Lex discs (3). The studies that used Sof-Lex discs did not show significant differences between nanofills and microhybrids. When SiC papers were used, 3 comparisons showed no significant differences between materials, whereas 1 comparison indicated a better performance, and 1 comparison showed poorer results for nanofills.

Table 2.5 - Smoothness retention according to the different polishing systems used in the studies

Polishing system	Author	Method of analysis	Aging method	N	Material	Baseline roughness (Ra, μm)	Final roughness (Ra, μm)	Δ Ra (%)	Conclusion
Carbide bur + PoGo	Turssi et al., 2005 [76]	Rugosi-meter	Wear (100K cycles, 2 Hz, 20 N - 6 mm linear path)	10	Filtek Supreme	0.1057 (0.0181)	0.3212 (0.0604)	204	There were no differences among the final roughness values of the materials tested.
					Filtek Z250	0.1061 (0.0179)	0.3296 (0.0446)	211	
Carbide bur + Sof-Lex Brush	Turssi et al., 2005 [76]	Rugosi-meter	Wear (100K cycles, 2 Hz, 20 N - 6 mm linear path)	10	Filtek Supreme	0.1154 (0.0142)	0.3144 (0.0441)	172	There were no differences among the final roughness values of the materials tested.
					Filtek Z250	0.1231 (0.0237)	0.3372 (0.0354)	174	
Diamond bur + PoGo	Turssi et al., 2005 [76]	Rugosi-meter	Wear (100K cycles, 2 Hz, 20 N - 6 mm linear path)	10	Filtek Supreme	0.2845 (0.0652)	0.3522 (0.0362)	24	There were no differences among the final roughness values of the materials tested.
					Filtek Z250	0.3350 (0.0741)	0.3701 (0.0442)	10	
Diamond bur + Sof-Lex Brush	Turssi et al., 2005 [76]	Rugosi-meter	Wear (100K cycles, 2 Hz, 20 N - 6 mm linear path)	10	Filtek Supreme	0.1516 (0.0226)	0.3390 (0.0310)	124	There were no differences among the final roughness values of the materials tested.
					Filtek Z250	0.1564 (0.0366)	0.3228 (0.0720)	106	
Polyester matrix	Senawongse & Pongprueksa 2007 [71]	Rugosi-meter	Toothbrushing (20K strokes, 80 strokes/min, 500 gf)	10	Filtek Supreme XT (dentin shade)	0.016 (0.003)	0.052 (0.016)	213	Two nanofills (Filtek Z350 and Filtek Supreme XT - dentin shade) presented the lowest final roughness values. Those were followed by the other nanofill (Filtek Supreme XT - translucent) together with two microhybrids (Filtek Z250 and Premise). Submicron composite presented higher final roughness values than those aforementioned.
					Filtek Supreme XT (transparent shade)	0.020 (0.004)	0.183 (0.081)	800	
					Filtek Z350	0.017 (0.003)	0.051 (0.009)	194	
					Estelite Σ	0.021 (0.002)	0.369 (0.115)	1662	
					Ceram•X	0.018 (0.003)	0.411 (0.131)	2178	
					Filtek Z250	0.017 (0.002)	0.148 (0.010)	782	
					Premise	0.026 (0.003)	0.207 (0.057)	708	
					Tetric Ceram	0.024 (0.003)	0.235 (0.074)	858	
					Tetric	0.029 (0.009)	0.428 (0.071)	1383	

					EvoCeram				
SiC Paper - 1200 grit	Catelan et al., 2009 [80]	Rugosi- meter	Ultraviolet light (8 h) + Condensation (4 h) + Heat ($65 \pm 3^\circ\text{C}$ or $45 \pm 3^\circ\text{C}$) + 100% humidity	10	Filtek Supreme XT	n.i.*	0.050 (0.009)	n.i.*	Nanofill composite together with one microhybrid (Vit-I- escence) presented lower roughness values than the other microhybrid.
					Opallis	n.i.*	0.059 (0.011)	n.i.*	
					Vit-I-escence	n.i.*	0.052 (0.007)	n.i.*	
	Teixeira et al., 2005 [78]	AFM	Toothbrushing (100K cycles, 1.5 strokes/s, 250 g)	10	Filtek Supreme	0.017 (0.006)	0.037 (0.009)	135	Nanofill composite presented lower final roughness value than the microhybrid.
					Filtek Z250	0.051 (0.041)	0.118 (0.017)	135	
	Teixeira et al., 2005 [78]	Rugosi- meter	Toothbrushing (100K cycles, 1.5 strokes/s, 250 g)	10	Filtek Supreme	0.200 (0.000)	0.536 (0.089)	170	Nanofill composite presented higher final roughness value than the microhybrid.
					Filtek Z250	0.200 (0.000)	0.410 (0.050)	105	
	Turssi et al., 2005 [76]	Rugosi- meter	Wear (100K cycles, 2 Hz, 20 N - 6 mm linear path)	10	Filtek Supreme	0.1266 (0.0180)	0.3444 (0.0455)	172	There were no differences among the final roughness values of the materials tested.
					Filtek Z250	0.1394 (0.0277)	0.3565 (0.0377)	156	
SiC Paper - 4000 grit	Barucci- Pfister & Görling, 2009 [48]	Rugosi- meter	Ethanol bath (240 h, ethanol 75%) + Toothbrushing (18K strokes, 60 strokes/min, 250 g) + Thermal cycling (3K cycles, 5 - 50°C, in artificial saliva)	10	Filtek Supreme	0.0264 (0.0030)	0.0845 (0.0118)	208	Nanofill composite together with two microhybrids (Ceram•X and Enamel Plus HFO) presented the lowest final roughness values.
					Artemis	0.0315 (0.0028)	0.3304 (0.0499)	965	
					Ceram•X	0.0357 (0.0024)	0.0780 (0.0067)	150	
					Enamel Plus HFO	0.0297 (0.0028)	0.0659 (0.0052)	133	
					Miris	0.0315 (0.0040)	0.2044 (0.0334)	545	
					Tetric Ceram	0.0337 (0.0041)	0.2182 (0.0293)	547	
					Venus	0.0335 (0.0024)	0.2645 (0.0264)	688	
Sof-Lex	de Moraes et al., 2009 [56]	Rugosi- meter	Toothbrushing (30K strokes, 4 Hz)	8	Filtek Supreme XT	0.09 (0.02)	0.12 (0.02)	33	Nanofill composite together with one microhybrid (Premise) presented the lowest final roughness values.
					Concept Advanced	0.09 (0.01)	0.16 (0.01)	78	
					Filtek Z250	0.24 (0.09)	0.27 (0.08)	13	
					Grandio	0.24 (0.04)	0.36 (0.04)	50	
					Premise	0.08 (0.01)	0.11 (0.02)	38	

				TPH 3	0.25 (0.08)	0.30 (0.09)	20	
Penteado et al., 2010 [79]	AFM	pH cycling (10 days: 6 h demineralizing solution + 18 h remineralizing solution)	12	Filtek Supreme	0.055 (0.006)	0.0522 (0.011)	-9,1	There were no differences among the final roughness values of the materials tested.
				Filtek Z250	0.056 (0.013)	0.0518 (0.0182)	-11	
Penteado et al., 2010 [79]	AFM	pH cycling (10 days: 6 h demineralizing solution + 18 h remineralizing solution) + Toothbrushing (50K cycles, 374 strokes/min, 200 g)	12	Filtek Supreme	0.055 (0.006)	0.2371 (0.0337)	336	There were no differences among the final roughness values of the materials tested.
				Filtek Z250	0.056 (0.013)	0.2287 (0.0218)	311	

* The paper did not provide baseline roughness values. It was not possible to calculate ΔRa .

2.4.2.4 Gloss retention

Toothbrushing was the surface challenge in 3 comparisons of gloss retention, and it was observed that nanofills and microhybrids performed similarly in 2 of those. Five comparisons were carried out after using another challenging methods or a combination of techniques, and none of those found differences among materials.

In total, 8 comparisons for the retention of gloss from 3 papers were analyzed (Table 2.6). Seven found no significant differences between materials, and 1 showed better results for nanofills compared with microhybrids. The positive result found for nanofills demonstrated that 2 microhybrids were poorer than the nanofill tested. One of those microhybrids performed similar to the nanofills in other tests. No submicron composite was tested in the papers selected for analysis of gloss retention.

Two variations of nanofills were tested. Filtek Supreme Plus was compared 3 times; in 2 comparisons, it was not different from at least 1 of the microhybrids to which it was compared. In the other comparison, the nanofill was better than the microhybrid. Filtek Supreme was tested 5 times, and it was always similar to at least one of the microhybrids tested.

Among the 8 comparisons, 4 performed the analysis with a measurement angle of 60°; 3 of these showed similar results for nanofills and microhybrids, and 1 indicated that the nanofill performed better than the microhybrids. The other 4 comparisons did not inform the angle used for analysis; they showed no significant differences between materials. Sof-Lex discs were the method mostly used for surface finishing (4), and no significant differences were observed between nanofills and microhybrids. The other 3 comparisons were performed with Enhance/PoGo as the finishing method, with only 1 comparison showing better results for nanofills.

Table 2.6 - Gloss retention according to the different polishing systems used in the studies

Polishing system	Author	Measurement angle	Aging method	N	Material	Baseline gloss (GU)	Final gloss (GU)	Δ GU (%)	Conclusion
Enhance / PoGo	da Costa et al., 2010 [35]	60°	Toothbrushing - Colgate Total (5760 strokes, 1 Hz, 100 g)	5	Filtek Supreme Plus	66 (8)	55 (12.55)	-17	Nanofill composite together with one microhybrid (Premise) presented the highest final gloss values.
					Filtek Z250	64 (5.26)	22 (2.13)	-66	
					Premise	64 (7.61)	45 (8.73)	-30	
	da Costa et al., 2010 [35]	60°	Toothbrushing - Colgate baking soda & peroxide whitening (5760 strokes, 1 Hz, 100 g)	5	Filtek Supreme Plus	68 (10.53)	36 (6)	-47	Nanofill composite presented higher final gloss values than the microhybrids.
					Filtek Z250	62 (10)	5 (2.25)	-92	
					Premise	71 (4.71)	23 (2.83)	-68	
	da Costa et al., 2010 [35]	60°	Toothbrushing - Colgate tartar control / whitening (5760 strokes, 1 Hz, 100 g)	5	Filtek Supreme Plus	66 (8.4)	33 (10.46)	-50	Nanofill composite together with one microhybrid (Premise) presented the highest final gloss values.
					Filtek Z250	63 (13.31)	8 (3)	-87	
					Premise	66 (5.34)	27 (3.32)	-59	
SiC paper	Barucci-Pfister & Göring, 2009 [48]	60°	Ethanol bath (240 h, ethanol 75%) + Toothbrushing (18K strokes, 60 strokes/min, 250 g) + Thermal cycling (3K cycles, 5 - 50 °C, in artificial saliva)	10	Filtek Supreme	51.0 (1.4)	46.3 (1.4)	-9,2	Nanofill composite together with two microhybrids (Ceram•X and Enamel Plus HFO) presented the highest final gloss values.
					Artemis	38.6 (6.1)	34.6 (3.0)	-10	
					Ceram•X	25.8 (3.2)	46.6 (0.8)	81	
					Enamel Plus HFO	32.9 (6.4)	49.2 (1.1)	50	
					Miris	27.9 (2.4)	37.1 (2.8)	33	
					Tetric Ceram	38.8 (4.0)	37 (2.1)	-4.6	
					Venus	32.4 (2.4)	37.6 (2.7)	16	
Sof-Lex	Gurgan & Yalcin Cakir, 2008 [52]	n.i.	10% carbamide peroxide (14 days, 2 h per day)	10	Filtek Supreme	94.7 (n.i.)	92.6 (n.i.)	-2.2	There were no differences among the final gloss values of the materials tested.
					Simile	94.6 (n.i.)	92.6 (n.i.)	-2.1	

Gurgan & Yalcin Cakir, 2008 [52]	n.i.	10% carbamide peroxide (14 days, 2 h per day) and Mouthrinse Oral-B (12 h immersion)	10	Filtek Supreme	95 (0.84)	90.9 (0.86)	-4.3	There were no differences among the final gloss values of the materials tested.
				Simile	94.7 (1.25)	90.7 (1.31)	-4.2	
Gurgan & Yalcin Cakir, 2008 [52]	n.i.	10% carbamide peroxide (14 days, 2 h per day) and Mouthrinse Listerine (12 h immersion)	10	Filtek Supreme	94.7 (1.02)	89.5 (1.01)	-5.5	There were no differences among the final gloss values of the materials tested.
				Simile	94.6 (1.04)	89.5 (0.98)	-5.4	
Gurgan & Yalcin Cakir, 2008 [52]	n.i.	10% carbamide peroxide (14 days, 2 h per day) and Mouthrinse Rembrandt Plus (12 h immersion)	10	Filtek Supreme	94.4 (0.88)	88.2 (0.94)	-6.6	There were no differences among the final gloss values of the materials tested.
				Simile	94.5 (1.06)	88.2 (1.04)	-6.7	

2.4.3 Overall results for polishing systems and composites

Figure 2.2 presents the results of surface roughness for clinically applicable finishing/polishing systems tested at least with 2 resin composites and evaluated with 3-D methods. The systems that presented the best results were the EP Esthetic polishing system (based on silicon carbide or aluminum coated discs) and polyester matrix. Both achieved the lowest roughness values as well as the most consistent results when applied with different composites. The poorest results were related to the use of either carbide or diamond burs. The burs were also the only systems presented herein that achieved roughness values above 0.3 μm , the threshold for clinical acceptability described by Jones et al. [39]. It is also important to highlight that Sof-Lex system was tested with 12 different resin composites; with all of them, Sof-Lex presented results below 0.2 μm , the threshold proposed by Bollen et al. [40].

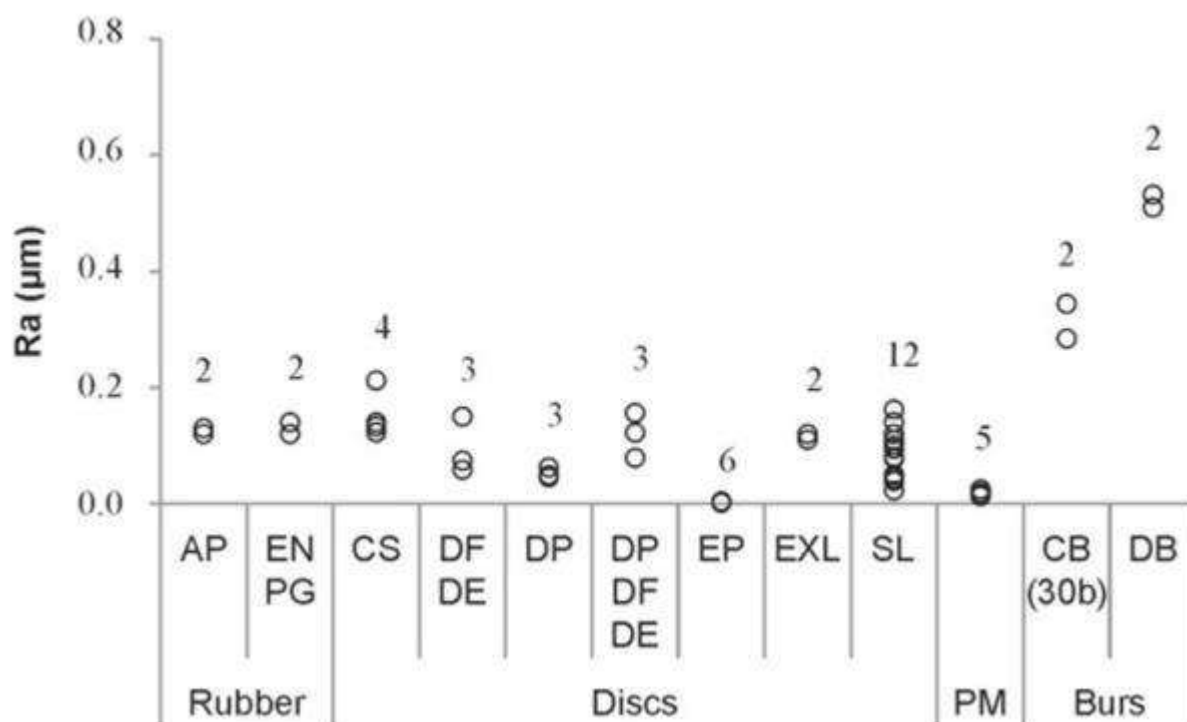


Figure 2.2 - Scatter chart of the roughness values achieved in 3-D evaluations by polishing system with clinical applicability, irrespective of the resin composite tested. Rubber = Rubber-based polishing systems: AP = Astropol, EN = Enhance, PG = PoGo; Discs = Disc-based polishing systems: CS = Compo system, DF = Diamond flex, DE = Diamond Excel, DP = Diamond pro, EP = EP Esthetic polishing system, EXL = EXL-695, SL = Sof-Lex; PM = Polyester matrix; Burs: CB (30b) = Carbide bur (30 blades), DB = Diamond bur.

Figure 2.3 presents the roughness results for resin composites tested with at least two polishing systems with clinical applicability and evaluated by 3-D methods. Filtek Supreme Plus, Esthet-X, Filtek Z250, Grandio, Synergy D6, and Tetric Ceram always presented roughness values lower than $0.3\text{ }\mu\text{m}$ [39]. The above-mentioned materials, except for Grandio, also presented results below $0.2\text{ }\mu\text{m}$ [40]. Filtek Supreme XT and Point 4 were the only composites that exceeded either of the thresholds for clinical acceptance.

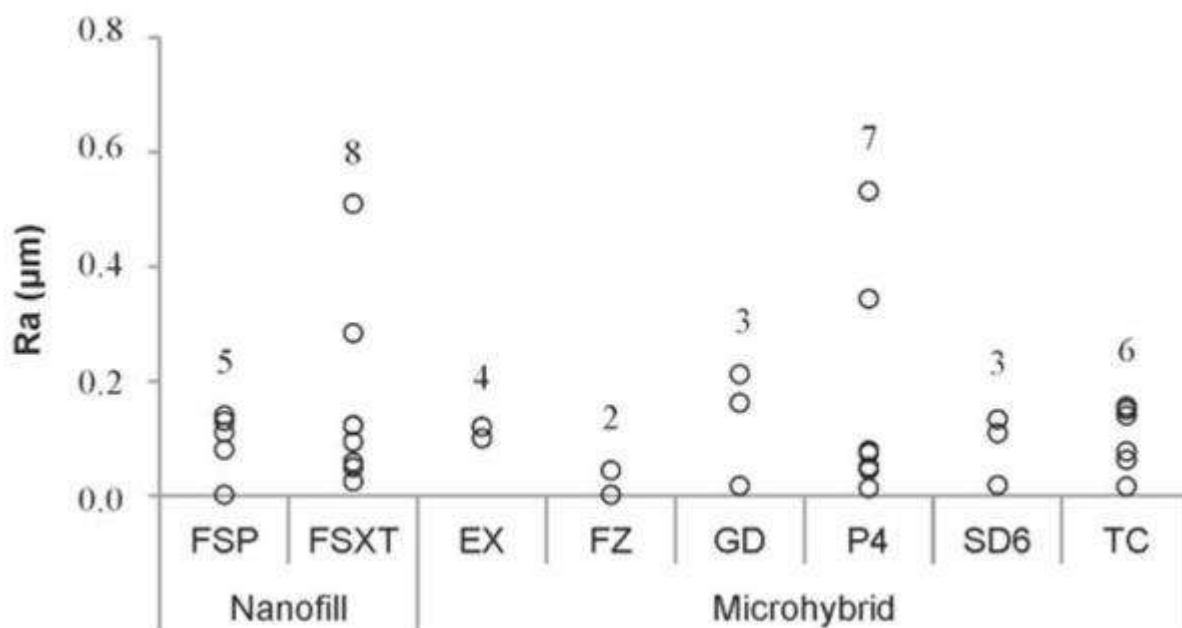


Figure 2.3 - Scatter chart of the roughness values achieved in 3-D evaluations by resin composites tested more than once, irrespective of the polishing system tested. Nanofill: FSP = Filtek Supreme Plus, FSXT = Filtek Supreme XT; Microhybrid: EX = Esthet-X, FZ = Filtek Z250, GD = Grandio, P4 = Point 4, SD6 = Synergy D6, TC = Tetric Ceram.

Figure 2.4 presents the roughness results of finishing/polishing systems and resin composites that behaved consistently when analyzed in Figures 2.2 and 2.3. Only materials tested more than once with 3-D methods and that did not present roughness values higher than the threshold of $0.2\text{ }\mu\text{m}$ [40] were included. Figure 2.4-A presents the results separately for finishing/polishing system. It is possible to observe that the EP Esthetics polishing system achieved much smoother surfaces than did other systems (consider results presented in logarithmic scale) but was tested only in one study. This was followed by polyester matrix, with only slight differences among the other systems. Figure 2.4-B presents the results separately for resin composites. The materials included herein were not greatly sensitive to the

polishing system applied except for those using the EP Esthetics polishing system. It is important to point out, however, that only the materials (finishing/polishing system + resin composite) with the best and more consistent results were included in these analyses.

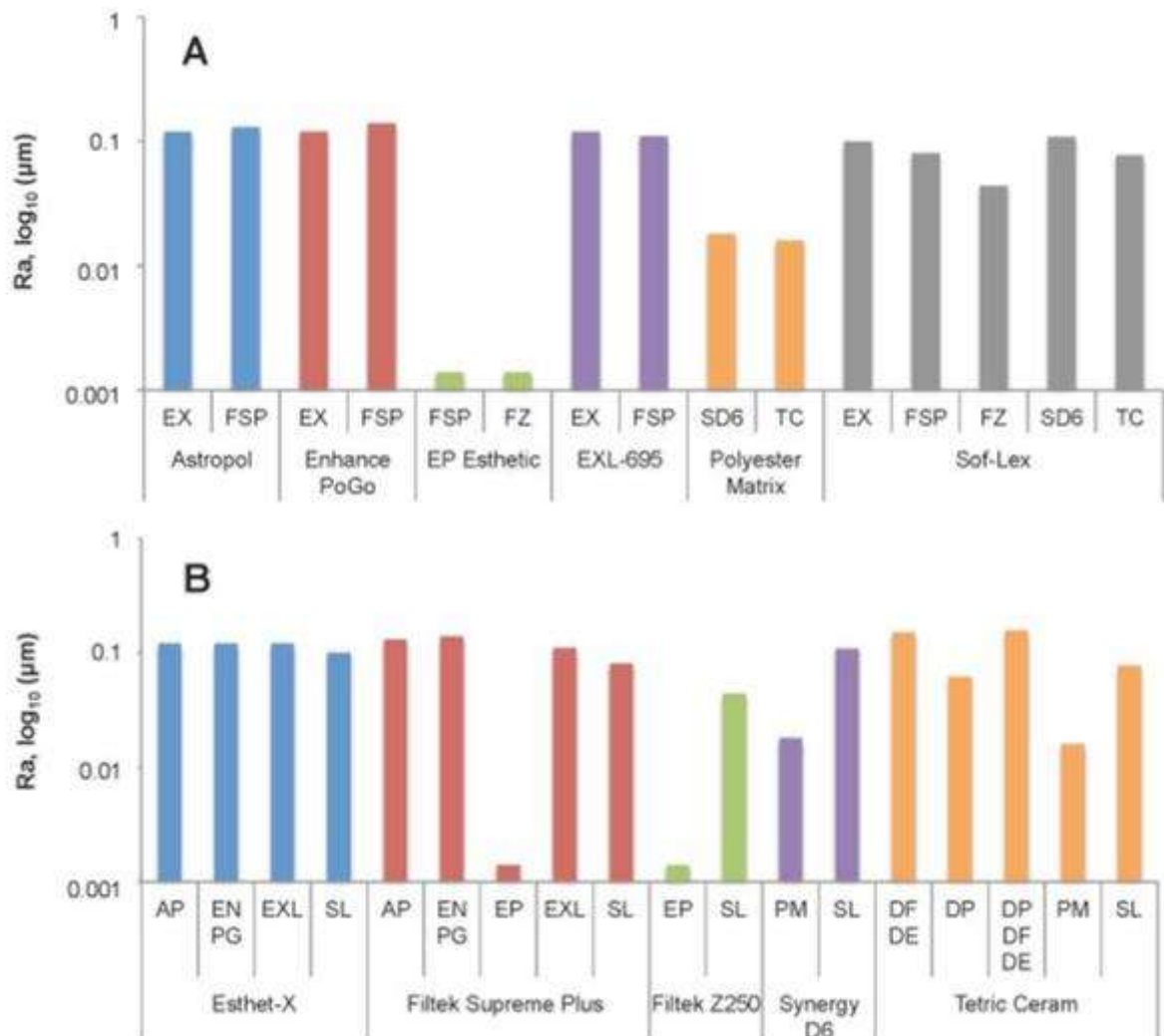


Figure 2.4 - Smoothness behavior of polishing systems (A) and resin composites (B). Only the resin composites and polishing systems that presented roughness values lower than 0.2 µm showed in Figure2.1 and Figure2.2, and also that were tested at least twice were considered in this analysis. (A): EX = Esthet-X, FSP = Filtek Supreme Plus, FZ = Filtek Z250, SD6 = Synergy D6, TC = Tetric Ceram. (B) AP = Astropol, DE = Diamond Excel, DF = Diamond Flex, DP = Diamond Pro, EN = Enhance, EP = EP Esthetic polishing system, EXL = EXL-695, PG = PoGo, PM = Polyester matrix, SL = Sof-Lex.

2.5 Discussion

Numerous studies have evaluated in vitro the smoothness and gloss of composites after finishing/polishing procedures, comparing nanofills or submicrons and traditional microhybrids (Tables 2.3 and 2.4). No solid evidence has been found to state conclusively that nanofills or submicrons present superior early smoothness or gloss (after finishing/polishing) than do microhybrids. Submicrons showed a slightly better smoothness performance than did nanofills when compared to microhybrids. However, submicrons were tested about six times less than were nanofills; thus, it is impossible to state that submicrons are indeed better than nanofills.

Dental materials manufacturers and the literature in general state that nanofills (and perhaps submicrons) may perform better than microhybrids due to the smaller size of the particles. The smoothest surfaces that could be extracted from the included studies were achieved by the EP system when polishing a nanofill composite and five microhybrid composites. The roughness values achieved with EP system were at least 3.6 times smoother than the best result showed with any other polishing system tested. The EP system was used for polishing composites in only one included study. Therefore, a question to be solved in future research is whether other polishing systems than those normally tested can lead to a smoother surface in nanofill composites than in microhybrids. Another very smooth surface in the investigated studies was achieved by a polyester matrix, which is not a clinically relevant surface as normally the surface has to be shaped and polished after removal of the matrix.

A superior performance regarding smoothness and gloss cannot be confirmed currently based on clinical evidence [5]; in addition, there is no summarization of in vitro evidence abundant in the literature. This may be explained because different finishing and polishing methods are reported or that different approaches were used to evaluate the surface properties, hindering comparisons among studies.

Reduction in filler particle size of composites has been traditionally linked to smoother surfaces. Current microhybrids, in general, have an average particle size up to 1 μm (Table 2.1), which is still significantly higher than the fillers in nanofills and submicrons. The complexity related to surface smoothness may explain the lack of differences among materials observed here. The present results indicate that

different types of finishing/polishing systems affect the performance of materials. In corroboration, Botta et al. [41] tested three strategies for polishing one nanofill and two microhybrids and found that the nanofill was smoother than the microhybrids with one polishing system, no difference with a second system, and rougher with the third polishing procedure. Another study [42] compared a nanofill with microhybrids using two polishing systems and found that the nanofill was always better; however, when a polyester matrix was used as the finishing method in the same study, the nanofill was rougher than the microhybrids. A similar situation was presented by Botta et al. [43], who found similar results between a nanofill and microhybrids with two polishing methods and poorer results for the nanofill when the polyester matrix was used. These results point to a negative effect of the polyester matrix over nanofill composites, although the evidence is still too limited. In addition, the results indicate that the surface properties of dental composites are dependent on both the restorative material and finishing/polishing system used.

When comparing the four types of nanofill composites studied, the results indicate that these are similar if not identical materials. Manufacturers tend to sell materials under different brand names in different countries or continents; further, it is usually not clear whether there are compositional differences between these materials, bringing considerable problems for researchers when comparing proprietary materials. It would be wise if identical materials were sold under the same brand name worldwide for better comparison among materials in the current literature.

While the finishing/polishing procedure may affect the ranking of materials, the influence of the evaluation method should also be considered. Kakaboura et al. [38] compared submicron and microhybrid materials using both the rugosimeter and AFM. The authors reported no differences among materials and higher roughness values when using AFM, while poorer performance for submicron and lower roughness values were observed with the rugosimeter. Surface topography is naturally 3-D; however, 2-D tactile profilometry is the most common measurement method (see Table 2.3) since it is widely available and relatively inexpensive. Tactile profilometry has been linked to underestimation of dental composites' surface roughness [38]. About 30% of the comparisons investigated herein were performed with non-contact 3-D methods, while 70% of the investigations used 2-D contact methods. Once

again, there is no solid evidence that nanofills or submicrons perform better than microhybrids, irrespective of the evaluation method.

The smoothness level of the surface has a significant impact on the gloss of resin composites [8, 14], although the gloss is also affected by other factors. Diffuse reflection is lower in composites with smaller filler particles, making the surface looks glossy [44]. Based on that, it has been assumed that, after polishing, nanofills and submicrons would have glossier surfaces than do microhybrids; nonetheless, the data analyzed in the present review do not support this assumption. Several studies showed that the polishing system plays an important role on the gloss and smoothness performance of resin composites [8, 45-47]. da Costa et al. [32] tested six finishing/polishing systems to compare performance of one nanofill and three microhybrids, and better gloss for the nanofill occurred with only one of the tested systems. It is known that metallographic polishing produces more planar, smoother surfaces than uncontrolled methods; thus, the gloss should also be lower for specimens polished with uncontrolled methods. However, among the studies included in the baseline gloss analysis, only one comparison was performed using metallographic polishing [48], and it presented better results for a nanofill. Nonetheless, the gloss values presented by Barucci-Pfister & Göhring [48] cannot be numerically compared with those from the other studies included because Barucci-Pfister & Göhring's [48] was the only study to apply a 45° measurement angle in the gloss analysis.

According to ISO 2813, ASTHD 523 and 2457, and DIN 67530, semigloss surfaces such as resin composites should be measured with a 60° angle of illumination, which is close to the angle the average person would observe the surface [38]. The literature seems to disagree on the best measurement angle for resin composites. According to Silikas et al. [47], a 20° angle produces measurement that more sensitively resolves differences in specular gloss than does a 60° angle. In contrast, Barucci-Pfister & Göhring [48] tested angles of 85°, 60°, 45°, and 20° and demonstrated that a 45° angle better differentiates materials. Considering the studies included in the baseline gloss analyses (Table 2.4), a 60° angle was used more often, yet no evidence was found of better performance of nanofills or submicrons over microhybrids. Interestingly, angles of 20° and 45° were used only once each; both studies [47, 48] showed that nanofill and submicron materials performed better than microhybrids.

Smoothness and gloss properties of resin composites have no agreed threshold for unacceptable values, although some studies endeavored to draw correlations between values to other investigations and to their clinical relevance [8, 33, 38, 42]. It has been reported that a material incapable of attaining and/or maintaining an Ra value below 0.2 μm in vitro would be susceptible to an increase in plaque accumulation and higher risk for caries and periodontal inflammation [40]. Whether this holds true for all resin composites has not been investigated, and the overall clinical performance of resin composite restorations is unlikely to be predicted by in vitro tests alone [49]. A clinical trial has shown that most patients could detect rough surfaces only when the Ra values were above 0.3 μm [39]. In the smoothness analyses of the present review, nanofills presented final roughness values (after surface challenges) up to 0.3 μm in about half of the comparisons. However, at least one microhybrid achieved the same performance in all of those comparisons. Only one comparison involved a submicron material that presented final roughness value of 0.4 μm after toothbrushing. Chung [50], in contrast, reported that restorations with roughness values below 1 μm could still be seen as smooth and glossy in vitro. All comparisons included in the smoothness retention analyses showed materials with final roughness values lower than 1 μm ; therefore, one could expect that in the gloss retention analysis, all materials would present acceptable gloss performance. The gloss behavior of polymers was classified by Cook & Thomas [51], who reported that with a 60° measurement angle, poor finish is generally considered to be below 60 GU, an acceptable finish between 60 and 70 GU, a good finish between 70 and 80 GU, and an excellent finish above 80 GU. Based on that, all comparisons included in the gloss retention analyses using a 60° measurement angle could be classified as having poor final gloss. The materials tested by Gurgan et al. [52] presented final gloss values above 80 GU; however, the authors did not inform the measurement angle applied, so the results cannot be classified according to Cook & Thomas [51]. The results of this systematic review of in vitro studies of reported thresholds for smoothness and gloss, as well as comparisons among nanofills, submicrons, and microhybrids, again showed no solid evidence to support that nanofills or submicrons are capable of maintaining smoothness and/or gloss better than are microhybrids.

2.6 Conclusions

Within the limitations of the present review, our hypothesis was confirmed: there is no current in vitro evidence that nanofill or submicron resin composites show improved smoothness or gloss over traditional microhybrids. Nanofills and submicrons were compared with several microhybrid composites using many commercial polishing systems and were submitted to different surface challenges. There is not enough evidence to support the choice of contemporary nanofill or submicron composites over traditional microhybrid materials based upon better surface smoothness and/or gloss, or based upon the maintenance of those superficial characteristics after surface challenges.

2.7 References

1. Kaleem M, Satterthwaite JD, Watts DC. Effect of filler particle size and morphology on force/work parameters for stickiness of unset resin-composites. *Dent Mater*, 2009;25:1585-92.
2. Karabela MM, Sideridou ID. Synthesis and study of properties of dental resin composites with different nanosilica particles size. *Dent Mater*, 2011;27:825-35.
3. Gonçalves F, Kawano Y, Braga RR. Contraction stress related to composite inorganic content. *Dent Mater*, 2010;26:704-9.
4. da Rosa Rodolpho PA, Donassollo TA, Cenci MS, Loguércio AD, Moraes RR, Bronkhorst EM, Opdam NJ, Demarco FF. 22-Year clinical evaluation of the performance of two posterior composites with different filler characteristics. *Dent Mater*, 2011;27:955-63.
5. Demarco FF, Corrêa MB, Cenci MS, Moraes RR, Opdam NJ. Longevity of posterior composite restorations: not only a matter of materials. *Dent Mater* 2012;28:87-101.
6. Kahler B, Kotousov A, Swain MV. On the design of dental resin-based composites: a micromechanical approach. *Acta Biomater*, 2008;4:165-72.
7. Cavalcante LM, Masouras K, Watts DC, Pimenta LA, Silikas N. Effect of nanofillers' size on surface properties after toothbrush abrasion. *Am J Dent*, 2009;22:60-4.
8. Heintze SD, Forjanic M, Ohmiti K, Rousson V. Surface deterioration of dental materials after simulated toothbrushing in relation to brushing time and load. *Dent Mater*, 2010;26:306-19.
9. Moher D, Liberati A, Tetzlaff J, Altman DG; PRISMA Group. Preferred reporting items for systematic reviews and meta-analyses: the PRISMA statement. *PLoS Med*, 2009;6:e1000097.
10. Bayne SC, Heymann HO, Swift Jr EJ. Update on dental composite restorations. *J Am Dent Assoc*, 1994;125:687–701.
11. Ferracane JL. Resin composite--state of the art. *Dent Mater*, 2011;27:29-38.
12. Choi MS, Lee YK, Lim BS, Rhee SH, Yang HC. Changes in surface characteristics of dental resin composites after polishing. *J Mater Sci Mater Med*, 2005;16:347-53.

13. Lee YK, Lu H, Oguri M, Powers JM. Changes in gloss after simulated generalized wear of composite resins. *J Prosthet Dent*, 2005;94:370-6.
14. Lu H, Roeder LB, Lei L, Powers JM. Effect of surface roughness on stain resistance of dental resin composites. *J Esthet Restor Dent*, 2005;17:102-9.
15. Mourouzis P, Koulaouzidou EA, Vassiliadis L, Helvatjoglu-Antoniades M. Effects of sonic scaling on the surface roughness of restorative materials. *J Oral Sci*, 2009;51:607-14.
16. Rinastiti M, Özcan M, Siswomihardjo W, Busscher HJ, van der Mei HC. Effect of biofilm on the repair bond strengths of composites. *J Dent Res*, 2010;89:1476-81.
17. Rinastiti M, Özcan M, Siswomihardjo W, Busscher HJ. Effects of surface conditioning on repair bond strengths of non-aged and aged microhybrid, nanohybrid, and nanofilled composite resins. *Clin Oral Investig*, 2011;15:625-33.
18. Rinastiti M, Özcan M, Siswomihardjo W, Busscher HJ. Immediate repair bond strengths of microhybrid, nanohybrid and nanofilled composites after different surface treatments. *J Dent*, 2010;38:29-38.
19. Suzuki T, Kyoizumi H, Finger WJ, Kanehira M, Endo T, Utterodt A, Hisamitsu H, Komatsu M. Resistance of nanofill and nanohybrid resin composites to toothbrush abrasion with calcium carbonate slurry. *Dent Mater J*, 2009;28:708-16.
20. Yeh ST, Wang HT, Liao HY, Su SL, Chang CC, Kao HC, Lee BS. The roughness, microhardness, and surface analysis of nanocomposites after application of topical fluoride gels. *Dent Mater*, 2011;27:187-96.
21. Jung M, Eichelberger K, Klimek J. Surface geometry of four nanofiller and one hybrid composite after one-step and multiple-step polishing. *Oper Dent*, 2007;32:347-55.
22. Jung M, Sehr K, Klimek J. Surface texture of four nanofilled and one hybrid composite after finishing. *Oper Dent*, 2007;32:45-52.
23. Koh R, Neiva G, Dennison J, Yaman P. Finishing systems on the final surface roughness of composites. *J Contemp Dent Pract*, 2008;9:138-45.
24. Rodrigues SA Jr, Ferracane JL, Della Bona A. Influence of surface treatments on the bond strength of repaired resin composite restorative materials. *Dent Mater*, 2009;25:442-51.
25. Schmitt VL, Puppini-Rontani RM, Naufel FS, Nahsan FP, Alexandre Coelho Sinhoreti M, Baseggio W. Effect of the polishing procedures on color stability and surface roughness of composite resins. *ISRN Dent*, 2011;2011:617672.

26. Yesil ZD, Alapati S, Johnston W, Seghi RR. Evaluation of the wear resistance of new nanocomposite resin restorative materials. *J Prosthet Dent*, 2008;99:435-43.
27. Curtin JA, Lu H, Milledge JT, Hong L, Peterson J. In vitro staining of resin composites by liquids ingested by children. *Pediatr Dent*, 2008;30:317-22.
28. Endo T, Finger WJ, Kanehira M, Utterodt A, Komatsu M. Surface texture and roughness of polished nanofill and nanohybrid resin composites. *Dent Mater J*, 2010;29:213-23.
29. Wang L, Francisconi LF, Atta MT, Dos Santos JR, Del Padre NC, Gonini A Jr, Fernandes KB. Effect of bleaching gels on surface roughness of nanofilled composite resins. *Eur J Dent*, 2011;5:173-9.
30. Topcu FT, Erdemir U, Sahinkesen G, Yildiz E, Uslan I, Acikel C. Evaluation of microhardness, surface roughness, and wear behavior of different types of resin composites polymerized with two different light sources. *J Biomed Mater Res B Appl Biomater*, 2010;92:470-8.
31. Mitra SB, Wu D, Holmes BN. An application of nanotechnology in advanced dental materials. *J Am Dent Assoc*, 2003;134:1382-90.
32. da Costa J, Ferracane J, Paravina RD, Mazur RF, Roeder L. The effect of different polishing systems on surface roughness and gloss of various resin composites. *J Esthet Restor Dent*, 2007;19:214-26.
33. Ergücü Z, Türkün LS. Surface roughness of novel resin composites polished with one-step systems. *Oper Dent*, 2007;32:185-92.
34. Attar N. The effect of finishing and polishing procedures on the surface roughness of composite resin materials. *J Contemp Dent Pract*, 2007;8:27-35.
35. da Costa J, Adams-Belusko A, Riley K, Ferracane JL. The effect of various dentifrices on surface roughness and gloss of resin composites. *J Dent*, 2010;38:e123-8.
36. da Silva JM, da Rocha DM, Travassos AC, Fernandes VV Jr, Rodrigues JR. Effect of different finishing times on surface roughness and maintenance of polish in nanoparticle and microhybrid composite resins. *Eur J Esthet Dent*, 2010;5:288-98.
37. Valinoti AC, Neves BG, da Silva EM, Maia LC. Surface degradation of composite resins by acidic medicines and pH-cycling. *J Appl Oral Sci*, 2008;16:257-65.
38. Kakaboura A, Fragouli M, Rahiotis C, Silikas N. Evaluation of surface characteristics of dental composites using profilometry, scanning electron, atomic force microscopy and gloss-meter. *J Mater Sci Mater Med*, 2007;18:155-63.

39. Jones CS, Billington RW, Pearson GJ. The in vivo perception of roughness of restorations. *Br Dent J*, 2004;196:42-5.
40. Bollen CM, Lambrechts P, Quirynen M. Comparison of surface roughness of oral hard materials to the threshold surface roughness for bacterial plaque retention: a review of the literature. *Dent Mater*, 1997;13:258-69.
41. Botta AC, Duarte S Jr, Paulin Filho PI, Gheno SM, Powers JM. Surface roughness of enamel and four resin composites. *Am J Dent*, 2009;22:252-4.
42. Janus J, Fauxpoint G, Arntz Y, Pelletier H, Etienne O. Surface roughness and morphology of three nanocomposites after two different polishing treatments by a multitechnique approach. *Dent Mater*, 2010;26:416-25.
43. Botta AC, Duarte S Jr, Paulin Filho PI, Gheno SM. Effect of dental finishing instruments on the surface roughness of composite resins as elucidated by atomic force microscopy. *Microsc Microanal*, 2008;14:380-6.
44. Alexander-Katz R, Barrera RG. Surface correlation effects on gloss. *J Polym Sci [B]*, 1998; 36:1321-34.
45. Antonson SA, Yazici AR, Kilinc E, Antonson DE, Hardigan PC. Comparison of different finishing/polishing systems on surface roughness and gloss of resin composites. *J Dent*, 2011;39:e9-17.
46. da Costa JB, Goncalves F, Ferracane JL. Comparison of two-step versus four-step composite finishing/polishing disc systems: evaluation of a new two-step composite polishing disc system. *Oper Dent*, 2011;36:205-12.
47. Silikas N, Kavvadia K, Eliades G, Watts D. Surface characterization of modern resin composites: a multitechnique approach. *Am J Dent*, 2005;18:95-100.
48. Barucci-Pfister N, Göhring TN. Subjective and objective perceptions of specular gloss and surface roughness of esthetic resin composites before and after artificial aging. *Am J Dent*, 2009;22:102-10.
49. Ferracane JL. Resin-based composite performance: Are there some things we can't predict? *Dent Mater*, 2013;29:51-8.
50. Chung KH. Effects of finishing and polishing procedures on the surface texture of resin composites. *Dent Mater*, 1994;10:325-30.
51. Cook MP, Thomas K. Evaluation of gloss meters for measurement of moulded plastics. *Polym Test*, 1990;9:233-44.

52. Gurgan S, Yalcin Cakir F. The effect of three different mouthrinses on the surface hardness, gloss and colour change of bleached nano composite resins. *Eur J Prosthodont Restor Dent*, 2008;16:104-8.
53. Sabbagh J, Ryelandt L, Bachérius L, Biebuyck JJ, Vreven J, Lambrechts P, Leloup G. Characterization of the inorganic fraction of resin composites. *J Oral Rehabil*, 2004;31:1090-101.
54. Hubbezoglu I, Akaoğlu B, Dogan A, Keskin S, Bolayir G, Ozçelik S, Dogan OM. Effect of bleaching on color change and refractive index of dental composite resins. *Dent Mater J*, 2008;27:105-16.
55. Hosoya Y, Shiraishi T, Odatsu T, Ogata T, Miyazaki M, Powers JM. Effects of specular component and polishing on color of resin composites. *J Oral Sci*, 2010;52:599-607.
56. de Moraes RR, Gonçalves L de S, Lancellotti AC, Consani S, Correr-Sobrinho L, Sinhoreti MA. Nanohybrid resin composites: nanofiller loaded materials or traditional microhybrid resins? *Oper Dent*, 2009;34:551-7.
57. Çelik EU, Aladağ A, Türkün LŞ, Yılmaz G. Color changes of dental resin composites before and after polymerization and storage in water. *J Esthet Restor Dent*, 2011;23:179-88.
58. Erdemir U, Yildiz E, Eren MM, Ozsoy A, Topcu FT. Effects of polishing systems on the surface roughness of tooth-colored materials. *J Dent Sci*. 2013; DOI: 10.1016/j.jds.2012.05.007.
59. Gönülol N, Yılmaz F. The effects of finishing and polishing techniques on surface roughness and colour stability of nanocomposites. *J Dent*, 2012;40:e64-70.
60. Sideridou ID, Karabela MM, Vouvoudi EC. Physical properties of current dental nanohybrid and nanofill light-cured resin composites. *Dent Mater*, 2011;27:598-607.
61. Ilie N, Hickel R. Investigations on mechanical behaviour of dental composites. *Clin Oral Investig*, 2009;13:427-38.
62. Furuse AY, Gordon K, Rodrigues FP, Silikas N, Watts DC. Colour-stability and gloss-retention of silorane and dimethacrylate composites with accelerated aging. *J Dent*, 2008;36:945-52.
63. Melander J, Dunn WP, Link MP, Wang Y, Xu C, Walker MP. Comparison of flexural properties and surface roughness of nanohybrid and microhybrid dental composites. *Gen Dent*, 2011;59:342-9.

64. Zhou M, Drummond JL, Hanley L. Barium and strontium leaching from aged glass particle/resin matrix dental composites. *Dent Mater*, 2005;21:145-55.
65. Johnston WM, Reisbick MH. Color and translucency changes during and after curing of esthetic restorative materials. *Dent Mater*, 1997;13:89-97.
66. Papadogiannis DY, Lakes RS, Papadogiannis Y, Palaghias G, Helvatjoglu-Antoniades M. The effect of temperature on the viscoelastic properties of nano-hybrid composites. *Dent Mater*, 2008;24:257-66.
67. Rastelli AN, Jacomassi DP, Faloni AP, Queiroz TP, Rojas SS, Bernardi MI, Bagnato VS, Hernandez AC. The filler content of the dental composite resins and their influence on different properties. *Microsc Res Tech*, 2012;75:758-65.
68. Uhl A, Michaelis C, Mills RW, Jandt KD. The influence of storage and indenter load on the Knoop hardness of dental composites polymerized with LED and halogen technologies. *Dent Mater*, 2004;20:21-8.
69. Hadis M, Leprince JG, Shortall AC, Devaux J, Leloup G, Palin WM. High irradiance curing and anomalies of exposure reciprocity law in resin-based materials. *J Dent*, 2011;39:549-57.
70. Sabatini C, Campillo M, Hoelz S, Davis EL, Munoz CA. Cross-compatibility of methacrylate-based resin composites and etch-and-rinse one-bottle adhesives. *Oper Dent*, 2012;37:37-44.
71. Senawongse P, Pongprueksa P. Surface roughness of nanofill and nanohybrid resin composites after polishing and brushing. *J Esthet Restor Dent*, 2007;19:265-75.
72. Başeren M. Surface roughness of nanofill and nanohybrid composite resin and ormocer-based tooth-colored restorative materials after several finishing and polishing procedures. *J Biomater Appl*, 2004;19:121-34.
73. Marghalani HY. Effect of finishing/polishing systems on the surface roughness of novel posterior composites. *J Esthet Restor Dent*, 2010;22:127-38.
74. Ozel E, Korkmaz Y, Attar N, Karabulut E. Effect of one-step polishing systems on surface roughness of different flowable restorative materials. *Dent Mater J*, 2008;27:755-64.
75. Korkmaz Y, Ozel E, Attar N, Aksoy G. The influence of one-step polishing systems on the surface roughness and microhardness of nanocomposites. *Oper Dent*, 2008;33:44-50.
76. Turssi CP, Ferracane JL, Serra MC. Abrasive wear of resin composites as related to finishing and polishing procedures. *Dent Mater*, 2005;21:641-8.

77. Yap AU, Yap SH, Teo CK, Ng JJ. Comparison of surface finish of new aesthetic restorative materials. *Oper Dent*, 2004;29:100-4.
78. Teixeira EC, Thompson JL, Piascik JR, Thompson JY. In vitro toothbrush-dentifrice abrasion of two restorative composites. *J Esthet Restor Dent*, 2005;17:172-82.
79. Penteado RA, Tonholo J, Júnior JG, Silva MF, Queiroz C da S, Cavalli V, Rego MA, Liporoni PC. Evaluation of surface roughness of microhybrid and nanofilled composites after pH-cycling and simulated toothbrushing. *J Contemp Dent Pract*, 2010;11:E017-24.
80. Catelan A, Briso AL, Sundfeld RH, Dos Santos PH. Effect of artificial aging on the roughness and microhardness of sealed composites. *J Esthet Restor Dent*, 2010;22:324-30.

3Capítulo 2

One-step silica coating of crystalline, non-silicate ceramic nanoparticles –
Prospecting improved hybrid biomaterials¹

Marina R. Kaizer^a, Julia A. Rosa^a, Ana Paula R. Gonçalves^a, Hui Tong^b, Yu Zhang^b,
Sergio S. Cava^c, Rafael R. Moraes^a

^aSchool of Dentistry, Federal University of Pelotas, RS - Brazil

^bCollege of Dentistry, New York University, NY - USA

^cSchool of Materials Engineering, Federal University of Pelotas, RS - Brazil

Corresponding author:

Prof. Rafael R. Moraes – E-mail: moraesrr@gmail.com

School of Dentistry, Federal University of Pelotas

Rua Gonçalves Chaves 457, room 505

96015-560 Pelotas-RS, Brazil

Phone/Fax: 55 53 3225.6741 x.135

¹Artigo estruturado segundo as normas do periódico *RSC _ CrystEngComm*(FI JCR 2013: 3.86).

3.1 Abstract

This study was designed to develop and characterize an one-step silica coating method for

crystalline, non-silicate ceramic nanoparticles (Al_2O_3 , TiO_2 , and ZrO_2). This method would allow particle silanization and further use of the coated nanoparticles as reinforcing phase in the prospecting of improved hybrid biomaterials. The one-step silica coating was obtained by a sol-gel method. It involved immersing the particles into an aqueous hydrochloric acid solution, to which tetraethyl orthosilicate was added, followed by calcination for deposit of crystalline silica around the particles. The nanopowders had their chemical and microstructural characteristics evaluated before and after silica-coating by means of EDS, XRD, BET, FE-SEM, and TEM. Results of all analyses corroborated the success of the purposed one-step silica coating method. Two distinct aspects were observed depending on the type of nanoparticle modified: a silica shell on the nanoparticles' surface or clusters of nanoparticles embedded into a silica matrix. Therefore, the one-step silica coating method presented here is a viable and promising novel strategy for the use of crystalline, non-silicate ceramics as reinforcing phase of polymeric hybrid biomaterials.

Keywords: 3D scaffolds; ceramics; composites; core-shell; hybrid materials; nanoparticles; nanotechnology; non-silicate ceramics; porous structures; sol-gel; silica coating.

3.2 Introduction

The use of nanoparticles for the development or modification of hybrid biomaterials has been vastly investigated in recent years. A wide variety of particles has been tested, including calcium phosphate nanoparticles,¹ cross-linked polymeric nanogels,² and titanium dioxide or hydroxyapatite nanofibers.³ Nanoparticles used in hybrid biomaterials can have markedly distinct composition, characteristics, and properties, therefore distinct applicability, ranging from structural reinforcement to drug-delivery functionality and so on.¹⁻⁵

A relevant class within the hybrid biomaterials covers the polymer-based composites. Those are often reinforced by glass or ceramic nanoparticles⁶⁻⁹ or, more recently, by porous 3D scaffolds of pressed ceramic nanoparticles that are infiltrated by the polymer matrix.¹⁰ An effective reinforcement of the polymer matrix is yielded by using organo-silanes, also referred to as silane coupling agents.¹¹⁻¹⁸ These substances act at the interface of the matrix and the reinforcing particles, promoting chemical interfacial interaction between the two phases.¹¹⁻¹⁸

The need for silanization restricts the use of non-silicate ceramic particles for reinforcing hybrid materials, as non-silicate ceramics are not reactive to silanes. To the authors' knowledge, currently only one strategy is effectively used to overcome this drawback: the clustering of silica and zirconia nanoparticles.¹⁹ Although effective, this approach needs chemical interference with the crystals during their synthesis, thus it is not useful in the modification of crystallized ceramic powders. In addition, it is a proprietary approach and, since its publication, limited to one type of ceramic nanoparticle (zirconia).

The development of an innovative method to make each and every type of non-silicate ceramic particle prone to silanization would widen the investigation, development, and modification of hybrid biomaterials containing ceramic particles of varied chemistry and physical characteristics. Therefore, this study was designed to develop and characterize an one-step silica coating method for crystalline, non-silicate ceramic nanoparticles that would allow silanization and further use of the modified particles as reinforcing agents in polymeric improved hybrid biomaterials.

3.3 Experimental

3.3.1 Materials

Three types of crystalline, non-silicate ceramic nanoparticles were used as received (Nanoamor, Houston, USA): aluminum oxide gamma (Al_2O_3 - 99.97%), commercially available under the trade name 1020MR; titanium oxide anatase (TiO_2 - 99%), commercially available under the trade name 5420HT; and zirconium oxide monoclinic (ZrO_2 - 99%), commercially available under the trade name 5931HT. For the one-step silica coating process, the powders were immersed in a tetraethylorthosilicate (TEOS) solution (Sigma-Aldrich, St. Louis, MO, USA) and calcinated as further described in item 3.3.2. Therefore, six groups were tested: Alumina (Al), Silica-coated alumina (AlS), Titania (Ti), Silica-coated titania (TiS), Zirconia (Zr), and Silica-coated zirconia (ZrS).

3.3.2 One-step silica coating method

The as-received nanoparticles were coated with a silica layer applied by a sol-gel method. For the silica coating, the particles were dispersed in a solution of 1 M hydrochloric acid P.A. (Synth, São Paulo, SP, Brazil) and 10 M distilled water. The suspension was kept in vigorous magnetic stirring for 15 min to favor disaggregation due to ionization of the particles. According to a pilot study, TEOS was added to the suspension in the proportion of 40 vol% relative to the volume of nanoparticles, adjusting the amount of TEOS according to the density of each material. Vigorous magnetic stirring was maintained and the temperature risen to 60°C to evaporate the aqueous content. After drying, the particles were heat-treated in an air atmosphere oven with 5°C/min heating rate up to 900°C dwell temperature for 2 h.

3.3.3 Microstructural and chemical characterization of the ceramic powders

The micromorphology of the nanoparticles with and without silica coating was analyzed by field emission scanning electron microscopy – FE-SEM (Merlin, Zeiss, Jena, Germany) and by transmission electron microscopy – TEM (JEM 1400, JEOL, Tokyo, Japan). For elemental chemical composition, the nanopowders were analyzed using energy-dispersive X-ray spectroscopy – EDS (JSM 6610, JEOL). Crystalline phases and crystal sizes were determined by X-ray diffraction – XRD (XRD-6000; Shimadzu, Tokyo, Japan) with $\text{CuK}\alpha$ radiation at 40 kV and 40 mA,

scan rate of 4°/min, 10–80°, at room temperature. The specific surface area and average particle size of the powders were determined by BET method with a surface area analyzer (Quantachrome Nova 1000e; Boynton Beach, FL, USA), by means of N₂ adsorption/desorption isotherm analysis.

3.4 Results and Discussion

Results for the elemental composition, particle size, specific surface area, crystal size, and crystalline phases of all particles are shown in Table 3.1. The EDS elemental analysis showed the presence of silicon only for powders submitted to the silica coating method. It was noticed that higher specific surface area of the as-received powders (Al > Ti > Zr) was associated with higher percentage of silicon after silica-coating, both weight and atom percent. Nanoparticles have a significant part of their atoms on their surfaces and the smaller the particle the more pronounced is the quantum effect on them. The quantum effect or quantum confinement of nanoparticles makes them prone to distinct surface interactions, ranging from simple agglomeration within the powder particles to adsorption of other substances to which they are exposed to.^{20,21}

The particle size analysis before the silica coating showed that all three powders were below 100 nm, alumina being the smallest particles, followed by titania, then zirconia. The BET diameter increased after silica coating, although only TiS particles were above 100 nm, outside the nanometer range. This finding indicates a much greater increase in particle size for titania under the conditions of the silica coating method described here. The crystal size evaluated by XRD also showed increase in crystal size for TiS groups, whereas the same did not happen for alumina or zirconia powders. It may be assumed that the increase in particle size for AIS and ZrS was due to the crystalline silica shell deposited on the surface of the particles, with no association to crystal growth or phase transformation of Al and Zr (Fig. 3.1).^{22,23} This is also corroborated by the presence of quartz only in silica-coated particles. It should be pointed out that no silica peaks in the XRD analysis were detected for any particles tested because the content of quartz phase estimated in ~0.1% (Table 3.1) is below the 2% accuracy of the equipment.

TEM images of the nanopowders (Fig. 3.2) indicated the presence of a silica shell around zirconia and alumina particles. In Figure 3.2-a (red arrows) it is possible to observe the zirconia nanoparticle (darker area at the center) surrounded by a silica layer (grayish area). The thickness of the silica layer seems to vary according to the diameter of the zirconia particles, as visible when the two examples pointed by red arrows in Fig. 3.2-a are compared. Visual particle sizes corroborate the findings of BET and XRD, with AIS particles (Fig. 3.2-b) being much smaller than ZrS (Fig. 3.2-a) and TiS (Fig. 3.2-c) particles.

Table 3.1 - Characterizations of the ceramic powders: elemental composition (EDS), particle size and specific surface area (BET), crystal size and crystalline phases (XRD).

	EDS _ wt%			EDS _ atom%			Surface area, m ² /g	Particle size, nm	Crystal size, nm	Crystalline phases
	O	*	Si	O	*	Si				
Al	15.7	84.3	-	24.0	76.0	-	193.2	8.4	4.7	Gamma 100%
AlS	10.7	83.6	5.7	16.9	78.0	5.1	91.1	17.8	5.2	Gamma 99.99% + Quartz 0.1%
Ti	12.9	87.1	-	30.7	69.3	-	91.9	16.7	25.1	Anatase 100%
TiS	5.4	92.0	2.6	14.5	81.7	3.9	7.3	209.5	88.5	Anatase 97.2% + Rutile 2.7% + Quartz 0.1%
Zr	2.1	98.0	-	10.8	89.2	-	27.3	37.3	32.9	Monoclinic 100%
ZrS	2.4	96.5	1.1	12.1	84.9	3.1	12.5	81.2	36.2	Monoclinic 99.99% + Quartz 0.1%

*Content of Al, Ti, or Zr according to the material under evaluation.

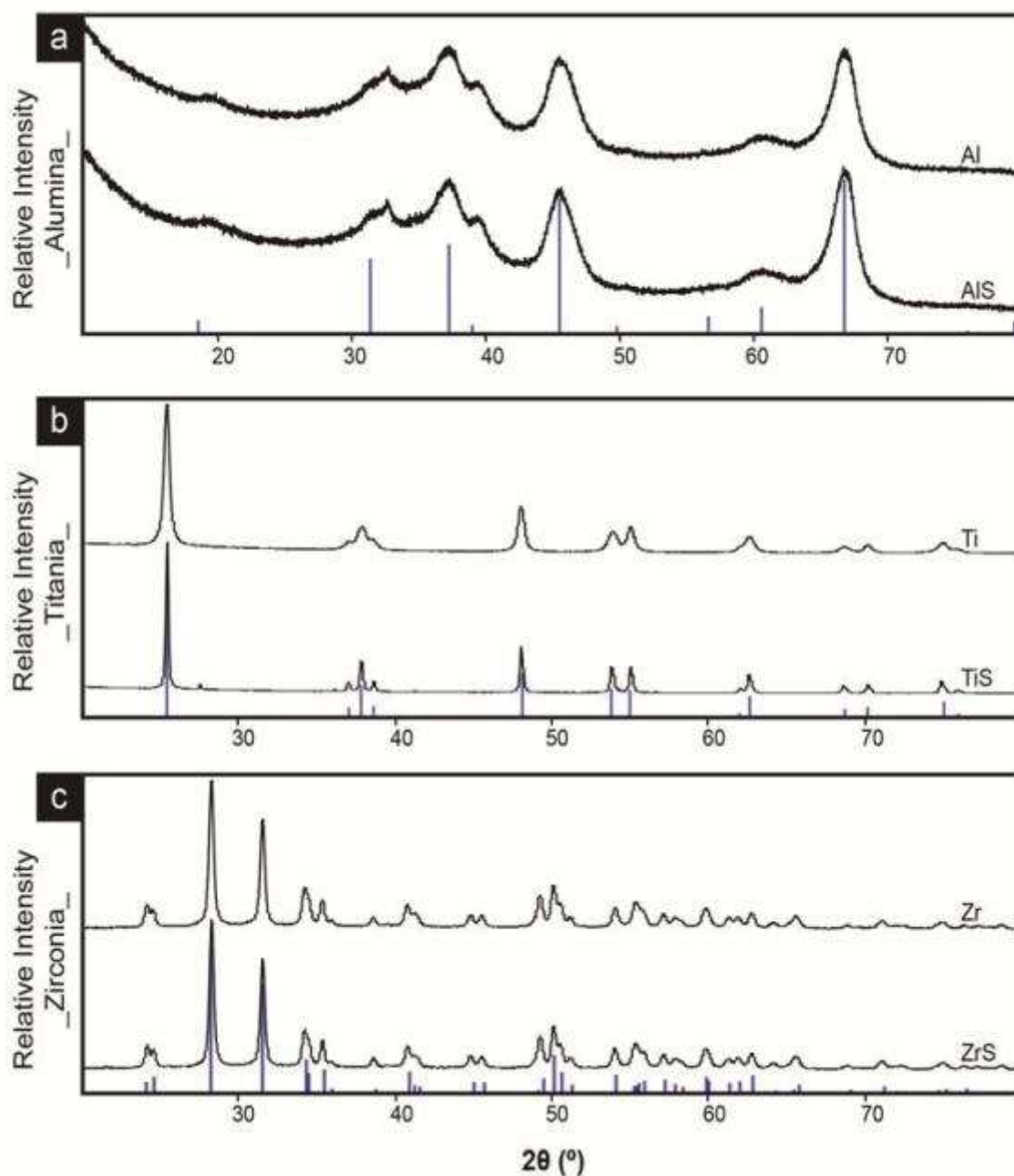


Figure 3.1 -X-ray diffraction spectra of the nanopowders with and without silica coating: (a) Spectral pattern of gamma alumina crystalline phase for Al and AIS. (b) Spectral pattern of anatase crystalline phase for Ti and predominantly anatase with rutile peaks for TiS. (c) Spectral pattern of monoclinic zirconia crystalline phase for Zr and ZrS. Silica peaks are not visible for any of the coated particles because the estimated content of quartz phase (0.1%) is below the 2% precision of the equipment.

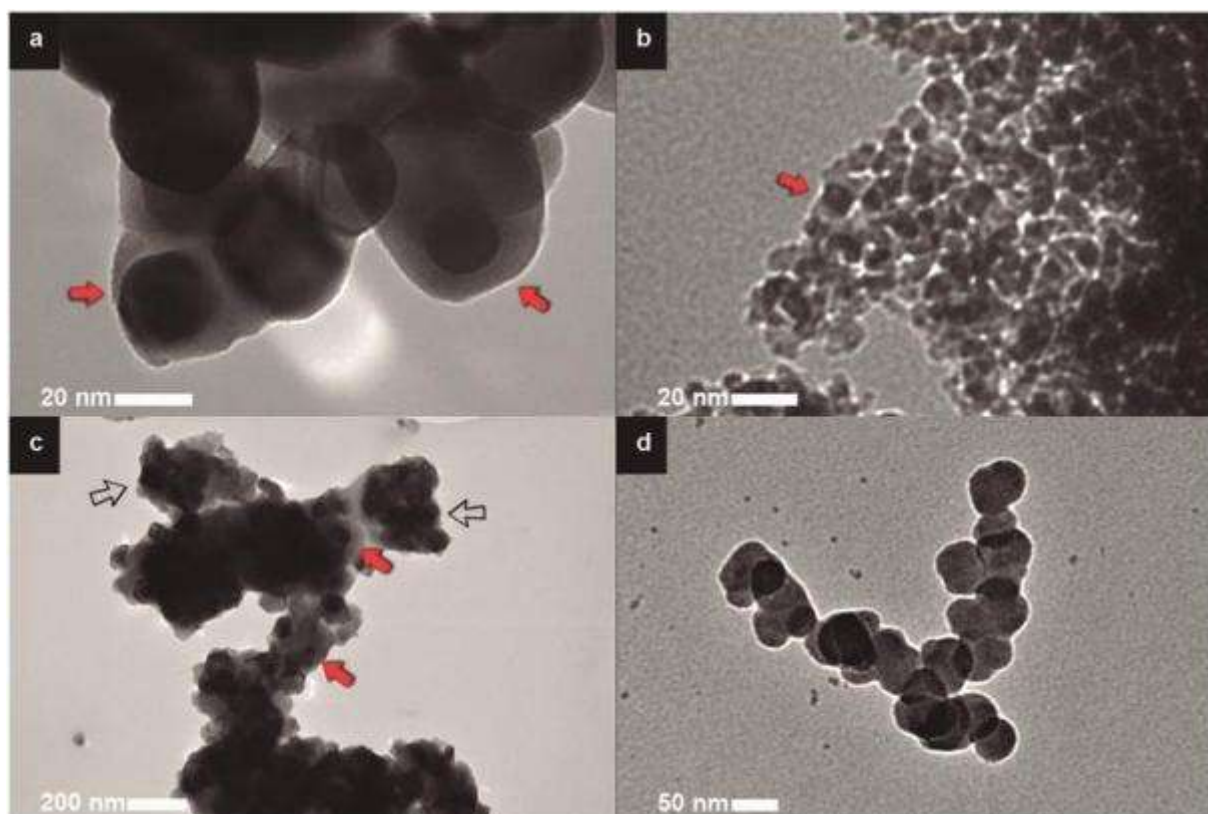


Figure 3.2 - TEM images of the nanopowders: (a) Silica-coated zirconia particles ($\times 1.2\text{M}$ magnification). The red arrows indicate the zirconia nanoparticle (darker area at the center) surrounded by a silica layer (grayish area). The thickness of the silica layer seems to vary according to the diameter of the zirconia particles, as visible when the two examples pointed by red arrows are compared. (b) Silica-coated alumina particles ($\times 1\text{M}$ magnification). Discrete nanoparticles much smaller than the other particles are observed. The red arrow points to an example of a coated particle. (c) Silica-coated titania particles ($\times 100\text{k}$ magnification). Most particles are seen embedded into clusters with a silica matrix (hollow black arrows), while some coated particles are also present (red arrows). (d) Silica nanoparticles ($\times 300\text{k}$ magnification) observed most likely as a result of a secondary phase formation during calcination of TEOS molecules not bounded to the nanopowders in the solution used in the silica coating method.

In contrast to the findings for AIS and ZrS particles, the coating method yielded a substantial increase in titania particle size, which may be attributed to crystal growth and phase transformation during coating.²⁴ After the silica-coating of Ti, 2.7% rutile was detected in the particles that were originally 100% anatase. XRD analyzes of the Ti nanopowders with and without silica coating are other evidences for the increase in particle size being a result of crystal growth and phase transformation. The TEM images further indicate that the increased BET diameter is not only explained by crystal growth and phase transformation, but also by clustering of titania particles embedded in a silica matrix (hollow black arrows in Figure 3.2-c), while some discrete coated particles are also present (red arrows). The clusters appear to be ~200 nm in diameter in the TEM images, which is in line with BET diameter measured for TiS. Successful silica coating was demonstrated in this study, with three types of non-silicate ceramic nanoparticle of distinct chemistry and physical characteristics. The presented method makes the particles prone to silanization and, therefore, prone to be used as effective reinforcement of a polymer matrix.¹¹⁻¹⁸ In the TEM analysis, the presence of silica nanoparticles was also observed (Figure 3.2-d), most likely a result of a secondary phase formation during calcination of TEOS molecules not bounded to the particles in the solution. Those particles are naturally reactive to silanes and would add to the reinforcement of the polymeric matrix. No negative effect is expected by their presence.

FE-SEM images of the nanopowders are presented in Figure 3.3. The FE-SEM analysis again corroborates that the Al group has the smallest particles (Fig. 3.3-a). It is important to point out that the particles of the three groups became highly reactive after silica coating. The images presented in Figure 3.3-b were taken using a shorter scanning time and yet for TiS group a wider field width was necessary for a precise imaging of the coated particles. These strategies were adopted to prevent fusing and apparent growth of particles as a reaction to the energy of the microscope beam and resulting heat generated with it. Most of the TiS particles are embedded into clusters with a silica matrix, which does not seem to happen with the other particles (Fig. 3.3-b), corroborating the findings of the TEM analysis. The effects of the high reactivity of the particles are shown in Figure 3.3-c, represented by the areas in the field pointed by red arrows showing particles fused together. This effect is clearly seen for ZrS (Fig. 3.3-c), where the fusing started at the reduced focus area in the center of the field. In addition, Figure 3.3-d shows the uncontrolled fusing of particles caused by the

energy of the beam, taking over the entire field, generating a 3D porous structure. Formation of these porous structures was not the primary aim of the silica coating method; however, there is potential applicability of those scaffolds as 3D networks preformed for further polymer infiltration and formation of hybrid biomaterials for CAD-CAM milling.^{10,25-28}

The investigation, development, and modification of polymer-based composites reinforced by glass or ceramic nanoparticles⁶⁻⁹ has been a constant throughout the years in biomaterials science. More recently, polymer-based composites with interpenetrating phases, a porous 3D ceramic scaffold infiltrated by a polymer matrix, has drawn the attention of some researchers with promising results.^{10,25-28} However, the use of crystalline, non-silicate particles has not yet been tested for the development of such materials. Therefore, the success of the versatile one-step silica coating method for non-silicate crystalline ceramic particles presented herein prospects the development of novel improved polymer-based composites reinforced by either ceramic particles or 3D porous scaffolds.

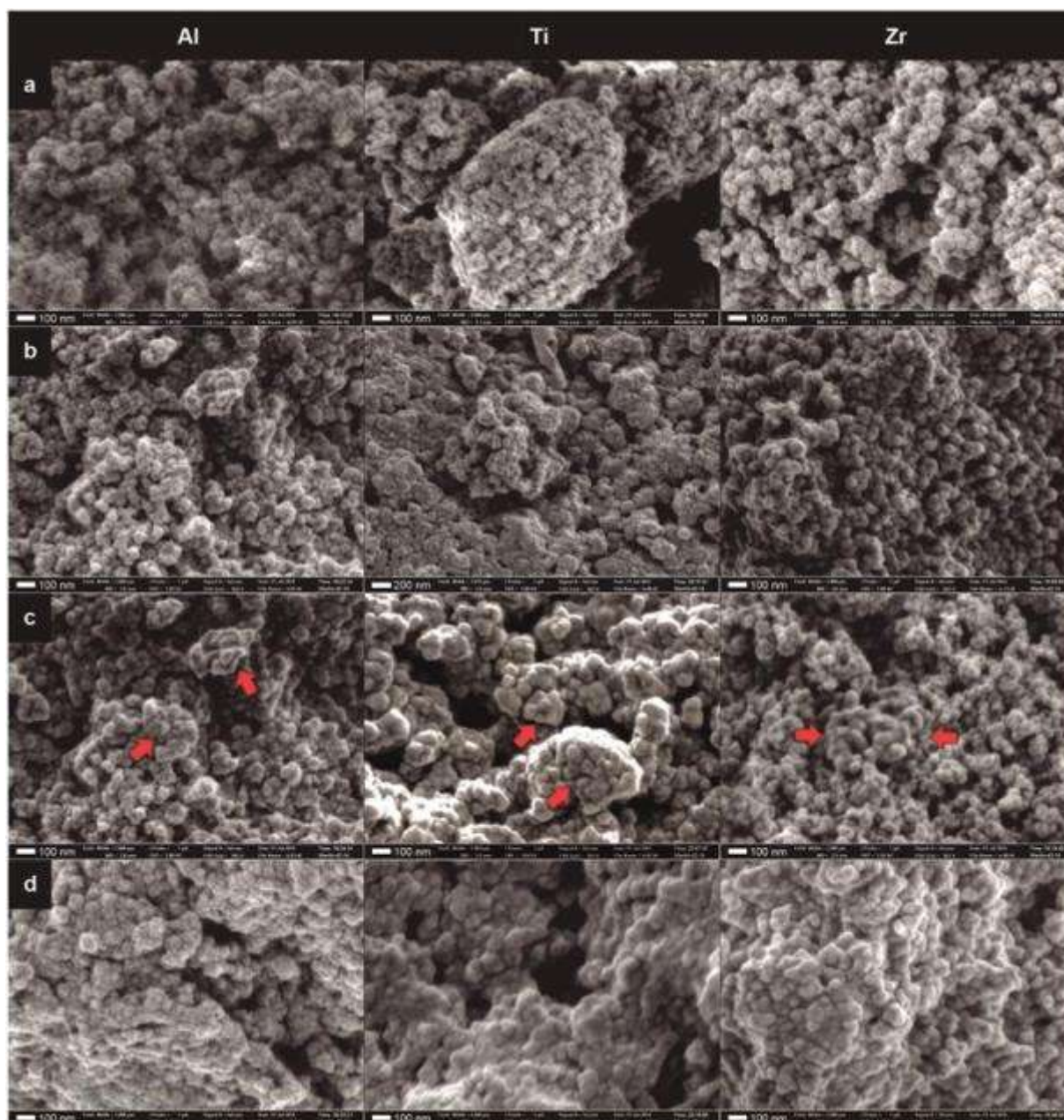


Figure 3.3– FE-SEM images of the nanopowders: (a) Image of the nanopowders as received in a field width of $2\text{ }\mu\text{m}$ (equivalent to approximately $\times 180\text{k}$ magnification). Alumina particles are visibly smaller than the other particles. (b) Image of the nanopowders after silica coating. Alumina and zirconia were imaged in a field width of $2\text{ }\mu\text{m}$, while for TiS a field width of $3.931\text{ }\mu\text{m}$ (equivalent to approximately $\times 90\text{k}$ magnification) was chosen for better imaging. Most of the Ti particles are embedded into clusters with a silica matrix, which does not seem to happen with the other particles. All particles became highly reactive after silica coating, as visible in (c), where some areas in the field pointed by red arrows show the particles fused together as a reaction to the energy of the microscope beam. This is clearly seen for the ZrS image, where the fusing started by the reduced focus area in the center of the field. (d) images showing the uncontrolled fusing of particles, caused by the energy of the beam, taking over the entire field, generating a 3D porous structure. For all images in (c) and (d) a field width of $2\text{ }\mu\text{m}$ was used.

3.5 Conclusion

The one-step silica coating proposed here was obtained by immersing the nanopowders in a tetraethyl orthosilicate solution, followed by appropriate calcination. The method presented in this study was successful, yielding two distinct aspects depending on the type of nanoparticle modified: silica shell on the surface of the nanoparticles, or clusters of nanoparticles embedded into a silica matrix. Therefore, this one-step silica coating method might be considered a promising novel strategy for the use of crystalline, non-silicate ceramic nanopowders as reinforcing phase of polymeric hybrid biomaterials.

3.6 Acknowledgements

CNPq – Conselho Nacional de Desenvolvimento Científico e Tecnológico – Brazil: Process # 141129/2011-5 (PhD scholarship - GD); Process # 241021/2012-0 (PhD internship abroad – SWE); Process # 475462/2012-2 (Grant – CNPq Universal).

Chemistry Department at New York University – USA. The Zeiss Merlin FESEM was acquired through the support of the National Science Foundation under Award Number DMR-0923251.

CEME-Sul – Centro de Microscopia Eletrônica da Zona Sul at Federal University of Rio Grande – Brazil for TEM support.

IQ-USP – Instituto de Química at University of São Paulo – Brazil for BET analysis.

3.7 References

1. M. C. Rodrigues, T. L. R. Hower, G. E. De Souza Brito, V. E. Arana-Chavez and R. R. Braga, *Materials Science & Engineering. C, Biomimetic Materials, Sensors and Systems*, 2014, **45**, 122-126.
2. R. R. Moraes, J. W. Garcia, N. D. Wilson, S. H. Lewis, M. D. Barros, B. Yang, C. S. Pfeifer and J. W. Stansbury, *Journal of Dental Research*, 2012, **91**, 179-184.
3. B. P. Santana, F. Nedel, E. Piva, R. V. Carvalho, F. F. Demarco and N. L. V. Carrenõ, *BioMed Research International*, 2013, **2013**, 1-6.
4. L. A. Frank, R. V. Contri, R. C. Beck, A. R. Pohlmann and S. S. Guterres, *Wiley Interdiscip Rev Nanomed Nanobiotechnol*, 2015. doi: 10.1002/wnan.1334. [Epub ahead of print]
5. L. O. Reis, M. R. Kaizer, F. A. Ogliari, F. M. Collares and R. R. Moraes, *International Journal of Adhesion and Adhesives*, 2014, **48**, 80-84.
6. G. Gao, A. F. Schilling, T. Yonezawa, J. Wang, G. Dai and X. Cui, *Biotechnology Journal*, 2014, **9**, 1304-1311.
7. M. R. Kaizer, A. De Oliveira-Ogliari, M. S. Cenci, N. J. Opdam and R. R. Moraes, *Dental Materials*, 2014, **30**, e41-78.
8. V. E. Salgado, L. M. Cavalcante, N. Silikas and L. F. J. Schneider, *Journal of Dentistry*, 2013, **45**, e45-e53.
9. A. A. Pesqueira, M. C. Goiato, D. M. Dos Santos, M. F. Haddad and A. Moreno, *Journal of Medical Engineering & Technology*, 2012, **36**, 217-221.
10. K. Okada, T. Kameya, H. Ishino and T. Hayakawa, *Dental Materials Journal*, 2014, **33**, 203-209.
11. I. D. Sideridou and M. M. Karabela, *Dental Materials*, 2009, **25**, 1315-1324.
12. K. S. Wilson, A. J. Allen, N. R. Washburn and J. M. Antonucci, *Journal of Biomedical Materials Research. Part A*, 2007, **81**, 113-123.
13. K. S. Wilson and J. M. Antonucci, *Dental Materials*, 2006, **22**, 995-1001.
14. K. S. Wilson, K. Zhang and J. M. Antonucci, *Biomaterials*, 2005, **26**, 5095-5103.
15. N. M. Mohsen and R. G. Craig, *Journal of Oral Rehabilitation*, 1995, **22**, 183-189.
16. N. Nishiyama, T. Ishizaki, K. Horie, M. Tomari and M. Someya, *Journal of Biomedical Materials Research*, 1991, **25**, 213-221.
17. J. G. Calais and K.-J. M. Söderholm K-JM, *Journal of Dental Research*, 1988, **67**, 836-840.

18. S. K. Brown, *British Polymer Journal*, 1980, **12**, 24-30.
19. S. B. Mitra, D. Wu and B. N. Holmes, *The Journal of the American Dental Association*, 2003, **134**, 1382-1390.
20. J. A. Scholl, A. L. Koh and J. A. Dionne, *Nature*, 2012, **483**, 421-428.
21. P. M. Paulus, A. Goossens, R. C. Thiel, A. M. van der Kraan, G. Schmid and L. J. de Jongh, *Physical Review B*, 2001, **64**, 205418.
22. T. Dallali Isfahani, J. Javadpour, A. Khavandi, M. Goodarzi and H. R. Rezaie, *Journal of Materials Science and Technology*, 2014, **30**, 387-393.
23. S. Cava, S. M. Tebcherani, I. A. Souza, S. A. Pianaro, C. A. Paskocimas, E. Longo and J. A. Varela, *Materials Chemistry and Physics*, 2007, **103**, 394-399.
24. J. Zhang J, M. Li, Z. Feng, J. Chen and C. Li, *The Journal of Physical Chemistry. B*, 2006, **110**, 927-935.
25. A. Della Bona, P. H. Corazza, and Y. Zhang, *Dental Materials*, 2014, **30**, 564-569.
26. J. F. Nguyen, D. Ruse, A. C. Phan, and M. J. Sadoun, *Journal of Dental Research*, 2014, **93**, 62-67.
27. A. Coldea, M. V. Swain and N. Thiel, *Dental Materials*, 2013, **29**, 419-426.
28. L. He and M. Swain, *Dental Materials*, 2011, **27**, 527-534.

4Capítulo 3

Mono or polycrystalline alumina-modified porcelain-ceramic hybrid biomaterials¹

Marina R. Kaizer^a, Ana Paula R. Gonçalves^a, Yu Zhang^b, Sergio S. Cava^c, Rafael R. Moraes^a

^aSchool of Dentistry, Federal University of Pelotas, RS - Brazil

^bCollege of Dentistry, New York University, NY - USA

^cSchool of Materials Engineering, Federal University of Pelotas, RS - Brazil

Corresponding author:

Prof. Rafael R. Moraes – E-mail: moraesrr@gmail.com

School of Dentistry, Federal University of Pelotas – Rua Gonçalves Chaves 457,
room 505

96015-560 Pelotas-RS, Brazil

Phone/Fax: 55 53 3225.6741 x.135

¹Artigo formatado segundo as normas do periódico *ACS_ Applied Materials & Interfaces* (FI JCR 2013: 5.90).

4.1 Abstract

The aim of the present study was to evaluate the effect of the addition of alumina particles (nanostructured: polycrystalline or translucent: monocrystalline), with or without silica coating, on the optical and mechanical properties of feldspar-based porcelain. The groups tested were: Control (C), Polycrystalline alumina (PA), Polycrystalline alumina-silica (PAS), Monocrystalline alumina (MA), Monocrystalline alumina-silica (MAS). The polycrystalline alumina powder was synthesized using a polymeric precursor method; a commercially available monocrystalline alumina powder (sapphire) was acquired. Silica coating was obtained by immersing alumina powders in a tetraethyl orthosilicate solution, followed by calcination. Electrostatic stable suspension method was used to ensure homogenous dispersion of the alumina particles within the porcelain powder. Porcelain-ceramic hybrid specimens were obtained by heat-pressing rods of porcelain with or without alumina addition. Microstructure, translucency parameter, contrast ratio, opalescence index, biaxial flexural strength, roughness, and elastic constants were characterized. It was noticed a better interaction between glass matrix and silica coated crystalline particles in comparison with the non-coated. The materials did not present significant differences in biaxial flexural strength, due to the presence of porosity in the groups with alumina addition. Elastic modulus was higher for MA and MAS groups. Also, these were the groups with optical qualities and roughness closer to control. The PA and PAS groups were considerably more opaque (Contrast ratio: C – 0.32; PA – 0.94; PAS – 0.93; MA – 0.55; MAS – 0.54), as well as rougher (Ra: C – 0.033; PA – 0.273; PAS – 0.184; MA – 0.054; MAS – 0.056). Therefore, feldspar-based porcelains with addition of translucent particles presented superior esthetic qualities in comparison to those with opaque particles. In order to eliminate the porosity in the ceramic materials investigated herein, processing parameters need to be optimized.

Keywords: ceramics; composites; feldspar; monocystals; polycrystals; porcelain; silica coating; single crystals.

4.2 Introduction

Advanced ceramics have been developed and tailor-made aiming distinct applications with specific demands: aerospace, nuclear, biomedical, electronics, cutting tools, and so forth. These materials are produced from high purity ceramic powders by employing controlled thermal and mechanical processing in order to attain the required properties. Advanced ceramics are usually divided into functional and structural categories. Functional ceramics are applied for their physical properties, having their performance modulated by optical, magnetic, dielectric, electric, and other characteristics.¹⁻³ Structural ceramics have been developed mainly to optimize mechanical strength, toughness, and hardness of diverse systems subjected to high tribological, mechanical, thermal and/or chemical conditions.^{4,5} In general terms, ceramics at the glass state will appear optically transparent and exhibit only moderate strength whereas fully polycrystalline ceramics will exhibit high strength but an opaque character.^{6,7} When needed, a compromise can be achieved by using ceramics that contain both glass and crystalline phases; these hybrid ceramics show higher strength than the glass itself and are more translucent than the fully crystalline material.

For some highly specialized applications both optical and mechanical properties are required for an excellent performance of ceramics. Amongst them is the use of ceramics as dental biomaterials, which need to be constructed into complex and stable-during-sintering shapes, and are subjected to sliding fatigue under mastication in a corrosive/moist environment.⁸⁻¹¹ In addition, dental ceramics are expected to last decades with an aesthetical natural-tooth-looking appearance.^{12,13} Ceramics used in dentistry that try to fulfill these expectations are usually feldspar-based porcelains with distinct crystal content.^{9,14} The crystalline phase can be obtained either by nucleation and crystallization within the glass matrix^{15,16} or by tailoring a hybrid-ceramic adding crystalline particles¹⁷ before sintering. Final properties of the porcelain-ceramic hybrid material are affected by the amount of crystalline phase, size and type of crystals, and their dispersion within the glass matrix.¹⁸⁻²¹

To date, only two porcelain-ceramic hybrid materials are commercially available for dental applications, both having zirconia particles added as crystal phase into a lithium silicate glass-ceramic system: Vita Suprinity (VITA Zahnfabrik,

Bad Säckingen, Germany) and Celtra DeguDent (DeguDent, Hanau, Germany). Despite the current appeal of zirconia, alumina is a technologically important material that is widely used in numerous applications^{2,22} but it is not being used in the tailoring of hybrid ceramics for dental applications. It is widely believed that alumina exists in more than 15 different crystallographic phases,^{23,24} which can determine distinct microstructures and properties if applied in hybrid ceramics. Nanostructured powders of simple oxides, such as Al_2O_3 , have been used in established applications,^{2,22,25} as well as considered a possibility for functional advanced materials. In addition, crystalline alumina has been given a lot of attention in its transparent monocrystalline state, known as artificial sapphire.²⁶⁻²⁸ To the best of the authors' knowledge, monocrystalline alumina powder was not yet tested in the development of porcelain-ceramic hybrid materials. Therefore, this study was designed to apply nanostructured polycrystalline or translucent monocrystalline alumina particles in the modeling optical and mechanical properties of feldspar-based porcelain. Silica coating method was used aiming a effective interfacial interaction between the alumina particles and porcelain matrix in the tailoring of porcelain-hybrid materials as dental biomaterials.

4.3 Experimental

4.3.1 Materials

The feldspar-based porcelain used as matrix of the porcelain-ceramic hybrid material is commercially available under the trade name Cerabien (Noritake Dental, Aichi, Japan). This porcelain was chosen because it has a coefficient of thermal expansion matching alumina, diminishing residual stresses near the interface of the two phases. Two types of alumina particles were used to manipulate the properties of the porcelain-matrix: polycrystalline alumina – sintered by means of a polymeric precursor method, and monocrystalline alumina – commercially available under the trade name Sapphire powder (GoodFellow, Huntingdon, England). The alumina particles were either silica-coated or not coated before addition to the porcelain powder. For the coating method, tetraethylorthosilicate (TEOS) was used as silica precursor (Sigma-Aldrich, St. Louis, MO, USA). Therefore, five groups were tested: Porcelain only (Control, C), Porcelain + Polycrystalline alumina (PA), Porcelain + Polycrystalline alumina-silica (PAS), Porcelain + Monocrystalline alumina (MA), and Porcelain + Monocrystalline alumina-silica (MAS).

4.3.2 Synthesis of polycrystalline alumina by a polymeric precursors method

Nanostructured alumina powder was produced by using a variation of methods previously described.²³ Briefly, 1 M aluminum nitrate ($\text{Al}(\text{NO}_3)_3 \cdot 9\text{H}_2\text{O}$) P.A. (Synth, São Paulo, SP, Brazil) and 3 M anhydrous citric acid ($\text{C}_6\text{H}_8\text{O}_7$) P.A. (Synth) were dissolved in water at 50°C for 1 h for the formation of aluminum citrate. Ethylene glycol ($\text{C}_2\text{H}_6\text{O}_2$) P.A. (Synth) was added at a 60:40 mass ratio of the citric acid/ethylene glycol. This mixture was then stirred at 80°C for 1 h, the temperature was then increased to 130°C to promote polymerization and remove excess solvents. The resin was then heat-treated in an air atmosphere oven, with 10°C/min heating rate up to 300°C dwell temperature for 2 h in order to burn the organic matter, yielding a black solid mass. This mass was finely hand-ground by using mortar and pestle. The powder obtained is referred as the “precursor”. In the furnace, the precursor was heat-treated with 10°C/min heating rate up to 1100°C dwell temperature for 2 h in the air in an Al_2O_3 boat, then cooled to room temperature. The final product is a white nanostructured α -alumina powder.

4.3.3 Silica coating of mono and polycrystalline alumina particles

The alumina particles were used either as-received (monocrystalline) and as-synthesized (polycrystalline) or coated with a silica layer applied by a sol–gel method. For silica coating, the particles were dispersed in a solution of 1 M hydrochloric acid (HCl) P.A. (Synth) and 10 M distilled water. The suspension was kept in vigorous magnetic stirring for 15 min to favor disaggregation. TEOS was added to the suspension in the proportion of 5 M% relative to the particles molar mass. Vigorous magnetic stirring was maintained and the temperature risen to 60°C to evaporate the aqueous content. After drying, the particles were heat-treated in an air atmosphere oven with 5°C/min heating rate up to 900°C dwell temperature for 2 h.

4.3.4 Microstructural and chemical characterization of the ceramic powders

The micromorphology of the alumina particles with and without silica coating was analyzed by scanning electron microscopy – SEM (JSM 6610, JEOL, Tokyo, Japan). For elemental chemical composition, the alumina powders were analyzed using energy-dispersive spectroscopy – EDS (JSM 6610, JEOL, Tokyo, Japan). Crystalline spectra were determined by X-ray diffraction – XRD (XRD-6000;

Shimadzu, Tokyo, Japan) with CuK α radiation at 40 kV and 40 mA, scan rate of 4°/min, 10–80°, at room temperature.

4.3.5 Homogenous dispersion/mixture of the porcelain-ceramic hybrid materials

A dispersant solution²⁹ was prepared by solubilizing 0.5 M citric acid (Synth) in deionized water and stirring for 10 min. To this solution 2 M triethylamine (Synth) was added and magnetic stirring was kept for 2 h, resulting in a solution with pH 7. This was used as dispersant for the addition of the alumina particles to the porcelain powder. It is important to notice that it does not leave residues in the material when it is sintered, does not cause any erosion at the acid sensitive porcelain particles, and it produces an efficient electrostatic repulsion between ceramic particles.²⁹ In order to incorporate 10 wt% of alumina particles into the porcelain powder in a homogenous, well dispersed way, these two powders were disaggregated together in a suspension containing isopropyl alcohol with 5% solid content (total powders). To that suspension, 10 wt% of the aforementioned dispersion solution²⁹ was poured. The suspension was sonicated at 9 W for 10 min in pulse mode (1 s cycles), and further placed into a round-bottom flask and taken to a rotary evaporator (RV10; IKA, Staufen, Germany) at 40°C under vacuum until complete elimination of the liquid content. The powder was yet kept in incubation at 150°C for 2 h to ensure complete solvent removal. After this process, the final material was porcelain-ceramic hybrid powder ready for use. For the control group, the porcelain powder without the addition of alumina was processed similarly to the others as described herein.

4.3.6 Production of hybrid porcelain-ceramic specimens by heat-pressing

The fabrication of both the control and hybrid porcelain-ceramic specimens followed the lost-wax technique and heat-pressing method for porcelains. For each group, five pre-sintered rod-shaped ingots (20 mm height, 12 mm diameter) were obtained by uniaxially pressing 4.5 g of each of the previously prepared porcelain(-hybrid) powders with 2 mL of distilled water at 3 ton, for 30 s. The green-bodies were heat-treated with a 45°C/min heating rate from 600°C to 750°C under vacuum, 1 min dwell at 750°C with vacuum, and 1 min at 750°C without vacuum. Rod-shaped wax patterns (10 mm height, 12 mm diameter) were produced using a silicone mold. Each wax pattern was individually attached to a pressing ring using a 3 mm round wax

sprue and a freshly vacuum mixed investment material was cast on a vibrating table. Following chemical setting time (45 min), the investment ring was transferred to a preheated oven at 750°C and left for 1 h to burn out the wax.

A pre-sintered ceramic ingot was placed in the ring and transferred to the heat-pressing oven (Kerampress; Kota, São Paulo, SP, Brazil), which was programmed to complete the sintering cycle: heating rate of 50°C/min from 700°C to 970°C, dwell 20 min + 8 min pressing at 3 bar (all under vacuum) + 1 min at 970°C without vacuum. Ideal sintering temperature was previously defined by a pilot study, considering the higher density and translucency achieved with temperature varying from 960°C (indicated by the manufacturer of the porcelain) up to 1000°C. One should consider that the addition of particles changes the viscosity of the porcelain above T_g , influencing the viscous flow during the heat-pressing process. After divesting and cleaning, the sintered rods were transversely sectioned using a precision circular saw coupled with a diamond-coated wafering blade under water cooling to produce disc-shaped specimens (1.1 mm thickness, 12 mm diameter). The specimens were polished up to 1 μm on both sides to a final thickness of 1 ± 0.05 mm.

4.3.7 Microstructural and chemical characterization of the hybrid ceramic

The micromorphology of the sintered hybrid samples was analyzed by SEM. The specimens were imaged both on their polished surface as well as after acid etching with 5% hydrofluoric acid for 10 s for better view of the crystals. Elemental chemical composition and mapping was carried out by EDS. The crystalline phases present in each group were determined by XRD as previously described. Surface roughness was analyzed by a contact profiler (SJ-410, Mitutoyo, Tokyo, Japan), used to measure roughness as *per* amplitude parameter R_a .

4.3.8 Optical properties

Optical properties were evaluated with a spectrophotometer (CM 3700d; Konica-Minolta, Tokyo, Japan), operating in the wavelength range of visible light (400 to 700 nm), both in reflectance and transmittance modes. Contrast ratio (CR) was calculated from the spectral reflectance of the light of the specimen (Y) on a black background (Y_b) and on a white background (Y_w),³⁰ according to the equation:

$$CR = Y_b / Y_w \quad (\text{Eq. 1}),$$

Translucency parameter (TP) was evaluated by calculating the color difference³¹ of the specimens on black and white backgrounds by using the equation:

$$TP=[(L^*_b-L^*_w)^2+(a^*_b-a^*_w)^2+(b^*_b-b^*_w)^2]^{1/2} \quad (\text{Eq. 2}),$$

where subscript b refers to color coordinates on the black background and subscript w refers to color coordinates on the white background.

Opalescence parameter (OP) was estimated as a difference in the chromaticity between the reflected and transmitted colors,³² according to the equation:

$$OP=[(a^*_t-a^*_r)^2+(b^*_t-b^*_r)^2]^{1/2} \quad (\text{Eq. 3}),$$

where subscripts t and r indicate the transmitted and the reflected color, respectively.

4.3.9 Elastic constants

The Poisson's ratio (ν) and elastic modulus (E) were determined by the ultrasonic pulse-echo method³³ using a 200 MHz ultrasonic pulser-receiver (5900 PR; Panametrics, Waltham, MA, USA), 20 MHz longitudinal and shear transducers with a delay material, and a coupling paste (Panametrics) applied between the sample and transducer. The time of flight of ultrasonic pulse was measured with an oscilloscope (TDS 1002; Tektronix, Shanghai, China) and the thickness of the sample was measured with a digital micrometer (Mitutoyo). Sonic velocities were calculated as two times the thickness divided by the time of flight, since in the pulse-echo method only one transducer (longitudinal or shear mode) is used to emit and capture the back-reflected wave. ν and E values were calculated using the equations:

$$\nu=0.5 \left(\frac{V_l^2-2V_t^2}{V_l^2-V_t^2} \right) \quad (\text{Eq. 4})$$

$$E=\rho \left(\frac{3V_l^2V_t^2-4V_t^4}{V_l^2-V_t^2} \right) \quad (\text{Eq. 5}),$$

where ρ is density measured by Archimedes principle, V_l is longitudinal velocity, and V_t is shear velocity.

4.3.10 Biaxial flexural strength (σ_f)

A ball-on-ring test configuration was used to determine the failure loads of the materials tested herein. Each disc-shaped specimen was placed in contact with a flat sheet of Parafilm (Bemis NA, Neenah, WI, USA), which covered the 10 mm diameter knife-edge ring support, and centrally loaded with a 4 mm diameter ball indenter at 1 mm/min. The Parafilm compensated for geometric variation and permitted small lateral displacements to minimize friction and shear.³⁴ The biaxial flexure stress at failure was calculated using a monolayer analytical solution:³⁴

$$\sigma_f = \frac{P}{h^2} \left\{ (1+\nu) \left[0.485 \ln \left(\frac{a}{h} \right) + 0.52 \right] + 0.48 \right\} \quad (\text{Eq. 6}),$$

where σ_f was the maximum tensile stress, P the measured fracture load, a was the radius of the knife-edge support, h was the mean specimen thickness measured from fragments at the point of fracture with a digital micrometer, and ν was the Poisson's ratio measured according to item 2.9.

4.3.11 Sample size and statistical analysis

For σ_f , 20 specimens were tested. For optical properties, roughness and elastic constants, 10 specimens were evaluated. Significant differences among homoscedastic data (σ_f , E , ν , and R_a) were evaluated by calculating 95% confidence intervals for the mean. Groups were considered significantly different when the 95% confidence interval bounds did not overlap. Optical properties data were heteroscedastic, thus were transformed to ranks and submitted to one-way Analysis of Variance. All pairwise multiple comparison procedures were conducted using the Student-Newman-Keuls' method. The significance level of all analyses was set at $\alpha = 5\%$. Weibull analysis of σ_f data was performed with Weibull++ software (Reliasoft, Tucson, AZ, USA). Weibull modulus (m) and characteristic strength (σ_0) were calculated based on the maximum likelihood method, and 95% confidence intervals were calculated using the likelihood ratio.³⁵ For σ_0 , and m groups were considered significantly different when their confidence interval bounds did not overlap.

4.4 Results and Discussion

4.4.1 Microstructural and chemical characterization of the alumina powders

Both alumina particles had similar particle size ($<60\mu\text{m}$) yet distinct particle shape (Figure 4.1): PA particles were irregular and porous, while MA particles were spherical and dense (Fig 4.1-a). A detailed surface observation of the PA particles denotes the boundaries of the nanosized crystals (red arrows in Fig 4.1-b), whereas no boundaries are present in MA particles. The silica coating applied is visible comparing the surfaces of MA and MAS groups (blue arrows in Fig 4.1-b). The dense structure of MA particles yields a superficial deposition of silica during the coating process. By comparison, PA had silica deposited both at the surface and within the porosity of the particles, hindering visualization of a uniform silica layer.

Figure 1-c shows the mapping of Si (red pixels) and Al (blue pixels), being Al the core of the particles for all groups, and Si identified as a coating layer covering the surface of the alumina particles for the groups PAS and MAS. Although the silica layer was not clearly visible by SEM imaging, the presence of Si on the surface of coated powders was clear. The EDS analysis corroborated the SEM images showing that the size of MA and PA particles is not greatly modified by silica coating. The hollow arrows identify the presence of silica nanoparticles that were likely crystallized during calcination of TEOS molecules not bound to the alumina particles during silica coating. Formation of a secondary silica phase during coating was observed in previous analyses and will be addressed in a separate report, whilst no negative effect is anticipated by the presence of silica in porcelain-hybrid materials since the particles are chemically alike to the glass matrix (see supplementary information SI 4.1 for elemental quantification in atom % and weight % - EDS).

4.4.2 Microstructural and chemical characterization of the sintered specimens

Microstructure of the sintered porcelain-ceramic hybrid specimens is shown in Figure 4.2. Uniform distribution of crystalline phases within the porcelain was observed for all groups (Fig 4.2-a). Although even the control porcelain had pores, higher porosity was generally observed for alumina-modified hybrid materials (Fig 4.2-a). Pores may act as stress concentration/magnification areas and reduce the load bearing capacity of materials, determining a significant reduction in strength.^{21,36,37} Porosity also scatter light and may reduce translucency.^{38,39,43}

Therefore, the presence of porosity may be detrimental to materials properties, thus it needs to be reduced as much as possible in the modified materials.

The group MA had porosity at the interface between alumina particles and porcelain (red arrows in Figs 4.2-a and 4.2-d). The lack of interfacial interaction between matrix and reinforcing phase compromise any reinforcement effect expected. The gap between phases prevent the propagation of stress from the matrix to the tougher particles, but the gap may also work as pores within the matrix.^{21,36,37} In contrast, the group MAS had no interface porosity, indicating positive effect of the silica coating in the interaction between MA particles and porcelain matrix. The highly magnified images of the group MAS showed glass bridging from the porcelain toward the alumina particles (blue arrows in Fig 4.2-d), again suggesting the effectiveness of the silica coating in improving the chemical interaction between these two phases.

PA particles seemed not to work as discrete particles but rather as nanoclusters, which is indicated by the crystal dislodgement observed during polishing (yellow arrows in Fig 4.2-d). The use of nanoclusters as reinforcing phase of polymeric dental biomaterials has been previously described.^{40,41} This approach considers that the progressive dislodgement of nanocrystals, instead of the loss of a whole microparticle during sliding fatigue under mastication, would benefit wear, fatigue, and esthetic properties.^{40,41} However, none of these effects has yet been tested in porcelain-ceramic hybrid materials, whilst the PA particles presented here may open that possibility.

The elemental mapping for Si and Al across the polished surface of the specimens (Fig 4.2-b) showed that Si is present both in the glass matrix and in the crystals nucleated during sintering, while Al is concentrated within the alumina particles added (see supplementary information SI 4.1 for elemental quantification in atom % and weight % - EDS; and, SI 4.2 for crystalline phase characterization - XRD). Surface imaging after 5% hydrofluoric acid-etching for 10 s (for better view of crystals) was able to show the crystalline phases present (Figs 4.2-c and 4.2-d): (1) SiO₂ crystals (hollow arrows) nucleated and grew in all groups during sintering. It is important to point out that these silica crystals are not related to the silica nanoparticles observed within the alumina powders, otherwise those crystals would not be present in the control group; (2) Al₂O₃ particles added (white arrows).

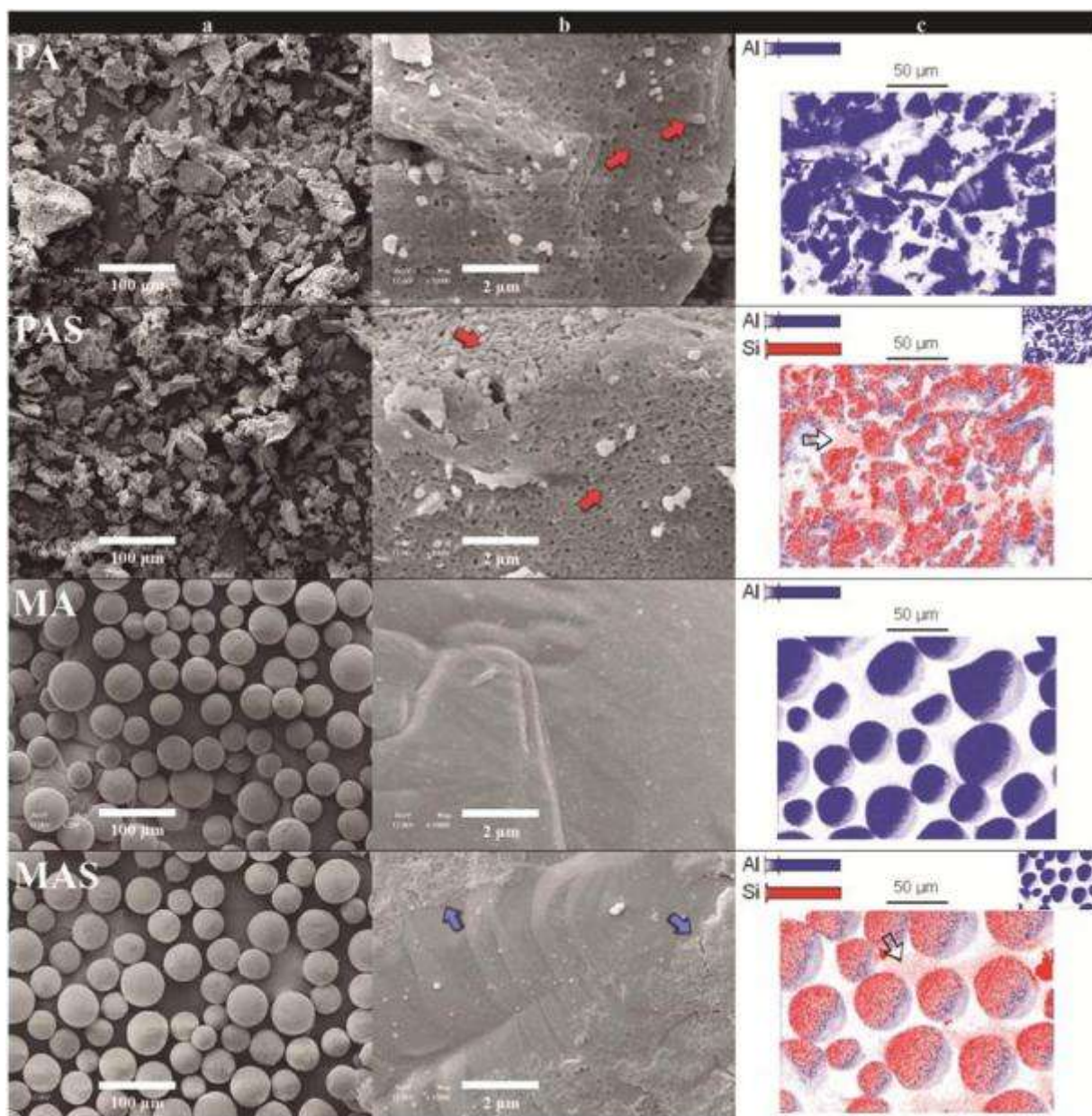


Figure 4.1-SEM images of the alumina powders: Polycrystalline alumina (PA); Polycrystalline alumina coated with silica (PAS); Monocrystalline alumina (MA); Monocrystalline alumina coated with silica (MAS). Column (a) shows magnifications of $\times 200$, and column (b) magnifications of $\times 10k$. The polycrystalline nanostructure (red arrows) of the irregular-shaped particles is clear in high magnification of PA and PAS powders. The thin silica coat layer (blue arrows) is visible comparing the highly magnified regular particles' surfaces of MA and MAS groups. Column (c) shows the mapping of Si and Al, being Al the core of the particles for all groups, and Si identified as a coating layer covering the surface of the alumina particles for the groups PAS and MAS. Red pixels among the alumina main particles (hollow arrows) identify the presence of silica nanoparticles as a secondary result of the TEOS calcination.

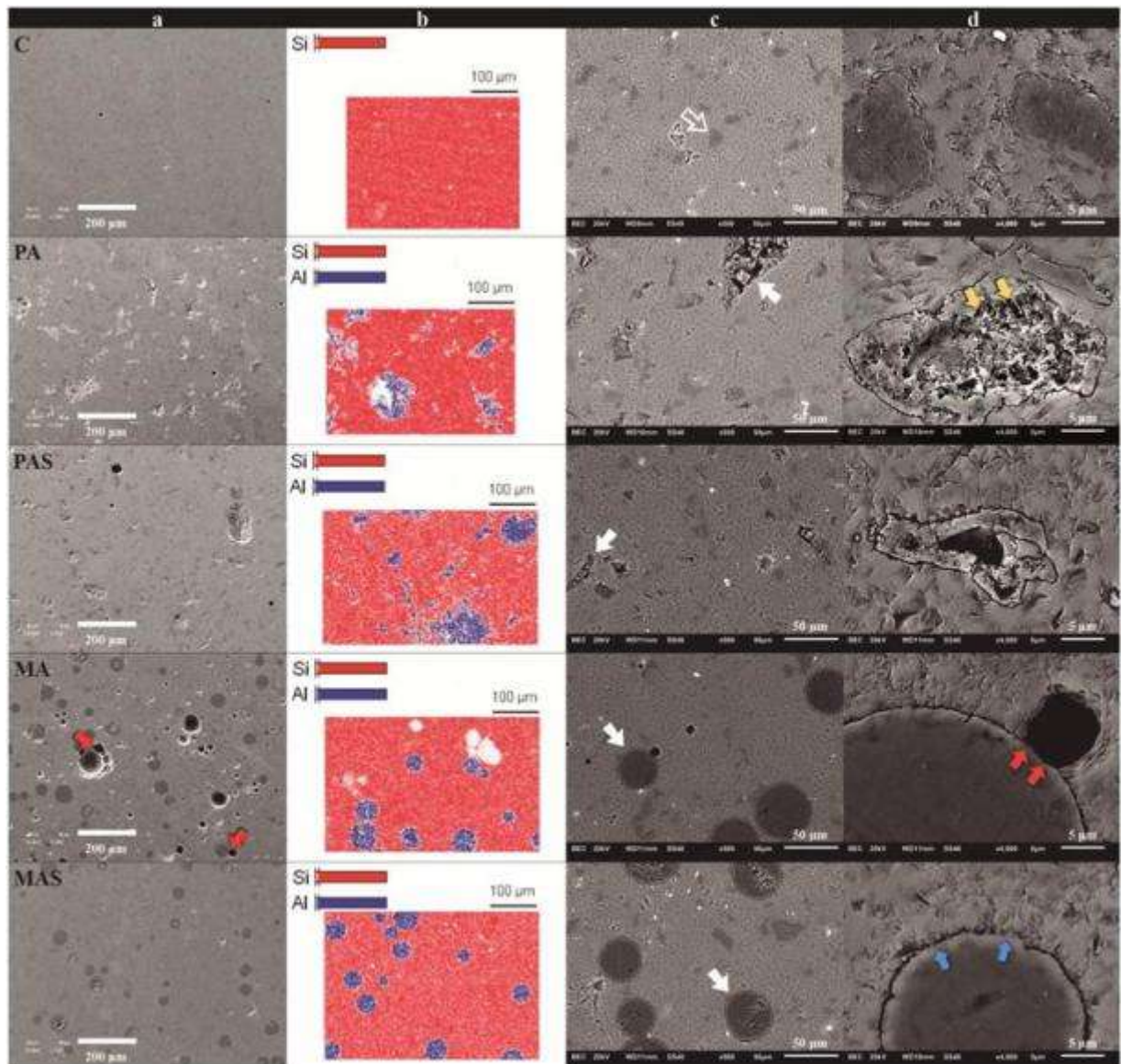


Figure 4.2-SEM images of sintered specimens: Polycrystalline alumina (PA); Polycrystalline alumina coated with silica (PAS); Monocrystalline alumina (MA); Monocrystalline alumina coated with silica (MAS). a) polished surfaces ($\times 100$) showing uniform distribution of crystalline phases as well as considerable porosity in groups with alumina addition. b) elemental mapping showing Si both in the glass matrix and crystals nucleated during sintering and Al concentrated within the alumina particles. c and d) microstructure after acid-etching with 5% hydrofluoric acid for 10 s for better view of the crystals (magnifications $\times 500$ and $\times 4k$). Crystalline SiO_2 (hollow arrow) nucleated and grew in all groups, while Al_2O_3 particles (white arrows) were not present in the control group. PA particles seemed to work as nanoclusters, with crystal dislodgement during polishing procedures (yellow arrows). Pores and defects were observed in the interface of glass matrix and alumina particles mainly for the group MA (red arrows). Bridges of glass between alumina particle and porcelain are observed (blue arrows), indicating that the silica coating was effective in improving the chemical interaction between these two phases.

4.4.3 Optical properties

Figure 4.3-a shows the apparent translucency of specimens and Figure 4.3-b shows the spectra of total light transmittance. C, MA, and MAS are the most translucent materials, whereas PA and PAS are significantly more opaque having less than 50% of the total light transmittance of C. Light transmittance generally increased with the increase in wavelength. Silica coating determined slightly higher light transmittance, which is explained by a better interfacial interaction of the porcelain and particles, reducing light scattering and dispersion between these two phases.^{38,39} The translucency of all groups with alumina addition could be improved by reducing porosity, which has been already mentioned as a shortcoming to be addressed.^{38,39,43}

Results for TP and CR (Table 4.1) corroborate the observations of light transmittance and visual translucency: C is the most translucent group, closely followed by MA and MAS. PA and PAS were significantly more opaque than the other groups. Silica coating yielded a general slight increase in translucency. CR was in general ~40% lower and TP was ~85% higher for monocrystalline compared to polycrystalline groups. The addition of particles into a matrix increases opacity due to increased light scattering, reflection, and dispersion.⁴² For hybrid-materials with same crystalline content and particles of similar size, the refractive index mismatch between the two phases is usually the most important aspect to be considered to estimate translucency.⁴³ PA and MA particles have similar refractive indices (between 1.71 and 1.79), which are quite different to the refractive index of porcelain (between 1.5 and 1.53). Therefore, one could expect all hybrid-materials tested to present high opacity, yet it was only true for PA-modified materials. Two aspects are hypothesized to be causing this effect: (i) MA particles are intrinsically translucent and dense,²⁸ minimizing light scattering, while PA particles are intrinsically opaque and porous, increasing light scattering within the particles;⁷ (ii) the difference in particle shape might have a role in light scattering, affecting the translucency of the experimental materials.⁴⁴⁻⁴⁶

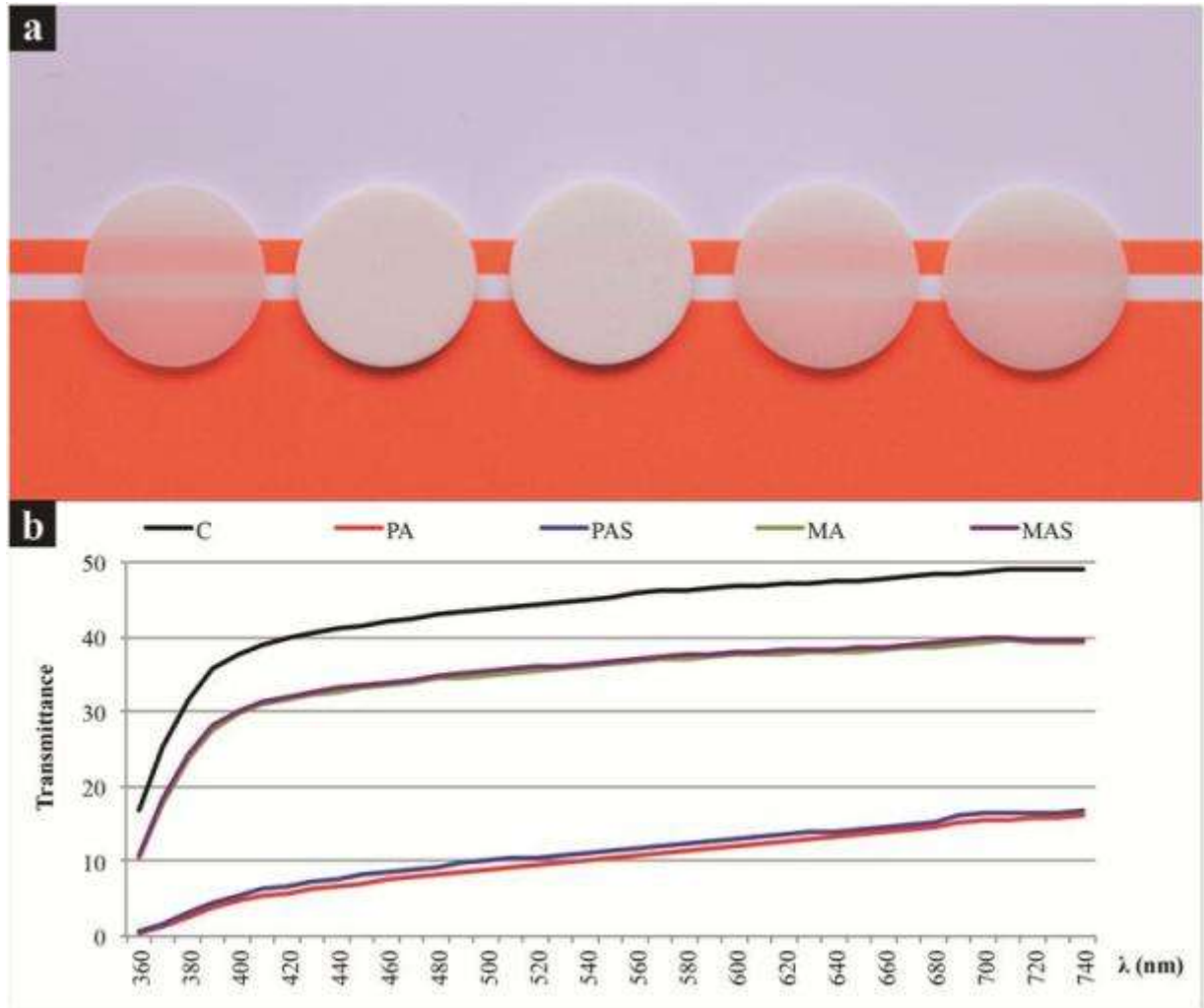


Figure 4.3 - a) apparent translucency of specimens from groups Control (C), Polycrystalline alumina (PA), Polycrystalline alumina coated with silica (PAS), Monocrystalline alumina (MA), and Monocrystalline alumina coated with silica (MAS). b) spectra of total light transmittance, indicating that transmittance increases with the increase in light wavelength. MA and MAS have similar translucency to C, while PA and PAS are noticeably more opaque.

Table 4.1 - Median (25% - 75%) of optical properties: CR = contrast ratio; TP = translucency parameter; OP = opalescence parameter.

	CR	TP	OP
C	0.32 ^e (0.31-0.32)	35.1 ^a (35.0-35.3)	5.7 ^c (5.6-5.9)
PA	0.94 ^a (0.94-0.95)	2.9 ^d (2.8-3.0)	9.1 ^a (8.9-9.4)
PAS	0.94 ^b (0.93-0.94)	3.2 ^c (3.2-3.3)	8.6 ^b (8.2-8.9)
MA	0.55 ^c (0.54-0.55)	21.6 ^b (21.2-21.8)	4.1 ^e (4.0-4.1)
MAS	0.54 ^d (0.54-0.54)	21.9 ^b (21.7-22.0)	4.2 ^d (4.2-4.2)

Data were transformed to ranks before the analysis. Distinct letters within the same column indicate significant differences among materials ($p < 0.05$).

A previous study⁴⁷ showed that spherical particles scatter more light than irregular particles, which further reinforces that the higher translucency of MA and MAS groups in comparison to PA and PAS is mostly due to the translucency of the MA particles. It is important to notice that the porcelain used in this study is highly translucent, used in thin increments in dental restorations (usually less than 0.5 mm), otherwise would render a low-value, unpleasing appearance to the restoration.⁴⁸⁻⁵¹ In this context, the addition of MA yielded a degree of translucency close to the porcelains generally used to build the body of the dental porcelain restorations,⁴⁸⁻⁵¹ thus ideal for monolithic restorations. On the other hand, the opaque character of PA and PAS groups might be proper for situations where masking a discolored background is needed.⁴⁸⁻⁵¹

Addition of PA increased OP, while MA particles decreased OP (Table 4.1). All OP values measured for the materials under investigation are within the range of values previously reported for commercial dental ceramics.^{32,52,53} The phenomenon of opalescence is due to the light scattering of the shorter wavelengths of the visible spectrum in translucent materials.^{32,52,53} The presence of PA particles containing nanocrystals and their multiple boundaries is most likely to be causing the scattering of short wavelength photons, which would explain the increase in OP for groups PA and PAS.⁴³ The presence of dense and translucent MA particles only slightly attenuated the opalescence. Within the same type of particle, the very discreet variation observed in OP values for groups with and without silica coating is not expected to cause any important effect in the final optical appearance.

4.4.4 Physical properties

Table 4.2 presents comparisons for σ_f , showing similar results for all groups except for PA, which presented lower σ_f than the control. The effect of addition of alumina particles was not clear for the σ_f of the porcelain due to the porosity observed for these groups. As mentioned, pores are areas of stress concentration during loading, which causes faster and unstable crack propagation resulting in fracture in lower maximum loads.^{21,36,37} A structure with porosity has reduced cross-section load bearing area of material, having a significant reduction in strength.^{21,36,37} Results for m and σ_0 are also presented in Table 4.2. The maximum likelihood estimation plot is presented in Figure 4.4, showing that most of the groups fit perfectly to a two-parameter Weibull model (for one type of failure mode) and there was no effect of the experimental factors (no difference in m). The similar m might be associated with the high variability in flexural strength values,³⁵ which are associated with unstable crack propagation and defects population within the structure.^{21,36} This finding further indicates that the porosity compromised the reinforcing effect of the alumina particles. The group PA, in contrast, would fit better a five-parameter Weibull model, indicating that for this group there is a second type of failure mode that is not active in the other groups, because it has the lowest strength in addition to the shape of distribution that is characteristic of multiple failure modes. A five-parameter Weibull model was also plotted, but the confidence intervals were too wide. Considering that m and σ_0 values were almost identical between the two models and that the other groups fitted better the two-parameter Weibull model, this model was chosen to be reported. Nevertheless, the five-parameter Weibull model confirmed the observation of the existence of a second type of failure mode for PA group: rate of failure mode 1: 0.54(95% CI 0.33- 0.75); rate of failure mode 2: 0.46(95% CI 0.06 - 0.92).

Table 4.2 also presents comparisons for elastic constants and surface roughness across groups. Addition of MA increased E , while PA particles determined lower E . While higher crystalline content can increase E , higher porosity might decrease it.^{37,54} The higher E of MAS in comparison to all other groups indicates that the silica coating was successful in promoting better interaction of the MA particles with the glass matrix. In that case, the positive effect of increased crystalline content overcame the negative effect of porosity.^{37,54} For PA and PAS groups, the lower E compared to C is explained by the negative effect of porosity within the glass matrix combined with the inherent porosity of the particles.^{37,54} No variation in v with the

addition of alumina particles was observed though, meaning that the effect of crystalline content and porosity are much less important in the variation of ν than E .^{37,54} Finally, regarding the surface roughness, MA and MAS groups were rougher than C, yet these three groups presented Ra values consistent with polished commercial dental porcelains.⁵⁵ This was not the case for PA and PAS groups, markedly rougher than the others. For these two latter groups, the cluster-like PA particles played a key role in increasing surface roughness by allowing crystal dislodgment during polishing. The same effect is likely to occur if these materials are subjected to any type of friction process during function.

Table 4.2 - Means (95% confidence interval) of biaxial flexural strength (σ_f), characteristic strength (σ_0), Weibull modulus (m), elastic modulus (E), Poisson's ratio (ν), and surface roughness (Ra)

	σ_f (MPa)	σ_0 (MPa)	m	E (GPa)	ν	Ra (nm)
C	137 ^a (± 10)	145 ^a (138-153)	8.6 ^a (6.0-12.0)	70.1 ^c (± 0.4)	0.18 ^a (± 0.01)	33 ^c (± 10)
PA	117 ^b (± 6)	122 ^b (117-128)	11.0 ^a (7.7-15.5)	66.7 ^d (± 0.6)	0.16 ^a (± 0.01)	273 ^a (± 52)
PAS	125 ^{ab} (± 6)	130 ^b (126-135)	12.2 ^a (8.7-17.0)	65.7 ^d (± 0.8)	0.17 ^a (± 0.01)	184 ^a (± 37)
MA	128 ^{ab} (± 7)	134 ^{ab} (128-140)	10.5 ^a (7.4-14.8)	73.4 ^b (± 0.5)	0.18 ^a (± 0.01)	54 ^b (± 9)
MAS	120 ^{ab} (± 7)	126 ^b (120-132)	9.4 ^a (6.8-13.0)	74.7 ^a (± 0.6)	0.17 ^a (± 0.01)	56 ^b (± 7)

Distinct letters within the same column indicate significant differences among materials. The 95% confidence interval of the mean was calculated for σ_f , E , ν , and Ra; while the 95% confidence interval for σ_0 , and m were calculated using likelihood ratio.

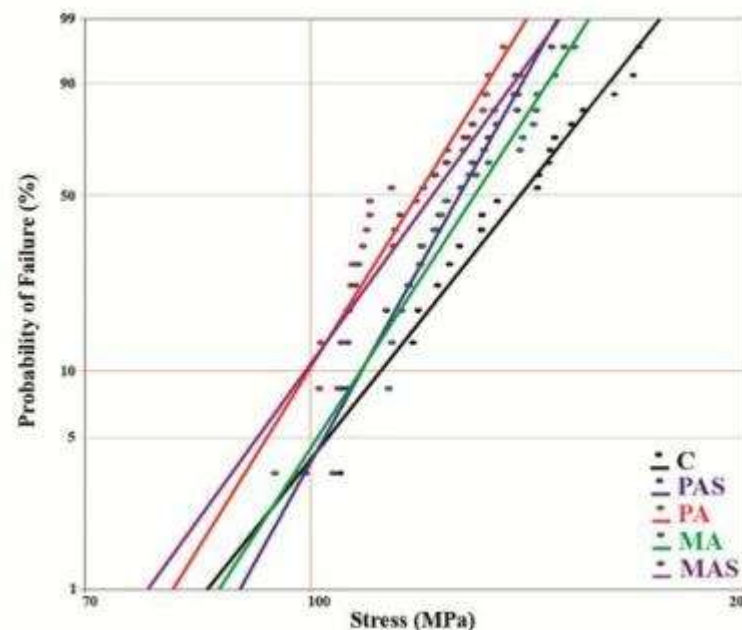


Figure 4.4 - Maximum likelihood estimation plots for the Weibull analysis. Most groups (Control (C); Polycrystalline alumina coated with silica (PAS); Monocrystalline alumina (MA); and Monocrystalline alumina coated with silica (MAS)) fitted well a two-parameter Weibull model without effect of the experimental factors. The group Polycrystalline alumina (PA) would fit better a five-parameter Weibull model, indicating that for this group there is a second type of failure mode that is not active in the other groups; this group has the lowest strength in addition to the shape of distribution that is characteristic of multiple failure modes.

4.5 Conclusion

Mono or polycrystalline alumina porcelain-ceramic hybrid materials presenting distinct characteristics and, therefore, potential varied applications were prepared by heat-pressing. Polycrystalline nanostructured alumina powder was synthesized using a polymeric precursor method, while monocrystalline alumina particles were purchased. Silica-coating of the alumina particles was obtained by calcination of tetraethyl orthosilicate precursor and confirmed by SEM-EDS. The presence of glass bridging from the porcelain to the alumina particles suggested effectiveness of the silica coating in improving the chemical interaction between these two phases. Polycrystalline alumina particles seemed to work as nanoclusters, where crystal dislodgement may occur due to friction. The addition of monocrystalline particles yielded more translucent hybrid materials, while polycrystalline particles determined higher opacity. The effect of addition of alumina particles on the strength of the hybrid materials was not clear due to porosity. In order to eliminate the porosity in the materials investigated herein, processing parameters need to be further optimized.

4.6 Supporting information (SI)

Supporting information is presented in the end of this chapter and consists of:

- SI4.1- (a) Distinct characterizations of the powders: Elemental composition, Crystal size, Particle size, Specific surface area; and (b) Chemical characterizations of the porcelain-ceramic hybrid materials – Elemental composition.
- SI4.2- (a) X-ray diffraction spectra of the alumina and porcelain powders; and (b) X-ray diffraction spectra of the sintered specimens of each group.

4.7 Acknowledgments

CNPq – Conselho Nacional de Desenvolvimento Científico e Tecnológico – Brazil: Process # 141129/2011-5 (PhD scholarship - GD); Process # 241021/2012-0 (PhD internship abroad – SWE); Process # 475462/2012-2 (Grant – CNPq Universal).

CEME-Sul – Centro de Microscopia Eletrônica da Zona Sul at Federal University of Rio Grande – Brazil.

4.8References

1. Delbrücke, T.; Schmidt, I.; Cava, S.; Sousa, V. C. Electrical Properties of a TiO₂-SrO Varistor System. *Advanced Materials Research***2014**, 975, 168-172.
2. Delbrücke, T.; Gouvêa, R. A.; Moreira, M. L.; Raubach, C. W.; Varela, J. A.; Longo, E.; Gonçalves, M. R. F.; Cava, S. Sintering of porous alumina obtained by biotemplate fibers for low thermal conductivity applications. *Journal of the European Ceramic Society***2013**, 33, 1087-1092.
3. Raubach, C. W.; Krolow, M. Z.; Mesko, M. F.; Cava, S.; Moreira, M. L.; Longo, E.; Carreno, N. L. V. Interfacial photoluminescence emission properties of core/shell Al₂O₃/ZrO₂. *CRYSTENGCOMM***2012**, 14, 393-396.
4. Zhang, X. P.; Ouyang, J. H.; Liu, Z. G.; Wang, Y. J.; Wang, Y. M.; Zhou, Y. Crack-healing ability and strength recovery of different hot-pressed TZ3Y20A-SiC ceramics by heat treatment in air. *Materials & Design***2015**, 67, 324-329.
5. Michalek, M.; Kasiarova, M.; Michalkova, M.; Galusek, D. Mechanical and functional properties of Al₂O₃-ZrO₂-MWCNTs nanocomposites. *Journal Of The European Ceramic Society***2014**, 34, 3329-3337.
6. Harianawala, H. H.; Kheur, M. G.; Apte, S. K.; Kale, B. B.; Sethi, T. S.; Kheur, S. M. Comparative analysis of transmittance for different types of commercially available zirconia and lithium disilicate materials. *The Journal of Advanced Prosthodontics***2014**, 6, 456-461.
7. Zhang, Y. Making yttria-stabilized tetragonal zirconia translucent. *Dental Materials***2014**, 30, 1195-1203.
8. Ferrari, M.; Vichi, A.; Zarone, F. Zirconia abutments and restorations: From laboratory to clinical investigations. *Dental Materials***2015**. doi: 10.1016/j.dental.2014.11.015.
9. Denry, I.; Kelly, J. R. Emerging ceramic-based materials for dentistry. *Journal of Dental Research***2014**, 93, 1235-1242.
10. Joshi, G. V.; Duan, Y. Y.; Della Bona, A.; Hill, T. J.; John, K. S.; Griggs, J. A. Contributions of stress corrosion and cyclic fatigue to subcritical crack growth in a dental glass-ceramic. *Dental Materials*, **2014**, 30, 884-890.
11. Rekow, E. D.; Silva, N. R.; Coelho, P. G.; Zhang, Y.; Guess, P.; Thompson V. P. Performance of dental ceramics: challenges for improvements. *Journal of Dental Research***2011**, 90, 937-952.

12. Håff, A.; Löf, H.; Gunne, J.; Sjögren, G. A retrospective evaluation of zirconia-fixed partial dentures in general practices: An up to 13-year study. *Dental Materials***2015**, 31, 162-170.
13. Beier, U. S.; Dumfahrt, H. Longevity of silicate ceramic restorations. *Quintessence International***2014**, 45, 637-644.
14. Li, R. W.; Chow, T. W.; Matinlinna, J. P. Ceramic dental biomaterials and CAD/CAM technology: state of the art. *Journal of Prosthodontic Research***2014**, 58, 208-216.
15. Fredericci, C.; Yoshimura, H. N.; Molisani, A. L.; Pinto, M. M.; Cesar, P. F. Effect of temperature and heating rate on the sintering of leucite-based dental porcelains. *Ceramics International***2011**, 37, 1073-1078.
16. Denry, I. L.; Holloway, J. A. Elastic constants, Vickers hardness, and fracture toughness of fluorrichterite-based glass-ceramics. *Dental Materials***2004**, 20, 213-219.
17. Lohbauer, U.; Frankenberger, R.; Krämer, N. Surface quality controls mechanical strength and fatigue lifetime of dental ceramics and resin composites. *Ceramic Materials***2010**, 9, 176-197.
18. Della Bona, A.; Nogueira, A. D.; Pecho, O. E. Optical properties of CAD-CAM ceramic systems. *Journal of Dentistry***2014**, 42, 1202-1209.
19. Borba, M.; De Araújo, M. D.; Fukushima, K. A.; Yoshimura, H. N.; Cesar, P. F.; Griggs, J. A.; Della Bona, A. Effect of the microstructure on the lifetime of dental ceramics. *Dental Materials***2011**, 27, 710-721.
20. Cesar, P. F.; Soki, F. N.; Yoshimura, H. N.; Gonzaga, C. C.; Styopkin, V. Influence of leucite content on slow crack growth of dental porcelains. *Dental Materials***2008**, 24, 1114-1122.
21. Albakry, M.; Guazzato, M.; Swain, M.V. Biaxial flexural strength, elastic moduli, and x-ray diffraction characterization of three pressable all-ceramic materials. *The Journal of Prosthetic Dentistry***2003**, 89, 374-380.
22. Cava, S.; Tebcherani, S. M.; Souza, I. A.; Paskocimas, C. A.; Longo, E.; Varela, J. A. Structural and spectroscopic characterization of $\text{Al}_{2-x}\text{Cr}_x\text{O}_3$ powders obtained by polymeric precursor method. *Journal of Sol-Gel Science and Technology***2007**, 43, 131-136.

23. Cava, S. ; Tebcherani, S. M. ; Souza, I. A. ; Pianaro, S. A. ; Paskocimas, C. A. ; Longo, E. ; Varela, J. A. .Structural characterization of phase transition of Al_2O_3 nanopowders obtained by polymeric precursor method. *Materials Chemistry and Physics***2007**, 103, 394-399.
24. Levin, I.; Brandon, D. Metastable alumina polymorphs: crystal structure and transition sequences. *Journal of the American Ceramic Society***1998**, 81, 1995-2012.
25. Janeway, P. A. Nanotechnology – it's more than size. *American Ceramic Society Bulletin***2003**, 82, 31-38.
26. Ozturk, I. K.; Basar, G.; Er, A.; Guzelcimen, F.; Basar, G.; Kreger, S. New energy levels of atomic niobium by laser induced fluorescence spectroscopy in the near infrared. *Journal Of Physics B-Atomic Molecular And Optical Physics***2015**, 48, 015005.
27. Yao, G.; Tang, Y. Q.; Fu, Y. J.; Jiang, Z. Q.; An, X. Y.; Chen, Y.; Liu, Y. D. Fabrication of high-quality ZnCdO epilayers and ZnO/ZnCdO heterojunction on sapphire substrates by pulsed laser deposition. *Applied Surface Science***2015**, 326, 271-275.
28. Scott, C.; Kaliszewski, M.; Greskovich, C.; Levinson, L. Conversion of polycrystalline Al_2O_3 into single-crystal sapphire by abnormal grain growth. *Journal of the American Ceramic Society***2002**, 85, 1275-1280.
29. De Riccardis, M. F.; Carbone, D.; Rizzo, A. A novel method for preparing and characterizing alcoholic EPD suspensions. *Journal of Colloid and Interface Science***2007**, 307, 109-115.
30. Anusavice, K. J.; Zhang, N. Z.; Moorhead, J. E. Influence of P205, AgNO_3 , and FeCl_3 on color and translucency of lithia-based glass-ceramics. *Dental Materials***1994**, 10, 230-235.
31. CIE Technical Committee 1.3. CIE colorimetry committee-working program on color differences. *Journal of the Optical Society of America***1974**, 64, 894-895.
32. Cho, M. S.; Yu, B.; Lee, Y. K. Opalescence of all-ceramic core and veneer materials. *Dental Materials***2009**, 25, 695-702.
33. Japanese Industrial Standards. *Testing methods for elastic modulus of high performance ceramics*. JIS R 1602, 1986.
34. Addison, O.; Fleming, G. J. Application of analytical stress solutions to bi-axially loaded dental ceramic-dental cement bilayers. *Dental Materials***2008**, 24, 1336-1342.

35. Griggs, J.A.; Zhang, Y. Determining the confidence intervals of Weibull parameters estimated using a more precise probability estimator. *Journal of Materials Science Letters***2003**, 22, 1771-1773.
36. Quinn, G. D.; Hoffman, K.; Quinn, J. B. Strength and fracture origins of a feldspathic porcelain. *Dental Materials***2012**, 28, 502-511.
37. Yoshimura, H. N.; Molisani, A. L.; Narita, N. E.; Cesar, P. F.; Goldenstein, H. Porosity dependence of elastic constants in aluminum nitride ceramics. *Materials Research***2007**, 10, 127-133.
38. Lee, Y. K. Influence of scattering/absorption characteristics on the color of resin composites. *Dental Materials***2007**, 23, 124-131.
39. Pecho, O. E.; Ghinea, R.; Ionescu, A. M.; Cardona, J. C.; Della Bona, A.; Pérez, M. Del M. Optical behavior of dental zirconia and dentin analyzed by Kubelka-Munk theory. *Dental Materials***2015**, 31, 60-67.
40. Kaizer, M. R.; De Oliveira-Ogliari, A.; Cenci, M. S.; Opdam, N. J.; Moraes, R. R. Do nanofill or submicron composites show improved smoothness and gloss? A systematic review of in vitro studies. *Dental Materials***2014**, 30, e41-78.
41. Mitra, S. B.; Wu D.; Holmes, B. N. An application of nanotechnology in advanced dental materials. *The Journal of the American Dental Association***2003**, 134, 1382-1390.
42. Lee, Y. K. Influence of filler on the difference between the transmitted and reflected colors of experimental resin composites. *Dental Materials***2008**, 24, 1243-1247.
43. Yoshimura, H. N.; Goldenstein, H. Light scattering in polycrystalline alumina with bi-dimensionally large surface grains. *Journal of the European Ceramic Society***2009**, 29, 293-303.
44. Turssi, C. P.; Ferracane, J. L.; Vogel, K. Filler features and their effects on wear and degree of conversion of particulate dental resin composites. *Biomaterials***2005**, 26, 4932-4937.
45. Kelly, K. L.; Coronado, E.; Zhao, L. L.; Schatz, G. C. The Optical Properties of Metal Nanoparticles: The Influence of Size, Shape, and Dielectric Environment. *The Journal of Physical Chemistry B***2003**, 107, 668-677.
46. Foss Jr., C. A.; Hornyak, G. L.; Stockert, J. A.; Martin, C. R. Template-Synthesized Nanoscopic Gold Particles: Optical Spectra and the Effects of Particle Size and Shape. *The Journal of Physical Chemistry***1994**, 98, 2963-2971.

47. Arikawa, H.; Kanie, T.; Fujii, K.; Takahashi, H.; Ban, S. Effect of filler properties in composite resins on light transmittance characteristics and color. *Dental Materials Journal***2007**, 26, 38-44.
48. Barizon, K. T.; Bergeron, C.; Vargas, M. A.; Qian, F.; Cobb, D. S.; Gratton, D. G.; Geraldeli, S. Ceramic materials for porcelain veneers. Part I: Correlation between translucency parameters and contrast ratio. *Journal of Prosthetic Dentistry***2013**, 110, 397-401.
49. Barizon, K. T.; Bergeron, C.; Vargas, M. A.; Qian, F.; Cobb, D. S.; Gratton, D. G.; Geraldeli, S. Ceramic materials for porcelain veneers: part II. Effect of material, shade, and thickness on translucency. *Journal of Prosthetic Dentistry***2014**, 112, 864-870.
50. Heffernan, M.J.; Aquilino, S. A.; Diaz-Arnold, A. M.; Haselton, D. R.; Stanford, C. M.; Vargas, M. A. Relative translucency of six all-ceramic systems. Part I: core materials. *Journal of Prosthetic Dentistry***2002**, 88, 4-9.
51. Heffernan, M.J.; Aquilino, S. A.; Diaz-Arnold, A. M.; Haselton, D. R.; Stanford, C. M.; Vargas, M. A. Relative translucency of six all-ceramic systems. Part II: core and veneer materials. *Journal of Prosthetic Dentistry***2002**, 88, 10-15.
52. Yu, B.; Lee, Y. K. Difference in opalescence of restorative materials by the illuminant. *Dental Materials***2009**, 25, 1014-1021.
53. Primus, C. M.; Chu, C. C.; Shelby, J. E.; Buldrini, E.; Heckle, C. E. Opalescence of dental porcelain enamels. *Quintessence International***2002**, 33, 439-449.
54. Yoshimura, H. N.; Gonzaga, C. C.; Cesar, P. F.; Miranda, W. G. Relationship between elastic and mechanical properties of dental ceramics and their index of brittleness. *Ceramics International***2012**, 38, 4715-4722.
55. Flury, S.; Lussi, A.; Zimmerli, B. Performance of different polishing techniques for direct CAD/CAM ceramic restorations. *Operative Dentistry***2010**, 35, 470-481.

4.9 Supplementary information

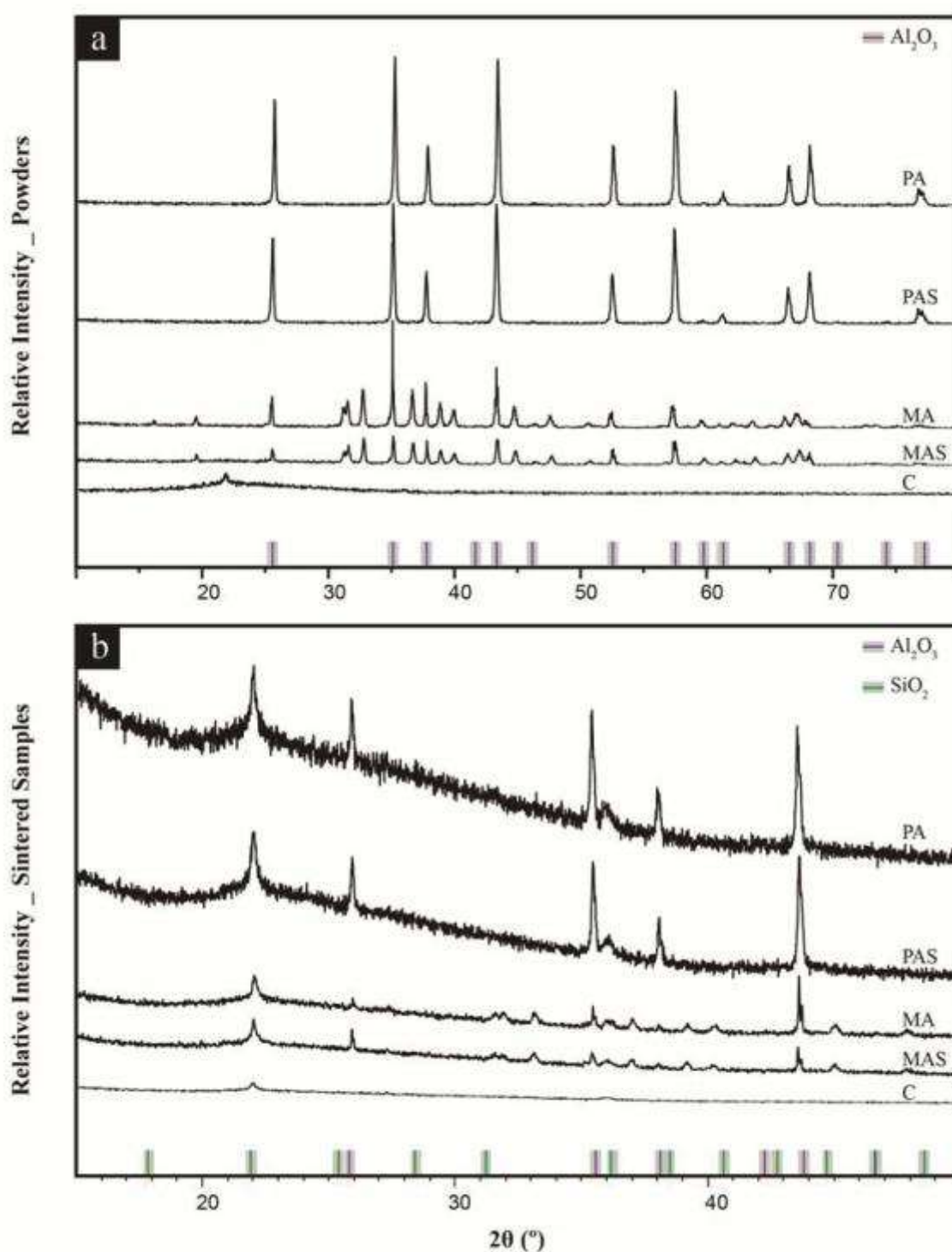
SI 4.1 (a) - Characterizations of the alumina powders: Elemental composition (EDS _ wt% & atom%), Particle size (BET _ μm), Specific surface area (BET _ m^2/g).

	EDS _ wt%			EDS _ atom%		
	O	Al	Si	O	Al	Si
PA	13.0	87.0	-	20.1	79.9	-
PAS	14.5	81.4	4.0	22.3	74.2	3.5
MA	12.6	87.4	-	19.6	80.4	-
MAS	12.1	68.2	19.7	19.0	63.4	17.6

SI 4.1 (b) - Chemical characterizations of the porcelain-ceramic hybrid materials _ Elemental composition (EDS _ wt% & atom%).

		Elemental Composition					
		O	Na	Mg	Al	Si	K
C	wt%	16.7	5.2	0.4	7.4	62.7	7.6
	atom%	26.2	5.7	0.4	6.8	56.0	4.9
PA	wt%	16.1	3.9	0.3	17.3	56.2	6.3
	atom%	25.2	4.2	0.3	16.1	50.1	4.0
PAS	wt%	20.5	3.9	-	17.7	52.3	5.5
	atom%	31.2	4.1	-	16.0	45.3	3.4
MA	wt%	10.5	3.9	0.4	15.5	62.3	7.6
	atom%	17.1	4.4	0.4	15.0	58.1	5.1
MAS	wt%	14.3	4.0	0.3	14.8	59.4	7.1
	atom%	22.8	4.4	0.3	14.0	53.9	4.6

The elemental composition of the alumina powders (SI 4.1-a) indicated that Si was observed only for powders submitted to silica coating. Si% is much higher for MAS compared to PAS group. The dense structure of the monocrystalline particles yields a complete superficial deposition of silica during the coating process, thus the EDS analysis estimated elevated percentage of Si. By contrast, silica is deposited both at the surface and within the porosity of the polycrystalline particles. In this case, due to the limited depth penetration, EDS only partially estimates the percentage of Si on polycrystalline particles. The full elemental composition (SI 4.1-b) indicates a typical feldspar porcelain composed of varied combination of Na, Mg, Al, Si, and K oxides. Groups with addition of alumina particles have higher percentage of Al than the control. Silica coating only slightly increases the Si content, thus this increase was not detectable for the sintered specimens that already have a high amount of Si in the porcelain matrix itself.



SI 4.2 - (a) X-ray diffraction spectra of the alumina and porcelain powders. Polycrystalline alumina (PA) and polycrystalline alumina coated with silica (PAS) show the spectral pattern of alpha alumina crystalline phase. Monocrystalline alumina (MA) and Monocrystalline alumina coated with silica (MAS) also matches the main peaks for crystalline alumina lattice. Porcelain _ control (C) group present the typical slope of amorphous material. (b) X-ray diffraction spectra of the sintered specimens of each group. For all groups it was observed the slope of the amorphous phase and the peaks of crystalline SiO_2 crystals nucleated and grown during sintering. Crystalline alumina peaks are not present only for the control group, which did not have addition of alumina particles.

5 Considerações finais

Respeitadas as limitações do presente estudo, é importante ressaltar os seguintes achados:

- Não há evidência *in vitro* de que compósitos resinosos nanoparticulados e submicrométricos demonstram menor rugosidade e maior brilho que os compósitos microhíbridos tradicionais;
- Dentre os compósitos resinosos estudados pelos artigos incluídos na revisão sistemática, em geral apenas partículas vítreas contendo silício são empregadas como reforço da fase polimérica;
- Observou-se que o método de recobrimento por sílica proposto resultou na deposição de uma camada de sílica na superfície das nanopartículas; ou ainda, na formação de aglomerados de nanopartículas envoltas em uma matriz de sílica;
- As partículas funcionalizadas pelo recobrimento por sílica cristalina demonstraram alta reatividade superficial, de forma que antecipam-se resultados promissores na sua interação interfacial com silanos ou porcelanas, ou mesmo na formação de estruturas tridimensionais para materiais restauradores indiretos;
- O uso do método de recobrimento por sílica também mostrou-se efetivo com micropartículas de alumina em materiais híbridos porcelana-cerâmica, observando-se “pontes” de matriz vítrea unindo porcelana e partículas de alumina;
- Partículas de alumina policristalina nanoestruturadas foram sintetizadas pelo método dos precursores poliméricos, recobertas ou não por sílica, e empregadas no desenvolvimento de materiais híbridos porcelana-cerâmica. Estas partículas parecem funcionar como nanoaglomerados na matriz vítrea, apresentando deslocamento de nanocristais por fricção.
- Também partículas de alumina monocristalina (adquiridas comercialmente) recobertas ou não por sílica, foram empregadas na obtenção de materiais híbridos porcelana-cerâmica. Os materiais com adição de partículas monocristalinas foram consideravelmente mais translúcidos que aqueles com partículas policristalinas.

- O efeito de reforço pela adição das partículas de alumina na matriz de porcelana não foi observado devido à porosidade presente nos materiais híbridos testados.

Desta forma, a alta reatividade das partículas recobertas por sílica e a efetiva interação superficial entre porcelana e partículas recobertas, observadas neste estudo, são resultados promissores para o desenvolvimento de materiais restauradores híbridos reforçados por partículas cerâmicas cristalinas sem silício. Antecipam-se materiais com propriedades distintas e melhoradas em relação aos atuais materiais restauradores híbridos em uso em odontologia.

Referências

ADDISON, O.; FLEMING, G. J. Application of analytical stress solutions to bi-axially loaded dental ceramic-dental cement bilayers. **Dental Materials**, v. 24, n. 10, p. 1336-1342, 2008.

ALBAKRY, M.; GUAZZATO, M.; SWAIN, M.V. Biaxial flexural strength, elastic moduli, and x-ray diffraction characterization of three pressable all-ceramic materials. **The Journal of Prosthetic Dentistry**, v. 89, n. 4, p. 374-380, 2003.

ALEXANDER-KATZ, R.; BARRERA, R. G. Surface correlation effects on gloss. **Journal of Polymer Science Part B: Polymer Physics**, v. 36, n. 8, p. 1321-1334, 1998.

ANTONSON, S. A. et al. Comparison of different finishing/polishing systems on surface roughness and gloss of resin composites. **Journal of Dentistry**, v. 39, n. 1, p. e9-17, 2011.

ANUSAVICE, K. J.; ZHANG, N. Z.; MOORHEAD, J. E. Influence of P205, AgNO₃, and FeCl₃ on color and translucency of lithia-based glass-ceramics. **Dental Materials**, v. 10, n. 4, p. 230-235, 1994.

ARIKAWA, H. et al. Effect of filler properties in composite resins on light transmittance characteristics and color. **Dental Materials Journal**, v. 26, n. 1, p. 38-44, 2007.

ATTAR, N. The effect of finishing and polishing procedures on the surface roughness of composite resin materials. **The Journal of Contemporary Dental Practice**, v. 8, n. 1, p. 27-35, 2007.

BARIZON, K. T. et al. Ceramic materials for porcelain veneers. Part I: Correlation between translucency parameters and contrast ratio. **The Journal of Prosthetic Dentistry**, v. 110, n. 5, p. 397-401, 2013.

BARIZON, K. T. et al. Ceramic materials for porcelain veneers: part II. Effect of material, shade, and thickness on translucency. **The Journal of Prosthetic Dentistry**, v. 112, n. 4, p. 864-870, 2014.

BARUCCI-PFISTER, N.; GÖHRING, T. N. Subjective and objective perceptions of specular gloss and surface roughness of esthetic resin composites before and after artificial aging. **American Journal of Dentistry**, v. 22, n. 2, p. 102-110, 2009.

BAŞEREN, M. Surface roughness of nanofill and nanohybrid composite resin and ormocer-based tooth-colored restorative materials after several finishing and polishing procedures. **Journal of Biomaterials Applications**, v. 19, n. 2, p. 121-134, 2004.

BAYNE, S. C.; HEYMANN, H. O.; SWIFT Jr., E. J. Update on dental composite restorations. **The Journal of the American Dental Association**, v. 125, n. 6, p. 687-701, 1994.

BEIER, U. S.; DUMFAHRT, H. Longevity of silicate ceramic restorations. **Quintessence International**, v. 45, n. 8, p. 637-644, 2014.

BOLLEN, C. M.; LAMBRECHTS, P.; QUIRYNEN, M. Comparison of surface roughness of oral hard materials to the threshold surface roughness for bacterial plaque retention: a review of the literature. **Dental Materials**, v. 13, n. 4, p. 258-269, 1997.

BORBA, M. et al. Effect of the microstructure on the lifetime of dental ceramics. **Dental Materials**, v. 27, n. 7, p. 710-721, 2011.

BOTTA, A. C. et al. Effect of dental finishing instruments on the surface roughness of composite resins as elucidated by atomic force microscopy. **Microscopy and Microanalysis**, v. 14, n. 5, p. 380-386, 2008.

BOTTA, A. C. et al. Surface roughness of enamel and four resin composites. **American Journal of Dentistry**, v. 22, n. 5, p. 252-254, 2009.

BROWN, S. K. Mechanics of fracture in filled thermosetting resins. **British Polymer Journal**, v. 12, n. 1, p. 24-30, 1980.

CALAIS, J. G.; SÖDERHOLM, K-J. M. Influence of filler type and water exposure on flexural strength of experimental composite resins. **Journal of Dental Research**, v. 67, n. 5, p. 836-840, 1988.

CATELAN, A. et al. Effect of artificial aging on the roughness and microhardness of sealed composites. **Journal of Esthetic and Restorative Dentistry**, v. 22, n. 5, p. 324-330, 2010.

CAVA, S. et al. Structural and spectroscopic characterization of $\text{Al}_{2-x}\text{Cr}_x\text{O}_3$ powders obtained by polymeric precursor method. **Journal of Sol-Gel Science and Technology**, v. 43, p. 131-136, 2007.

CAVA, S. et al. Structural characterization of phase transition of Al_2O_3 nanopowders obtained by polymeric precursor method. **Materials Chemistry and Physics**, v. 103, p. 394-399, 2007.

CAVALCANTE, L. M. et al. Effect of nanofillers' size on surface properties after toothbrush abrasion. **American Journal of Dentistry**, v. 22, n. 1, p. 60-64, 2009.

ÇELİK, E. U. et al. Color changes of dental resin composites before and after polymerization and storage in water. **Journal of Esthetic and Restorative Dentistry**, v. 23, n. 3, p. 179-188, 2011.

CESAR, P. F. et al. Influence of leucite content on slow crack growth of dental porcelains. **Dental Materials**, v. 24, n. 8, p. 1114-1122, 2008.

CHO, M. S.; YU, B.; LEE, Y. K. Opalescence of all-ceramic core and veneer materials. **Dental Materials**, v. 25, n. 6, p. 695-702, 2009.

CHOI, M. S. et al. Changes in surface characteristics of dental resin composites after polishing. **Journal of Materials Science: Materials in Medicine**, v. 16, n. 4, p. 347-353, 2005.

CHUNG, K. H. Effects of finishing and polishing procedures on the surface texture of resin composites. **Dental Materials**, v. 10, n. 5, p. 325-330, 1994.

CIE TECHNICAL COMMITTEE 1.3. CIE colorimetry committee-working program on color differences. **Journal of the Optical Society of America**, v. 64, p. 894-895, 1974.

COLDEA, A.; SWAIN M.V.; THIEL, N. Mechanical properties of polymer-infiltrated-ceramic-network materials. **Dental Materials**, v. 29, n. 4, p. 419-426, 2013.

COOK, M. P.; THOMAS, K. Evaluation of gloss meters for measurement of moulded plastics. **Polymer Testing**, v. 9, n. 4, p. 233-244, 1990.

CURTIN, J. A. et al. In vitro staining of resin composites by liquids ingested by children. **Journal of Pediatric Dentistry**, v. 30, n. 4, p. 317-322, 2008.

DA COSTA, J. B.; GONCALVES, F.; FERRACANE, J. L. Comparison of two-step versus four-step composite finishing/polishing disc systems: evaluation of a new two-step composite polishing disc system. **Operative Dentistry**, v. 36, n. 2, p. 205-212, 2011.

DA COSTA, J. et al. The effect of different polishing systems on surface roughness and gloss of various resin composites. **Journal of Esthetic and Restorative Dentistry**, v. 19, n. 4, p. 214-226, 2007.

DA COSTA, J. et al. The effect of various dentifrices on surface roughness and gloss of resin composites. **Journal of Dentistry**, v. 38, n. 2, p. e123-128, 2010.

DA ROSA RODOLPHO, P. A. et al. 22-Year clinical evaluation of the performance of two posterior composites with different filler characteristics. **Dental Materials**, v. 27, n. 10, p. 955-963, 2011.

DA SILVA, J. M. et al. Effect of different finishing times on surface roughness and maintenance of polish in nanoparticle and microhybrid composite resins. **The European Journal of Esthetic Dentistry**, v. 5, n. 3, p. 288-298, 2010.

DALLALI ISFAHANI, T. et al. Nanocrystalline growth activation energy of zirconia polymorphs synthesized by mechanochemical technique. **Journal of Materials Science and Technology**, v. 30, n. 4, p. 387-393, 2014.

DE MORAES, R. R. et al. Nanohybrid resin composites: nanofiller loaded materials or traditional microhybrid resins? **Operative Dentistry**, v. 34, n. 5, p. 551-557, 2009.

DE RICCARDIS, M. F.; CARBONE, D.; RIZZO, A. A novel method for preparing and characterizing alcoholic EPD suspensions. **Journal of Colloid and Interface Science**, v. 307, n. 1, p. 109-115, 2007.

DELBRÜCKE, T. et al. Sintering of porous alumina obtained by biotemplate fibers for low thermal conductivity applications. **Journal of the European Ceramic Society**, v. 33, p. 1087-1092, 2013.

DELBRÜCKE, T. et al. Electrical Properties of a TiO₂-SrO Varistor System. **Advanced Materials Research**, v. 975, p. 168-172, 2014.

DELLA BONA, A.; CORAZZA, P. H.; ZHANG, Y. Characterization of a polymer-infiltrated ceramic-network material. **Dental Materials**, v. 30, n. 5, p. 564-569, 2014.

DELLA BONA, A.; NOGUEIRA, A. D.; PECHO, O. E. Optical properties of CAD-CAM ceramic systems. **Journal of Dentistry**, v. 42, n. 9, p. 1202-1209, 2014.

DEMARCO, F. F. et al. Longevity of posterior composite restorations: not only a matter of materials. **Dental Materials**, v. 28, n. 1, p. 87-101, 2012.

DENRY, I. L.; HOLLOWAY, J. A. Elastic constants, Vickers hardness, and fracture toughness of fluorrichterite-based glass-ceramics. **Dental Materials**, v. 20, n. 3, p. 213-219, 2004.

DENRY, I.; KELLY, J. R. Emerging ceramic-based materials for dentistry. **Journal of Dental Research**, v. 93, n.12, p. 1235-1242, 2014.

ENDO, T. et al. Surface texture and roughness of polished nanofill and nanohybrid resin composites. **Dental Materials Journal**, v. 29, n. 2, p. 213-223, 2010.

ERDEMIR, U. et al. Effects of polishing systems on the surface roughness of tooth-colored materials. **Journal of Dental Sciences**, v. 8, n. 2, p. 160-169, 2013.

ERGÜCÜ, Z.; TÜRKÜN, L. S. Surface roughness of novel resin composites polished with one-step systems. **Operative Dentistry**, v. 32, n. 2, p. 185-192, 2007.

FERRACANE, J. L. Resin composite--state of the art. **Dental Materials**, v. 27, n. 1, p. 29-38, 2011.

FERRACANE, J. L. Resin-based composite performance: Are there some things we can't predict? **Dental Materials**, v. 29, n. 1, p. 51-58, 2013.

FERRARI, M.; VICHI, A.; ZARONE, F. Zirconia abutments and restorations: From laboratory to clinical investigations. **Dental Materials**, 2015. doi: 10.1016/j.dental.2014.11.015.

FLURY, S.; LUSSI, A.; ZIMMERLI, B. Performance of different polishing techniques for direct CAD/CAM ceramic restorations. **Operative Dentistry**, v. 35, n. 4, p. 470-481, 2010.

FOSS JR., C. A. et al. Template-Synthesized Nanoscopic Gold Particles: Optical Spectra and the Effects of Particle Size and Shape. **The Journal of Physical Chemistry**, v. 98, n. 11, p. 2963-2971, 1994.

FRANK, L. A. et al. Improving drug biological effects by encapsulation into polymeric nanocapsules. **Wiley Interdisciplinary Reviews: Nanomedicine and Nanobiotechnology**, 2015. doi: 10.1002/wnan.1334.

FREDERICCI, C. et al. Effect of temperature and heating rate on the sintering of leucite-based dental porcelains. **Ceramics International**, v. 37, n. 3, p. 1073-1078, 2011.

FURUSE, A. Y. et al. Colour-stability and gloss-retention of silorane and dimethacrylate composites with accelerated aging. **Journal of Dentistry**, v. 36, n. 11, p. 945-952, 2008.

GAO, G. et al. Bioactive nanoparticles stimulate bone tissue formation in bioprinted three-dimensional scaffold and human mesenchymal stem cells. **Biotechnology Journal**, v. 9, n. 10, p. 1304-1311, 2014.

GIORDANO R. Materials for chairside CAD/CAM-produced restorations. **The Journal of the American Dental Association**, v. 137, p. 14S-21S, set. 2006.

GONÇALVES, F.; KAWANO, Y.; BRAGA, R. R. Contraction stress related to composite inorganic content. **Dental Materials**, v. 26, n. 7, p. 704-709, 2010.

GÖNÜLOL, N.; YILMAZ, F. The effects of finishing and polishing techniques on surface roughness and colour stability of nanocomposites. **Journal of Dentistry**, v. 40, n. 2, p. e64-70, 2012.

GRIGGS, J.A.; ZHANG, Y. Determining the confidence intervals of Weibull parameters estimated using a more precise probability estimator. **Journal of Materials Science Letters**, v. 22, n. 24, p. 1771-1773, 2003.

GURGAN, S.; YALCIN CAKIR, F. The effect of three different mouthrinses on the surface hardness, gloss and colour change of bleached nano composite resins. **European Journal of Prosthodontics and Restorative Dentistry**, v. 16, n. 3, p. 104-108, 2008.

HADIS, M. et al. High irradiance curing and anomalies of exposure reciprocity law in resin-based materials. **Journal of Dentistry**, v. 39, n. 8, p. 549-557, 2011.

HÄFF, A. et al. A retrospective evaluation of zirconia-fixed partial dentures in general practices: An up to 13-year study. **Dental Materials**, v. 31, n. 2, p.162-170, 2015.

HARIANAWALA, H. H. et al. Comparative analysis of transmittance for different types of commercially available zirconia and lithium disilicate materials. **The Journal of Advanced Prosthodontics**, v. 6, n. 6, p. 456-461, 2014.

HE, L.; SWAIN, M. A novel polymer infiltrated ceramic dental material. **Dental Materials**, v. 27, n.6, p. 527-534, 2011.

HEFFERNAN, M.J. et al. Relative translucency of six all-ceramic systems. Part I: core materials. **The Journal of Prosthetic Dentistry**, v. 88, n. 1, p. 4-9, 2002.

HEFFERNAN, M.J. et al. Relative translucency of six all-ceramic systems. Part II: core and veneer materials. **The Journal of Prosthetic Dentistry**, v. 88, n. 1, p. 10-15, 2002.

HEINTZE, S. D. et al. Surface deterioration of dental materials after simulated toothbrushing in relation to brushing time and load. **Dental Materials**, v. 26, n. 4, p. 306-319, 2010.

HOSOYA, Y. et al. Effects of specular component and polishing on color of resin composites. **Journal of Oral Sciences**, v. 52, n. 4, p. 599-607, 2010.

HUBBEZOGLU, I. et al. Effect of bleaching on color change and refractive index of dental composite resins. **Dental Materials Journal**, v. 27, n. 1, p. 105-116, 2008.

ILIE, N.; HICKEL, R. Investigations on mechanical behaviour of dental composites. **Clinical Oral Investigations**, v. 13, n. 4, p. 427-438, 2009.

JANEWAY, P. A. Nanotechnology – it's more than size. **American Ceramic Society Bulletin**, v.82, n.4, p.31-38, 2003.

JANUS, J. et al. Surface roughness and morphology of three nanocomposites after two different polishing treatments by a multitechnique approach. **Dental Materials**, v. 26, n. 5, p. 416-425, 2010.

JAPANESE INDUSTRIAL STANDARDS. **Testing methods for elastic modulus of high performance ceramics**. JIS R 1602, 1986.

JOHNSON, A. C. et al. Fracture strength of CAD/CAM composite and composite-ceramic occlusal veneers. **Journal of Prosthodontic Research**, v. 58, n. 2, p. 107-114, 2014.

JOHNSTON, W. M.; REISBICK, M. H. Color and translucency changes during and after curing of esthetic restorative materials. **Dental Materials**, v. 13, n. 2, p. 89-97, 1997.

JONES, C. S.; BILLINGTON, R. W.; PEARSON, G. J. The in vivo perception of roughness of restorations. **British Dental Journal**, v. 196, n. 1, p. 42-45, 2004.

JOSHI, G. V. et al. Contributions of stress corrosion and cyclic fatigue to subcritical crack growth in a dental glass-ceramic. **Dental Materials**, v. 30, n. 8, p. 884-890, 2014.

JUNG, M.; EICHELBERGER, K.; KLIMEK, J. Surface geometry of four nanofiller and one hybrid composite after one-step and multiple-step polishing. **Operative Dentistry**, v. 32, n. 4, p. 347-355, 2007.

JUNG, M.; SEHR, K.; KLIMEK, J. Surface texture of four nanofilled and one hybrid composite after finishing. **Operative Dentistry**, v. 32, n. 1, p. 45-52, 2007.

KAHLER, B.; KOTOUSOV, A.; SWAIN, M. V. On the design of dental resin-based composites: a micromechanical approach. **Acta Biomaterialia**, v. 4, n. 1, p. 165-172, 2008.

KAIZER, M. R. et al. Do nanofill or submicron composites show improved smoothness and gloss? A systematic review of in vitro studies. **Dental Materials**, v. 30, n. 4, p. e41-78, 2014.

KAKABOURA, A. et al. Evaluation of surface characteristics of dental composites using profilometry, scanning electron, atomic force microscopy and gloss-meter. **Journal of Materials Science: Materials in Medicine**, v. 18, n. 1, p. 155-163, 2007.

KALEEM, M.; SATTERTHWAIT, J. D.; WATTS, D. C. Effect of filler particle size and morphology on force/work parameters for stickiness of unset resin-composites. **Dental Materials**, v. 25, n. 12, p. 1585-1592, 2009.

KARABELA, M. M; SIDERIDOU, I. D. Synthesis and study of properties of dental resin composites with different nanosilica particles size. **Dental Materials**, v. 27, n. 8, p. 825-835, 2011.

KELLY, K. L. et al. The optical properties of metal nanoparticles: the influence of size, shape, and dielectric environment. **The Journal of Physical Chemistry B**, v. 107, n. 3, p. 668-677, 2003.

KOH, R. et al. Finishing systems on the final surface roughness of composites. **The Journal of Contemporary Dental Practice**, v. 9, n. 2, p. 138-145, 2008.

KORKMAZ, Y. et al. The influence of one-step polishing systems on the surface roughness and microhardness of nanocomposites. **Operative Dentistry**, v. 33, n. 1, p. 44-50, 2008.

LANGE, R.T.; PFEIFFER, P. Clinical evaluation of ceramic inlays compared to composite restorations. **Operative Dentistry**, v. 34, n. 3, p. 263-272, 2009.

LARSSON, C.; WENNERBERG, A. The clinical success of zirconia-based crowns: a systematic review. **The International Journal of Prosthodontics**, v. 27, n. 1, p. 33-43, 2014.

LEE, Y. K. et al. Changes in gloss after simulated generalized wear of composite resins. **The Journal of Prosthetic Dentistry**, v. 94, n. 4, p. 370-376, 2005.

LEE, Y. K. Influence of filler on the difference between the transmitted and reflected colors of experimental resin composites. **Dental Materials**, v. 24, n. 9, p. 1243-1247, 2008.

LEE, Y. K. Influence of scattering/absorption characteristics on the color of resin composites. **Dental Materials**, v. 23, n. 1, p. 124-131, 2007.

LEVIN, I.; BRANDON, D. Metastable alumina polymorphs: crystal structure and transition sequences. **Journal of the American Ceramic Society**, v. 81, n. 8, p. 1995-2012, 1998.

LI, R. W.; CHOW, T. W.; MATINLINNA, J. P. Ceramic dental biomaterials and CAD/CAM technology: state of the art. **Journal of Prosthodontic Research**, v. 58, n. 4, p. 208-216, 2014.

LOHBAUER, U.; FRANKENBERGER, R.; KRÄMER, N. Surface quality controls mechanical strength and fatigue lifetime of dental ceramics and resin composites. **Ceramic Materials**, v. 9, p. 176-197, 2010.

LU, H. et al. Effect of surface roughness on stain resistance of dental resin composites. **Journal of Esthetic and Restorative Dentistry**, v. 17, n. 2, p. 102-109, 2005.

MARGHALANI, H. Y. Effect of finishing/polishing systems on the surface roughness of novel posterior composites. **Journal of Esthetic and Restorative Dentistry**, v. 22, n. 2, p. 127-138, 2010.

MELANDER, J. et al. Comparison of flexural properties and surface roughness of nanohybrid and microhybrid dental composites. **General Dentistry**, v. 59, n. 5, p. 342-349, 2011.

MICHALEK, M. et al. Mechanical and functional properties of Al_2O_3 - ZrO_2 -MWCNTs nanocomposites. **Journal of The European Ceramic Society**, v. 34, n. 14, p. 3329-3337, 2014.

MITRA, S. B.; WU, D.; HOLMES, B. N. An application of nanotechnology in advanced dental materials. **The Journal of the American Dental Association**, v. 134, n. 10, p. 1382-1390, 2003.

MIYAZAKI, T. et al. A review of dental CAD/CAM: current status and future perspectives from 20 years of experience. **Dental Materials Journal**, v. 28, n. 1, p. 44-56, 2009.

MOHER, D. et al. Preferred reporting items for systematic reviews and meta-analyses: the PRISMA statement. **PLoS Medicine**, v. 6, n. 7, p. e1000097, 2009.
MOHSEN, N. M.; CRAIG, R. G. Effect of silanation of fillers on their dispersability by monomers systems. **Journal of Oral Rehabilitation**, v. 22, n. 3, p. 183-189, 1995.

MORAES, R. R. et al. Improved dental adhesive formulations based on reactive nanogel additives. **Journal of Dental Research**, v. 91, n. 2, p. 179-184, 2012.

MOUROUZIS, P. et al. Effects of sonic scaling on the surface roughness of restorative materials. **Journal of Oral Sciences**, v. 51, n. 4, p. 607-614, 2009.

NGUYEN, J.F. et al. High-temperature-pressure polymerized resin-infiltrated ceramic networks. **Journal of Dental Research**, v. 93, n. 1, p. 62-67, 2014.

NISHIYAMA, N. et al. Novel polyfunctional silanes for improved hydrolytic stability at the polymer-silica interface. **Journal of Biomedical Materials Research**, v. 25, n. 2, p. 213-221, 1991.

OKADA, K. et al. A novel technique for preparing dental CAD/CAM composite resin blocks using the filler press and monomer infiltration method. **Dental Materials Journal**, v. 33, n. 2, p. 203-209, 2014.

OZEL, E. et al. Effect of one-step polishing systems on surface roughness of different flowable restorative materials. **Dental Materials Journal**, v. 27, n. 6, p. 755-764, 2008.

OZER, F. et al. A retrospective survey on long-term survival of posterior zirconia and porcelain-fused-to-metal crowns in private practice. **Quintessence International**, v. 45, n. 1, p. 31-38, 2014.

OZTURK, I. K. et al. New energy levels of atomic niobium by laser induced fluorescence spectroscopy in the near infrared. **Journal of Physics B: Atomic, Molecular and Optical Physics**, v. 48, n. 1, p. 015005, 2015.

PAPADOGIANNIS, D. Y. et al. The effect of temperature on the viscoelastic properties of nano-hybrid composites. **Dental Materials**, v. 24, n. 2, p. 257-266, 2008.

PAULUS, P. M. et al. Surface and quantum-size effects in Pt and Au nanoparticles probed by ¹⁹⁷Au Mössbauer spectroscopy. **Physical Review B**, v. 64, p. 205418, 2001.

PECHO, O. E. et al. Optical behavior of dental zirconia and dentin analyzed by Kubelka-Munk theory. **Dental Materials**, v. 31, n. 1, p. 60-67, 2015.

PENTEADO, R. A. et al. Evaluation of surface roughness of microhybrid and nanofilled composites after pH-cycling and simulated toothbrushing. **The Journal of Contemporary Dental Practice**, v. 11, n. 6, p. E017-24, 2010.

PESQUEIRA, A. A. et al. Effect of disinfection and accelerated ageing on dimensional stability and detail reproduction of a facial silicone with nanoparticles. **Journal of Medical Engineering & Technology**, v. 36, n.4, p. 217-221, 2012.

PRIMUS, C. M. et al. Opalescence of dental porcelain enamels. **Quintessence International**, v. 33, n. 6, p. 439-449, 2002.

QUINN, G. D.; HOFFMAN, K.; QUINN, J. B. Strength and fracture origins of a feldspathic porcelain. **Dental Materials**, v. 28, n. 5, p. 502-511, 2012.

RAIGRODSKI, A.J. et al. Clinical efficacy of veneered zirconium dioxide-based posterior partial fixed dental prostheses: five-year results. **The Journal of Prosthetic Dentistry**, v. 108, n. 4, p. 214-222, 2012.

RASTELLI, A. N. et al. The filler content of the dental composite resins and their influence on different properties. **Microscopy Research and Technique**, v. 75, n. 6, p. 758-765, 2012.

RAUBACH, C. W. et al. Interfacial photoluminescence emission properties of core/shell Al₂O₃/ZrO₂. **CrystEngComm**, v. 14, n. 2, p. 393-396, 2012.

REIS, L. O. et al. Investigation on the use of triphenyl bismuth as radiopacifier for (di)methacrylate dental adhesives. **International Journal of Adhesion and Adhesives**, v. 48, p. 80-84, 2014.

REKOW, E. D. et al. Performance of dental ceramics: challenges for improvements. **Journal of Dental Research**, v. 90, n. 8, p. 937-952, 2011.

RINASTITI, M. et al. Effect of biofilm on the repair bond strengths of composites. **Journal of Dental Research**, v. 89, n. 12, p. 1476-1481, 2010.

RINASTITI, M. et al. Effects of surface conditioning on repair bond strengths of non-aged and aged microhybrid, nanohybrid, and nanofilled composite resins. **Clinical Oral Investigations**, v. 15, n. 5, p. 625-633, 2011.

RINASTITI, M. et al. Immediate repair bond strengths of microhybrid, nanohybrid and nanofilled composites after different surface treatments. **Journal of Dentistry**, v. 38, n. 1, p. 29-38, 2010.

RODRIGUES, M. C. et al. Calcium phosphate nanoparticles functionalized with a dimethacrylate monomer. **Materials Science & Engineering: C, Biomimetic Materials, Sensors and Systems**, v. 45, p. 122-126, 2014.

RODRIGUES, S. A. Jr.; FERRACANE, J. L.; DELLA BONA, A. Influence of surface treatments on the bond strength of repaired resin composite restorative materials. **Dental Materials**, v. 25, n. 4, p. 442-451, 2009.

SABATINI, C. et al. Cross-compatibility of methacrylate-based resin composites and etch-and-rinse one-bottle adhesives. **Operative Dentistry**, v. 37, n. 1, p. 37-44, 2012.

SABBAGH, J. et al. Characterization of the inorganic fraction of resin composites. **Journal of Oral Rehabilitation**, v. 31, n. 11, p. 1090-1101, 2004.

SALGADO, V. E. et al. The influence of nanoscale inorganic content over optical and surface properties of model composites. **Journal of Dentistry**, v. 45, n. 5, p. e45-e53, 2013.

SANTANA, B. P. et al. Preparation, Modification, and Characterization of Alginate Hydrogel with Nano-/Microfibers: A New Perspective for Tissue Engineering. **BioMed Research International**, v. 2013, p. 1-6, 2013.

SCHMITT, V. L. et al. Effect of the polishing procedures on color stability and surface roughness of composite resins. **ISRN Dentistry**, v. 2011, p. 617672, 2011.

SCHOLL, J. A.; KOH, A. L.; DIONNE J. A. Quantum plasmon resonances of individual metallic nanoparticles. **Nature**, v. 483, p. 421-428, 2012.

SCOTT, C. et al. Conversion of polycrystalline Al₂O₃ into single-crystal sapphire by abnormal grain growth. **Journal of the American Ceramic Society**, v. 85, n. 5, p. 1275-1280, 2002.

SENAWONGSE, P.; PONGPRUEKSA, P. Surface roughness of nanofill and nanohybrid resin composites after polishing and brushing. **Journal of Esthetic and Restorative Dentistry**, v. 19, n. 5, p. 265-275, 2007.

SIDERIDOU, I. D.; KARABELA, M. M. Effect of the amount of 3-methacyloxypropyltrimethoxysilane coupling agent on physical properties of dental resin nanocomposites. **Dental Materials**, v. 25, n. 11, p. 1315-1324, 2009.

SIDERIDOU, I. D.; KARABELA, M. M.; VOUVOUDI, E. C. H. Physical properties of current dental nanohybrid and nanofill light-cured resin composites. **Dental Materials**, v. 27, n. 6, p. 598-607, 2011.

SILIKAS, N. et al. Surface characterization of modern resin composites: a multitechnique approach. **American Journal of Dentistry**, v. 18, n. 2, p. 95-100, 2005.

SUZUKI, T. et al. Resistance of nanofill and nanohybrid resin composites to toothbrush abrasion with calcium carbonate slurry. **Dental Materials Journal**, v. 28, n. 6, p. 708-716, 2009.

TEIXEIRA, E. C. et al. In vitro toothbrush-dentifrice abrasion of two restorative composites. **Journal of Esthetic and Restorative Dentistry**, v. 17, n. 3, p. 172-182, 2005.

THOMPSON, J. Y. et al. Adhesion/cementation to zirconia and other non-silicate ceramics: Where are we now? **Dental Materials**, v. 27, n. 1, p. 71-82, 2011.

TOPCU, F. T. et al. Evaluation of microhardness, surface roughness, and wear behavior of different types of resin composites polymerized with two different light sources. **Journal of Biomedical Materials Research Part B: Applied Biomaterials**, v. 92, n. 2, p. 470-478, 2010.

TURSSI, C. P.; FERRACANE, J. L.; SERRA, M. C. Abrasive wear of resin composites as related to finishing and polishing procedures. **Dental Materials**, v. 21, n. 7, p. 641-648, 2005.

TURSSI, C. P.; FERRACANE, J. L.; VOGEL, K. Filler features and their effects on wear and degree of conversion of particulate dental resin composites. **Biomaterials**, v. 26, n. 24, p. 4932-4937, 2005.

UHL, A. et al. The influence of storage and indenter load on the Knoop hardness of dental composites polymerized with LED and halogen technologies. **Dental Materials**, v. 20, n. 1, p. 21-28, 2004.

VALINOTI, A. C. et al. Surface degradation of composite resins by acidic medicines and pH-cycling. **Journal of Applied Oral Science**, v. 16, n. 4, p. 257-265, 2008.

WANG, L. et al. Effect of bleaching gels on surface roughness of nanofilled composite resins. **European Journal of Dentistry**, v. 5, n. 2, p. 173-179, 2011.

WILSON, K. S. et al. Interphase effects in dental nanocomposites investigated by small-angle neutron scattering. **Journal of Biomedical Materials Research Part A**, v. 81, n. 1, p. 113-123, 2007.

WILSON, K. S.; ZHANG, K.; ANTONUCCI, J. M. Systematic variation of interfacial phase reactivity in dental nanocomposites. **Biomaterials**, v. 26, n. 25, p. 5095-5103, 2005.

WILSON, K.S.; ANTONUCCI, J.M. Interphase structure–property relationships in thermoset dimethacrylate nanocomposites. **Dental Materials**, v. 22, n. 11, p. 995-1001, 2006.

YAO, G. et al. Fabrication of high-quality ZnCdO epilayers and ZnO/ZnCdO heterojunction on sapphire substrates by pulsed laser deposition. **Applied Surface Science**, v. 326, p. 271-275, 2015.

YAP, A. U. et al. Comparison of surface finish of new aesthetic restorative materials. **Operative Dentistry**, v. 29, n. 1, p. 100-104, 2004.

YEH, S. T. et al. The roughness, microhardness, and surface analysis of nanocomposites after application of topical fluoride gels. **Dental Materials**, v. 27, n. 2, p. 187-196, 2011.

YESIL, Z. D. et al. Evaluation of the wear resistance of new nanocomposite resin restorative materials. **The Journal of Prosthetic Dentistry**, v. 99, n. 6, p. 435-443, 2008.

YOSHIMURA, H. N.; GOLDENSTEIN, H. Light scattering in polycrystalline alumina with bi-dimensionally large surface grains. **Journal of the European Ceramic Society**, v. 29, n. 2, p. 293-303, 2009.

YOSHIMURA, H. N. et al. Relationship between elastic and mechanical properties of dental ceramics and their index of brittleness. **Ceramics International**, v. 38, n. 6, p. 4715-4722, 2012.

YOSHIMURA, H. N. et al. Porosity dependence of elastic constants in aluminum nitride ceramics. **Materials Research**, v. 10, n. 2, p. 127-133, 2007.

YU, B.; LEE, Y. K. Difference in opalescence of restorative materials by the illuminant. **Dental Materials**, v. 25, n. 8, p. 1014-1021, 2009.

ZHANG, J. et al. UV Raman spectroscopic study on TiO_2 . I. Phase transformation at the surface and in the bulk. **The Journal of Physical Chemistry B**, v. 110, n. 2, p. 927-935, 2006.

ZHANG, X. P. et al. Crack-healing ability and strength recovery of different hot-pressed TZ3Y20A-SiC ceramics by heat treatment in air. **Materials & Design**, v. 67, p. 324-329, 2015.

ZHANG, Y. Making yttria-stabilized tetragonal zirconia translucent. **Dental Materials**, v. 30, n. 10, p. 1195-1203, 2014.

ZHOU, M.; DRUMMOND, J. L.; HANLEY, L. Barium and strontium leaching from aged glass particle/resin matrix dental composites. **Dental Materials**, v. 21, n. 2, p. 145-155, 2005.

Anexos

Anexo A –Licensa de uso do texto completo do artigo constante no Capítulo 1 desta tese.Os direitos autorais do referido artigo pertencem à editora Elsevier

1/25/2015

RightsLink - Your Account

ELSEVIER LICENSE TERMS AND CONDITIONS

Jan 25, 2015

This is a License Agreement between Marina R Kaizer ("You") and Elsevier ("Elsevier") provided by Copyright Clearance Center ("CCC"). The license consists of your order details, the terms and conditions provided by Elsevier, and the payment terms and conditions.

All payments must be made in full to CCC. For payment instructions, please see information listed at the bottom of this form.

Supplier	Elsevier Limited The Boulevard, Langford Lane Kidlington, Oxford, OX5 1GB, UK
Registered Company Number	1982084
Customer name	Marina R Kaizer
Customer address	2261 Tiradentes St, apt 201 Pelotas, None 96010
License number	3547571450932
License date	Jan 14, 2015
Licensed content publisher	Elsevier
Licensed content publication	Dental Materials
Licensed content title	Do nanofill or submicron composites show improved smoothness and gloss? A systematic review of in vitro studies
Licensed content author	None
Licensed content date	April 2014
Licensed content volume number	30
Licensed content issue number	4
Number of pages	38
Start Page	e41
End Page	e78
Type of Use	reuse in a thesis/dissertation
Portion	full article
Format	electronic
Are you the author of this Elsevier article?	Yes
Will you be translating?	No
Title of your thesis/dissertation	Direct and Indirect Hybrid Restorative Materials in Dentistry
Expected completion date	Feb 2015
Estimated size (number of pages)	
Elsevier VAT number	GB 494 6272 12
Price	0.00 USD
VAT/Local Sales Tax	0.00 USD / 0.00 GBP